



NRL/MR/7531--99-7240

Vertical Correlation Functions for Temperature and Relative Humidity Errors

RICHARD FRANKE

*Atmospheric Dynamics & Prediction Branch
Marine Meteorology Division*

19990319 020

January 1999

Approved for public release; distribution unlimited.

DTIC QUALITY INSPECTED 1

REPORT DOCUMENTATION PAGE

Form Approved
OMB No. 0704-0188

Public reporting burden for this collection of information is estimated to average 1 hour per response, including the time for reviewing instructions, searching existing data sources, gathering and maintaining the data needed, and completing and reviewing the collection of information. Send comments regarding this burden or any other aspect of this collection of information, including suggestions for reducing this burden, to Washington Headquarters Services, Directorate for Information Operations and Reports, 1215 Jefferson Davis Highway, Suite 1204, Arlington, VA 22202-4302, and to the Office of Management and Budget, Paperwork Reduction Project (0704-0188), Washington, DC 20503.

1. Agency Use Only (Leave Blank).	2. Report Date. January 1999	3. Report Type and Dates Covered. Final	
4. Title and Subtitle. Vertical Correlation Functions for Temperature and Relative Humidity Errors		5. Funding Numbers. PE 0602435N PN R3591	
6. Author(s). Richard Franke			
7. Performing Organization Name(s) and Address(es). Naval Research Laboratory Marine Meteorology Division Monterey, CA 93943-5502		8. Performing Organization Reporting Number. NRL/MR/7531- - 99 - 7240	
8. Sponsoring/Monitoring Agency Name(s) and Address(es). Office of Naval Research Arlington, VA 22217-5660		10. Sponsoring/Monitoring Agency Report Number.	
11. Supplementary Notes.			
12a. Distribution /Availability Statement. Approved for public release; distribution unlimited		12b. Distribution Code.	
13. Abstract (Maximum 200 words). This report gives the details and results of any investigation into the properties of the temperature and relative humidity errors from the Navy Operational Global Atmospheric Prediction System for a four-month period from March-June 1998. The spatial covariance data for temperature and for relative humidity was fit using eight different approximation functions/weighting methods. From these, two were chosen as giving good estimates of the parameters and variances of the prediction and observation errors and were used in further investigations. The vertical correlation between temperature errors at different levels and relative humidity errors at different levels was approximated using a combination of functional fitting and transformation of the pressure levels. The cross-covariance between temperature and relative humidity errors at various pressure levels were approximated in two ways: (1) by directly computing and approximating the cross-covariance data, and (2) by approximating variance of the difference of normalized data. The latter led to more consistent results. There are numerous figures illustrating the results obtained and tables give the pertinent data.			
14. Subject Terms. Covariance functions; Temperature error statistics; Relative humidity error statistics Temperature/humidity error correlation; NOGAPS		15. Number of Pages. 78	16. Price Code.
17. Security Classification of Report. UNCLASSIFIED	18. Security Classification of This Page. UNCLASSIFIED	19. Security Classification of Abstract. UNCLASSIFIED	20. Limitation of abstract. Same as report

CONTENTS

1. Introduction.....	1
2. Covariance Functions for Temperature and Relative Humidity.....	3
3. Estimation of Cross-Correlation of Temperature and Relative Humidity Errors by Direct Computation.....	8
4. Estimation of Cross-Correlation of Temperature and Relative Humidity Errors Through a Differencing Approach.....	10
5. Summary and Conclusions.....	13
Figures	15
Appendix	59
Reference	69

ACKNOWLEDGEMENT

This research was conducted while the author was working for Naval Research Laboratory/Monterey during FY98, supported under Program Element 0602435N. The author expresses his thanks to Ed Barker, who made the arrangements, and Nancy Baker, Roger Daley, and Andrew Van Tuyl, all of whom contributed to the effort by supplying data and many useful comments. Formatting and editing of this manuscript was done by Soheila Judy.

1. Introduction

Plans for increasing the vertical resolution of the Navy Operational Global Atmospheric Prediction System (NOGAPS) used by Fleet Numerical Meteorological and Oceanographic Center require that the covariance structure for temperature and relative humidity errors be modeled more accurately. This report details an investigation into the statistical properties of the innovation data for these quantities. For this purpose a four month time history of the data (March through June 1998, with the exception of one day, March 27 at 00 UTC) was used, independently for times 00 UTC and 12 UTC. All valid data from longitude 70° to 130° west and 25° to 55° north were used. Some preliminary computations were carried out using a two month history, but it was quickly determined that data for the four month period led to binned data that seemed more consistent in that the points have less scatter and can be better fit by a curve. This was less apparent at the very lowest and highest levels, but at intermediate levels was consistently true. Such a long period may obscure seasonal effects, and this will need to be investigated if such details are to be incorporated into the system.

Previous work that investigates the cross-correlation of temperature and relative humidity errors has been based on the "NMC method" (Parrish and Derber, 1992). There the idea is to use the 24 and 48 hour forecasts to estimate the prediction error, assuming that error growth is linear for that period of time. For vertical temperature error correlations ECMWF has found a close agreement between this method and those derived from innovation data (Courtier, et al, 1993). Steinle and Seaman (1995) also used the "NMC method" to estimate the cross-correlation between temperature and relative humidity.

The methods employed here are very much like those used previously by the investigator (see Franke, 1998) and others. The temperature and relative humidity innovation data were averaged at each level for each station over the 122 days. The mean values were then subtracted from the innovation data. Then the raw covariance data were formed and summed into bins of size 0.01 radians, keeping a count of the number of terms. True radian distance on the sphere was used. Use of great circle distance poses a potential difficulty with positive definiteness of the spatial covariance function approximation, but it is thought to not pose a problem over regions of the size

contemplated. Experiments were carried out using several different forms of the covariance function approximation and different weights for the squared residuals of the binned data. Complete details of all results are not given here, but sufficient data to indicate the nature of the results and reasons for the choices made are given.

The quantities measured by radiosondes are temperature and relative humidity (Federal Meteorological Handbook No. 3, OFCM, 1997). The data supplied from NOGAPS are the pressure p , predicted temperature T_p , and predicted specific humidity Q_p . In the data file along with the NOGAPS data is the observed temperature T_o and observed dewpoint depression D_o (which is actually reported), along with the quality control flags. Using the formulas given by (OFCM, 1997), the observed value of relative humidity is retrieved as follows: dewpoint temperature $T_d = T_o - D_o$, observed vapor pressure $e = c \exp\left(\frac{aT_d}{b+T_d}\right)$, saturation vapor pressure $e_s = c \exp\left(\frac{aT_o}{b+T_o}\right)$, and finally

observed relative humidity $u_o = \frac{e}{e_s}$. Here a , b , and c are constants,

$a = 17502$, $b = 240.97^\circ K$, $c = 6.1121$ mb. It is assumed that these calculations reverse those that obtained D_o from u_o . If not, the relative humidity may be contaminated by the observation error in T_o . Similar formulas allow the calculation of the predicted value of relative humidity from the predicted values of temperature, specific humidity, and

pressure p : mixing ratio $r = \frac{Q_p}{1 - Q_p}$, predicted vapor pressure $e = \frac{rp}{r + 0.622}$,

saturation vapor pressure at the predicted temperature, $e_s = c \exp\left(\frac{aT_p}{b+T_p}\right)$, and predicted

relative humidity $u_p = \frac{e}{e_s}$, where a , b , and c are as before.

As we will see later, the independence of the observation errors for temperature and relative humidity is questionable. Whether the values were cross contaminated from the

above operations, or whether the relative humidity observation error is somehow dependent on temperature measurement errors is unknown.

2. Covariance functions for temperature and relative humidity

Samples of the binned covariance data for temperature innovations at time 00 UTC are given in Figure 1 for the 850, 700, 500, and 400 mb levels, and a bar chart showing the number of measurements, N , included in each bin for these cases is given in Figure 2. The corresponding data for the relative humidity is given in Figures 3 and 4. For curve fitting purposes, only data out to a maximum distance of 0.40 radians was used, with the data at greater distances shown for completeness only.

The choice of functions to fit data such as this is not clear cut. It is important that the function be positive definite and that it embody enough parameters to give a good estimate of the intercept value for the dependent variable using only data for positive distances since the zero distance covariance is a sum of the observation and prediction error variances. It is assumed that the observation errors are spatially uncorrelated since different instruments (of the same type) are used at different stations. Thus we seek to fit the prediction error spatial covariance function, with the intercept then being the prediction error variance and the difference between the empirical innovation variance and the prediction error variance being the observation error variance. In previous studies a number of different functions and weights have been used (e.g., Franke, 1985, 1998). For this study we have used some that have been used previously, and some that we have not used before. The three basic functions used here are the special second order autoregressive function

$$F(d) = C(1 + ad)e^{-ad} , \quad (1)$$

a convex combination ($0 \leq c \leq 1$) of two second order autoregressive functions

$$F(d) = C[(c(1 + ad)e^{-ad} + (1 - c)(1 + bd)e^{-bd}] , \quad (2)$$

and the full third order autoregressive function

$$F(d) = [(\alpha \cos as + \beta \sin as)e^{-bs} + \gamma e^{-cs}] , \quad (3)$$

where $\alpha = \frac{(3b^2 - a^2 - c^2)ac}{\delta}$, $\beta = \frac{(b^2 - 3a^2 - c^2)bc}{\delta}$, $\gamma = \frac{-2(b^2 + a^2)ab}{\delta}$, with $\delta = (3b^2 - a^2 - c^2)ac - 2(b^2 + a^2)ab$.

Function (1) has been used extensively by the investigator and others. Note that function (2) was inspired by Mitchell, et al. (1990), where a sum of special third order autoregressive functions were used (but with specified weights and relation between constants in the exponential). Function (3) was chosen because it has more parameters and embodies two different exponential decay rates, giving considerably more flexibility than function (1), and with a different connection between the exponential decay terms than that of function (2). All nonlinear least squares fits were computed using the standard minimization function *fmins* in Matlab®, which uses a Nelder-Mead simplex algorithm. All nonlinear minimization routines are sensitive to the initial guess, and some effort was expended in trying different initial guesses.

Table 1 gives a list of the functions and weights we have used to fit the temperature and relative humidity innovations.

Ref #	weight	Function	Comments
1	N, d < 0.40	(1)	special second order AR, N-weighted (S2W1)
2	N, d < 0.20	(1)	special second order AR, limited distance (S2W2)
3	\sqrt{N} , d < 0.40	(1)	special second order AR, \sqrt{N} -weighted (S2W3)
4	1, d < 0.40	(1)	special second order AR, equi-weighted (S2W4)
5	N, d < 0.40	(2)	sum of two SAR2s, N-weighted (SS2W1)
6	N, d < 0.20	(2)	sum of two SAR2s, limited distance (SS2W2)
7	\sqrt{N} , d < 0.40	(2)	sum of two SAR2s, \sqrt{N} -weighted (SS2W3)
8	N, d < 0.40	(3)	Full third order AR, N-weighted (F3W1)

Table 1: Fitting functions and weighting for spatial least squares fits

The standard deviations of the temperature and relative humidity prediction errors (that is, the square roots of the intercepts) obtained from the 8 approximations indicated

in Table 1 are shown graphically for various levels at the two times in Figures 5 and 6. Two things are striking: The general consistency of the results for the special second order autoregressive fits (especially for temperature) and to a lesser extent the overall consistency when some non-equal weighting is applied to the binned data, and the rather different results obtained when using equal weighting.

The difficulties in obtaining appropriate approximations to the intercept (and hence the variance of the prediction error) is a long-standing problem. In some sense the data for short distances is most critical to defining that value, but on the other hand the amount of data is very much less (as seen in Figure 2). Of course, this goes hand-in-hand with a suitable assumption for the local behavior of the spatial covariance function for short distances. As in previous work (Franke, 1998), it is felt here that some form of non-equal weighting for the data is appropriate. The choice is not clear-cut, and somewhat arbitrarily I have decided to use the weighting of Ref#1, weighting of the squared residuals by the number of the data collected in the bin. Likewise I have decided to pursue further investigations using only two fitting functions with that weighting, the special second order autoregressive function and the full third order autoregressive function. These will be referred to hereafter as SAR2 and FAR3, respectively. It is presently unknown what restrictions on the parameters will guarantee that the full third order autoregressive function is positive definite in two dimensions, but the additional parameters and flexibility available will allow some different behavior by the approximating function for small distances. The FAR3 will also be used for the vertical correlation approximations.

The standard deviations of the error data implied by the two choices for fitting the spatial covariance functions is presented in Figures 7 and 8. Figure 7 shows the standard deviations of the temperature observation and prediction errors for the various levels for each of the two approximations at the two times. Figure 8 shows the corresponding data for relative humidity.

To estimate the vertical correlation between temperature errors and between relative humidity errors, the same strategy as has been used previously for pressure level height errors was used. That is, the spatial covariance functions for the differences in the errors between all possible pairs of (different) levels were approximated. Letting V_j represent

the error of the quantity in question (temperature, or relative humidity), we estimate $\text{var}(V_j - V_i)$. Then, since $\text{var}(V_j - V_i) = \text{var}(V_j) - 2\text{cov}(V_j, V_i) + \text{var}(V_i)$, we obtain

$$\text{cov}(V_j, V_i) = \frac{1}{2}(\text{var}(V_j) + \text{var}(V_i) - \text{var}(V_j - V_i)) \quad (4)$$

Having estimated each of the quantities on the right side of Eq. (4) by approximating the spatial covariance function for the quantity, we are able to obtain the vertical covariance.

The vertical correlation is then $\text{cor}(V_j, V_i) = \text{cov}(V_j, V_i) / (\text{var}(V_j) \text{var}(V_i))^{1/2}$.

It is desirable that the vertical correlation functions be expressed in a stationary isotropic form. In an attempt to achieve this, the simultaneous fit and transformation of the vertical coordinate that was used by Franke (1998) was applied to these eight cases for both prediction and observation error. Because there is appreciable negative correlation at short distances, the full autoregressive function of order three given by Eq. (3) was used. After translation of the values to the new coordinate system, the resulting approximations, along with the correlation points, are shown in Figures 9-12. The transformations generated for each of the approximations are shown in Figure 13-16. The previous application (to height error correlations) generated considerable improvement in terms of reducing the scatter and making the data look reasonably coherent when viewed as isotropic in the transformed coordinate, however we see less of this in Figures 9-12. At short distances the temperature prediction errors (Figure 9) are fit well, however the relative humidity prediction errors (Figure 11) are not so well fit, especially at 12 UTC. The situation is somewhat reversed with the observation errors, where the fit is generally better for the relative humidity observation error (Figure 12) than that for the relative humidity prediction error (Figure 10). The use of the full third order autoregressive function for the vertical correlation approximation induces some negative lobes in the approximation for the temperature prediction error and the relative humidity observation error. Generally the approximating correlation functions for temperature observation errors appear to be quite narrow, indicating the vertical errors are nearly uncorrelated. It is noted that the transformations associated with some fits (Figures 15 lower right and 16 lower left) both show extreme deformation between

certain points. It is also noted that some of the correlation values obtained through the FAR3 fits are larger than one, although this is obscured by Figure 10 (upper right) because the extent of the axis for the figure does not include the two points near "correlation value" 1.3. There is no such occurrence with SAR2.

While some interesting things can be seen by looking at Figures 9-16, the more realistic view comes by observing the fit to the correlation points and how the translation affects the correlation curve approximation. For this purpose there are sixteen figures that show the correlation curves mapped back to the log-pressure coordinate. The sixteen figures (Figures 17-32) correspond to the sixteen subfigures of Figures 8-12. The order the figures corresponds to the curves within each of Figures 8-12 from left to right, top to bottom. In each of Figures 17-32, the four subfigures show a separated subset of the correlation curves for correlation of the indicated error between pressure levels. The label indicates the correlation curve for the error at that level with other levels. Also shown in each figure are the data points giving the empirical correlation as computed by the indicated method for the particular error and time. It is noted that for purposes of computing the correlation curves the transformation between levels was obtained by piecewise linear interpolation. The figures can be perused at length, and yield considerable information about the approximate behavior of the vertical correlation functions for temperature and relative humidity prediction and observation error. The general conclusion is much the same as was observed in Figures 8-16. The curves are generally well-behaved for all cases, except those corresponding to Figures 15 lower right and 16 lower left. The corresponding curves are shown in Figures 28 and 31, respectively. Unfortunately, these two cases cut across both fitting methods, so that a clear choice of fitting method does not appear here.

The correlation distance parameter is of interest. For function (1) this is the reciprocal of the parameter a , while in function (3), there are two similar parameters, b and c . The correlation distance is generally a measure of the distance at which the function decays by a certain amount¹, but for (3) the term is taken to mean the larger of the reciprocals of b and c . Plots of the correlation distance parameters are given in

¹ In this and previous papers the investigator uses decay to $\exp(-1)$ of the maximum value, but others have used decay to 0.5 of the maximum value.

Figure 33. It is noted that the correlation distances arising from the SAR2 approximations are quite consistent between the two times, and generally well behaved. There is considerably more variation of the correlation distance over level and between the two times when the FAR3 approximation is used.

3. Estimation of cross-correlation of temperature and relative humidity errors by direct computation

The cross-correlation between temperature and relative humidity errors has not been extensively studied. The only work known to the investigator is that mentioned in the introduction, by Steinle and Seaman (1995) using the "NMC method" (see Parrish and Derber, 1992). The more important part of this work was to attempt to compute from the innovation data the behavior of the cross-correlation between temperature and relative humidity prediction errors.

First it is noted that the variance of the temperature prediction errors and the relative humidity prediction errors must be known (estimates, anyway) before the cross-correlation of the two quantities can be estimated from the innovation data. It is believed that reasonable estimates are available from the work reported in the previous section.

The first attempt was to directly compute the cross-covariance data from the innovation data, bin it, and then approximate the spatial cross-covariance function. In principle the observation errors should be independent, and only the zero distance empirical cross-covariance would need to be computed. In practice it was quickly discovered that this was not the case. In what follows, the innovations will be referred to as errors for simplicity. Figure 34 shows the binned cross-covariance data for relative humidity errors at 850 mb and the temperature errors at 925, 850, 700, and 500 mb at time 00 UTC. The fit using the SAR2 function is also shown for each case. The data for 925 mb temperature innovations is rather scattered, but the others appear reasonably well behaved and are fit reasonably well by the approximating function. The 700 mb temperature data seems to have an anomalous fit. Despite the fact that the function approximates the data fairly well, there is no good reason to believe that such functions would approximate well for other pairs of levels since cross-covariance functions need to satisfy fewer constraints than covariance functions. Note that the intercept of the

approximating function misses the value at zero distance, in each case, by a nontrivial amount. Perusal of other pairs of levels also exhibit apparent additional correlated error at zero distance. Whether this error is indeed due to correlated observation error, or whether it is contamination of the innovation values for relative humidity when calculated from predicted specific humidity and observed dewpoint depression is unknown. In any case, it cannot be ignored.

Because most of the software was readily available, it was decided to approximate the directly computed cross-covariance data using both the SAR2 fit and the FAR3 fit. Using the intercepts of these approximations, the cross-covariance matrix for zero distances between the 16 temperature levels and the 7 relative humidity levels was computed, and hence the vertical cross-correlation matrix for temperature and relative humidity. The seven figures showing the correlation between relative humidity error and temperature errors at various heights at time 00 UTC are shown in Figure 35, as derived from the SAR2 fits. Most notable is the strong negative correlation between temperature errors and relative humidity errors at the same level up to 850 mb, and lesser negative correlation at higher levels. Smaller amounts of data suggest one should be suspicious about the correlations between relative humidity error at 1000 mb and temperature error at the upper levels. Perusal of the fits to the cross-covariance data for relative humidity error at 1000 mb and temperature error at 200 mb and above show that in most cases the fits do not seem unreasonable, however. The corresponding plots for the cross-correlation data derived from the SAR2 fits at 12 UTC are shown in Figure 36.

Figures 37 and 38 show the cross-correlation data derived from the FAR3 fits at 00 and 12 UTC. For the most part, the correlations are fairly consistent between the two times. The correlation between relative humidity error at 925 mb and temperature error at 925 mb is a bad value. There are some cases where the points differ significantly for the two fits at the same time, and in particular two SAR2 fits that are very much wrong. These are the cross-correlations between relative humidity error at 700 mb and temperature error at 20 mb at 00 UTC, and relative humidity error at 850 mb and temperature error at 70 mb at 12 UTC. The correlations derived from the FAR3 fits appear to be much more consistent between the two times. The additional flexibility of

the FAR3 fits, and in particular the possibility of the spatial cross-covariance curve changing sign may be the reason for this.

Because of the unknown properties of spatial cross-covariance functions, it seemed desirable to attempt to derive the cross-correlation properties by fitting only spatial covariance data. The analogy on which this idea is based is that of estimating vertical covariances between different levels of the height error (see Franke, 1998) by treating the thickness error for all combinations of levels, just as the temperature and relative humidity data were treated in the previous section. In this case, unfortunately, we are dealing with quantities that have different units (degrees, and none), and various authors (e.g., Cressie, 1993) have warned against working with the difference of such quantities. In the next section an approach and the results will be presented.

4. Estimation of cross-correlation of temperature and relative humidity errors through a differencing approach

The primary problem with computing the spatial covariance of the difference of two quantities is assigning a meaning to it when the two quantities have different units. Thus, while one can plunge ahead and compute things such as $\text{var}(V_i - W_j)$ when V_i and W_j have different units, exactly what that means physically is questionable and troubling. Cressie (1993) suggests that the quantities need to be normalized in some way. Because it is necessary to compute the variances of the prediction errors for both temperature and relative humidity, it seems natural to normalize by the standard deviations of the error. To lend some consistency, the standard deviations derived from the same fitting function as is used to fit the spatial covariance of the difference will be used.

At this point the details of the equations for the case of temperature innovations and relative humidity innovations will be completely spelled out. Let σ_i and μ_j represent the standard deviations of the temperature prediction error at level i and the relative humidity prediction error at level j , respectively. Recall that the innovations are the differences between the observed value and the predicted value and are thus equal to the difference between the observation error and the prediction error. Having previously estimated the variances of the prediction errors for both temperature and relative

humidity, we now nondimensionalize the innovation for temperature at level i and relative humidity at level j by dividing by the appropriate standard deviation, σ_i for temperature and μ_j for relative humidity. Now, letting $\delta_i^o - \delta_i^p$ represent the normalized temperature innovation at level i , and correspondingly $\delta u_i^o - \delta u_i^p$ represent the normalized relative humidity innovation at level j , we now consider the variance of the difference. We have

$$\begin{aligned} \text{var}(\delta_i^o - \delta_i^p - \delta u_j^o + \delta u_j^p) &= -2 \text{cov}(\delta_i^o, \delta u_j^o) - 2 \text{cov}(\delta_i^p, \delta u_j^p) \\ &+ \text{var}(\delta_i^o) + \text{var}(\delta_i^p) + \text{var}(\delta u_j^o) + \text{var}(\delta u_j^p) \end{aligned}$$

(4) if we assume that the predicted values and the observed values are independent. Now consider Eq. (4) in a more general sense as describing spatial covariance of the difference on the left side. Because the observation error is independent for different stations, at distances greater than zero the right side becomes (here interpreting the quantities as spatial covariances)

$$-2 \text{cov}(\delta_i^p, \delta u_j^p) + \text{var}(\delta_i^p) + \text{var}(\delta u_j^p) . \quad (5)$$

Thus when the left side is approximated by the same techniques as used for temperature and relative humidity errors and extrapolated to zero distance, the intercept is an approximation to the quantity in Eq. (5) for zero distance. The actual empirical value at zero distance also includes the terms arising from observation errors, that is

$$-2 \text{cov}(\delta_i^o, \delta u_j^o) + \text{var}(\delta_i^o) + \text{var}(\delta u_j^o) .$$

It may be possible that there are other terms involving error that is correlated with observation error (such problems are assumed away here). In such a case the values of the covariance of observation errors would be impossible to separate from the other correlated errors.

Returning to Eq. (5) and denoting the intercept of the spatial approximation to the left side of Eq. (4) by $C_{i,j}^{t-u}$, we obtain

$$\text{cov}(\delta t_i^P, \delta u_j^P) = \frac{1}{2} \left(\text{var}(\delta t_i^P) + \text{var}(\delta u_j^P) - C_{i,j}^{t-u} \right)$$

Noting that δt_i^P and δu_j^P represent the normalized values of the predicted temperature and relative humidity errors, respectively, we see that the two variances have the value one. Further, the covariance on the left side is then seen to be the correlation between the two quantities, and thus we have

$$\text{cor}(\delta t_i^P, \delta u_j^P) = 1 - \frac{1}{2} C_{i,j}^{t-u} . \quad (6)$$

One of the key advantages of the difference approach is that all function approximations are to spatial covariances. Using the two approximations SAR2 and FAR3, the approximation of the correlation by the difference method was carried out. To illustrate some of the data involved, Figure 39 shows the binned covariance data for four different cases. These are the covariances between relative humidity error at 850 mb and temperature error at 925, 850, 700, and 500 mb. Some of the nuances of the third order autoregressive function are shown, as well. The 925 mb temperature data illustrates that the function may have a very sharp transition from zero slope at the origin to a rapid decrease. Some subtle “waviness” is shown for the 850 mb and 500 mb temperature data.

When the intercept values obtained from fitting all differences are used in Eq. (6) the correlation matrix for the relative humidity and temperature errors are then available. The results were computed for both the SAR2 and FAR3 fits.

The results obtained from the SAR2 fits at times 00 UTC and 12 UTC are shown in Figures 40 and 41, respectively. Figure 40 should be compared with Figure 35, and Figure 41 with Figure 36. Depending on the level, some graphs compare rather well, while there are significant differences in other cases. There are no “out of bounds” points resulting from the difference method, in contrast to the two resulting from SAR2 fits using the direct method. The difference method tends to show a significant drift toward positive correlations at the higher temperature levels (generally above 200 mb, but lower in a few cases) that are not shown in the direct method calculations. No explanation for this has come to mind, although the investigator would urge skepticism concerning the reality of such results.

For the FAR3 fits the plots for 00 UTC and 12 UTC are shown in Figures 42 and 43, and should be compared with Figures 37 and 38. In contrast to the SAR2 fits, the "out of bounds" points with FAR3 are now obtained using the difference method rather than the direct method. The curves in Figures 42 and 43 tend to show greater variation over the temperature levels than those of Figures 37 and 38. The strong negative correlation between relative humidity errors and temperature errors at the same level are somewhat suppressed, and in some cases the correlation is positive.

As a general rule, the correlation curves shown in Figures 37 and 38 are the most pleasing in the sense that they tend not to show large correlations between relative humidity errors and temperature errors at widely differing levels. A notable exception to this is the significant (varying positive and negative) correlation between relative humidity error at 1000 mb and temperature error at upper levels at time 00 UTC. The correlations are smaller at 12 UTC.

5. Summary and conclusions

This study has attempted to determine some of the properties of the spatial covariance and vertical correlation of temperature and relative humidity prediction errors, and their vertical cross-correlation. Use of different spatial approximations has led to consistent results in some respects such as the variance of prediction errors and correlation distances for both temperature and relative humidity. The attempt to approximate the vertical correlation functions with an isotropic function on a transformed domain led to somewhat inconsistent results when comparing those based on spatial fits with the SAR2 function with those based on FAR3 spatial fits. Although neither of the two approximations gave entirely satisfactory results, the SAR2 fits had the fewest real serious problems, such as "correlation" values between levels that are greater than one in value.

In attempting to fit the cross-correlation, the more pleasing results were obtained by fitting the spatial cross-covariance data directly, even though the difference method is based entirely on fitting spatial covariance functions (of differences) and might seem to pose less problem of an appropriate fitting function. With the direct method the

additional flexibility of the FAR3 function leads to better vertical cross-correlation curves between the two variables at different levels.

Fitting the normalized difference of the two variables in the spatial domain using SAR2 fits yields somewhat more pleasing results for the vertical cross-correlation than that using the FAR3 fits. There is, however, a disconcerting increase in the correlation between relative humidity errors and temperature errors as a function of height of the temperature errors for the results from the SAR2 fits. In the case of the difference scheme there are no "bad points" such as were noted in Figures 35 and 36 using the SAR2 fits directly on the spatial cross-covariance.

In two final figures, it is noted that the vertical correlation of temperature prediction errors and of temperature observation errors may not be isotropic in any transformed region. That is, for certain levels the negative lobe below the given level may not be matched by a negative lobe at upper levels. See Figure 44 for the sixteen plots of correlation of temperature prediction errors at 00 UTC derived from SAR2 at a given level with those at other levels, and note especially the curves for 300 and 70 mb, and to a lesser extent, 200 mb. Further it can be noted that the curves are different at different heights, indicating inhomogeneity, at least to some extent. The corresponding curves for the associated temperature observation errors are shown in Figure 45 and exhibit some of the same behavior. Whether such vertical correlation functions can be modeled using positive definite functions that have the right properties is not known to the investigator. As a matter of interest, it is noted that the empirical vertical correlation matrix for the temperature prediction errors shown in Figure 44 is not positive definite, although that for the temperature observation errors shown in Figure 45 is.

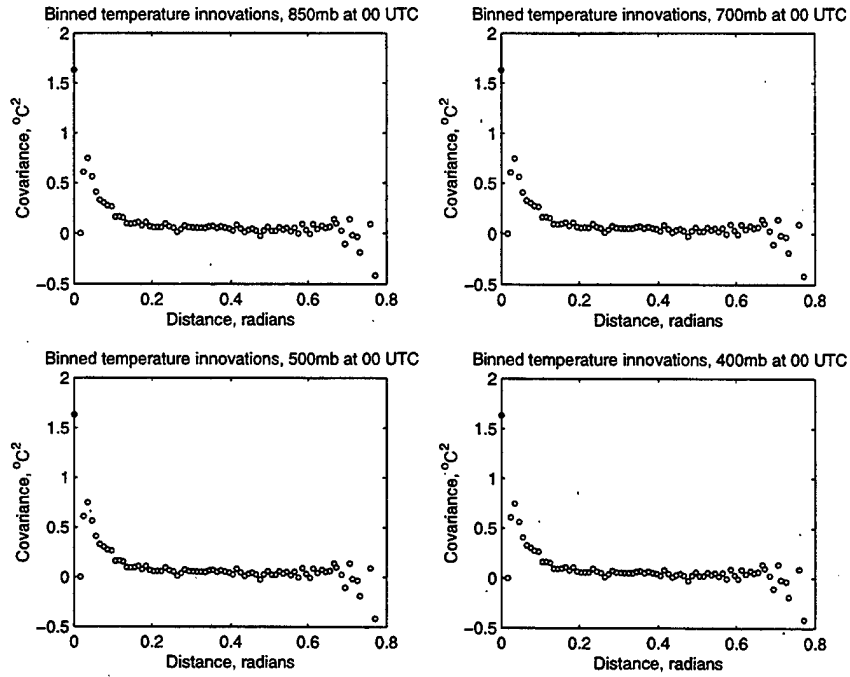


Figure 1: Binned temperature innovations for 00 UTC at 850, 700, 500, and 400 mb levels.

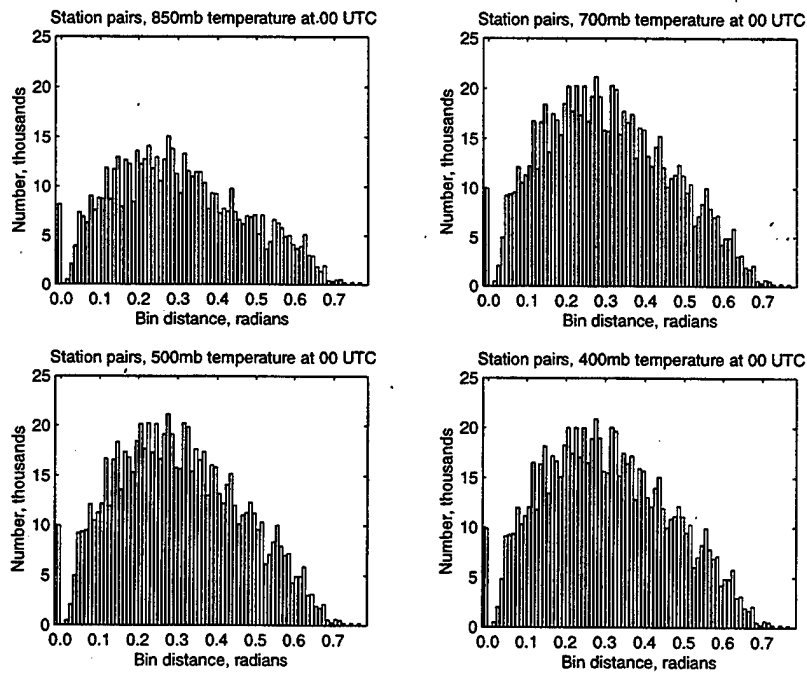


Figure 2: Bar chart showing number of terms in each bin for Figure 1.

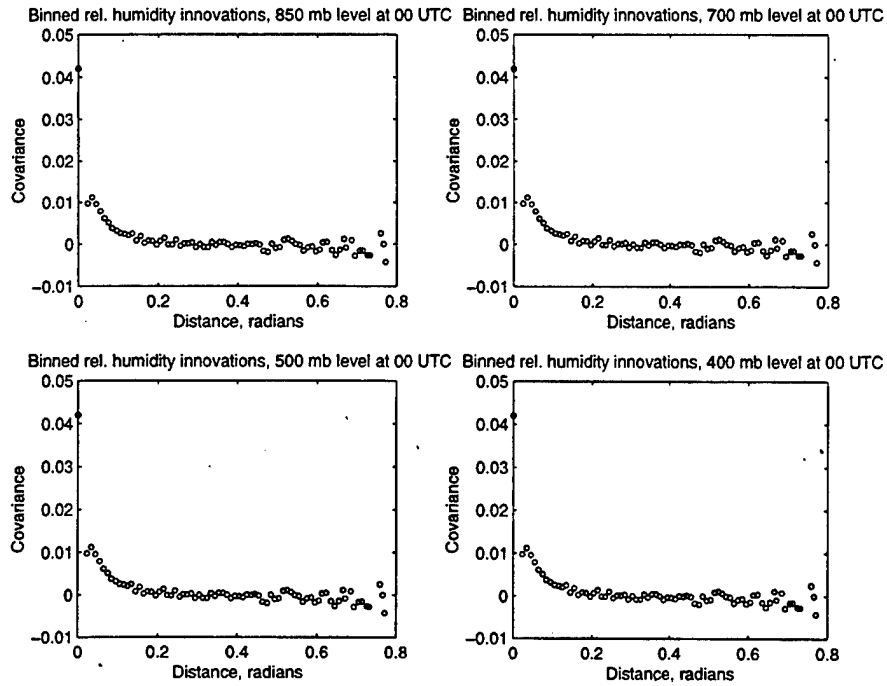


Figure 3: Binned relative humidity innovations for 00 UTC at 850, 700, 500, and 400 mb levels.

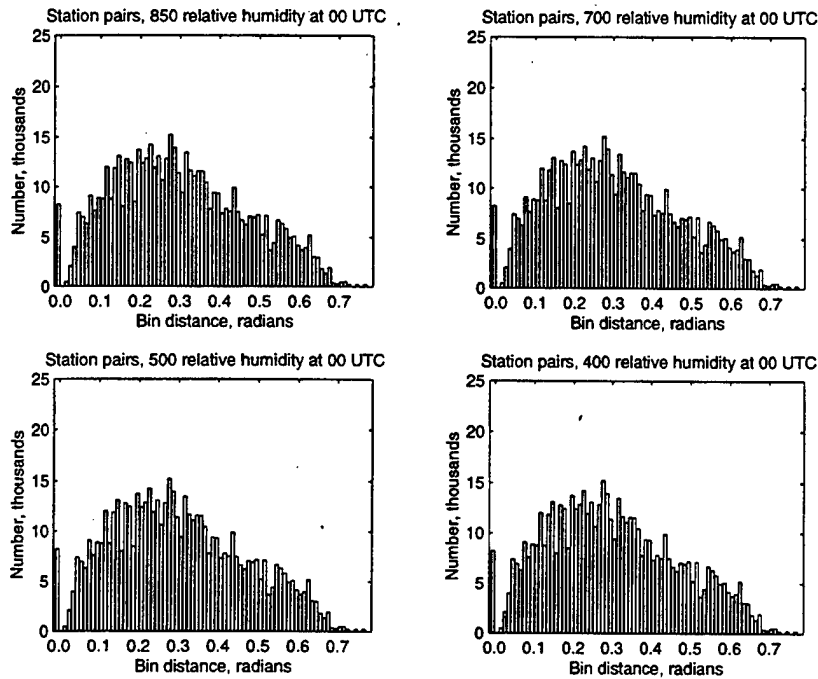


Figure 4: Bar chart showing number of terms in each bin for Figure 3.

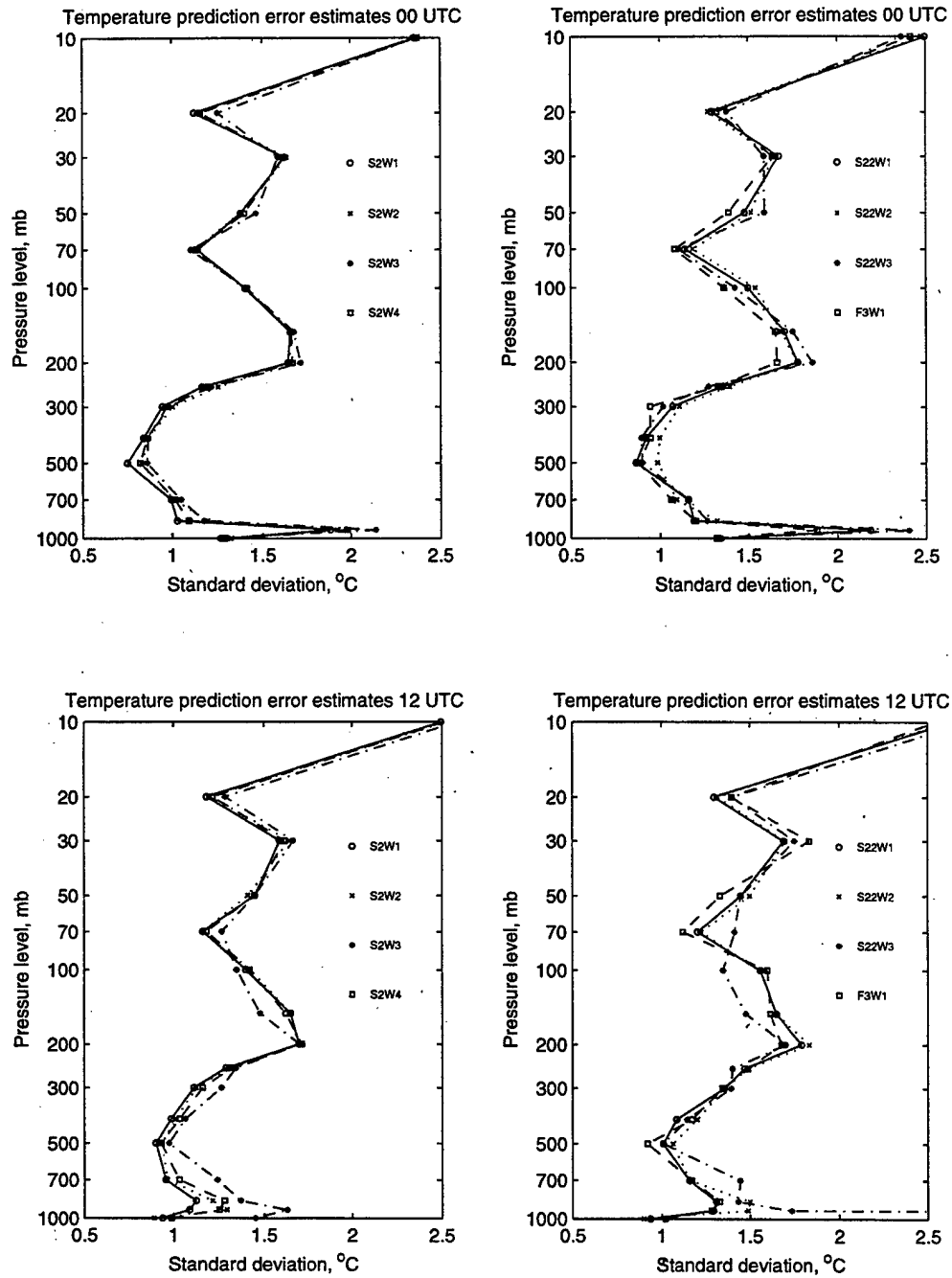


Figure 5: Plots of standard deviations of temperature prediction errors inferred from spatial covariance fits 1-8 in Table 1 for times 00 and 12 UTC.

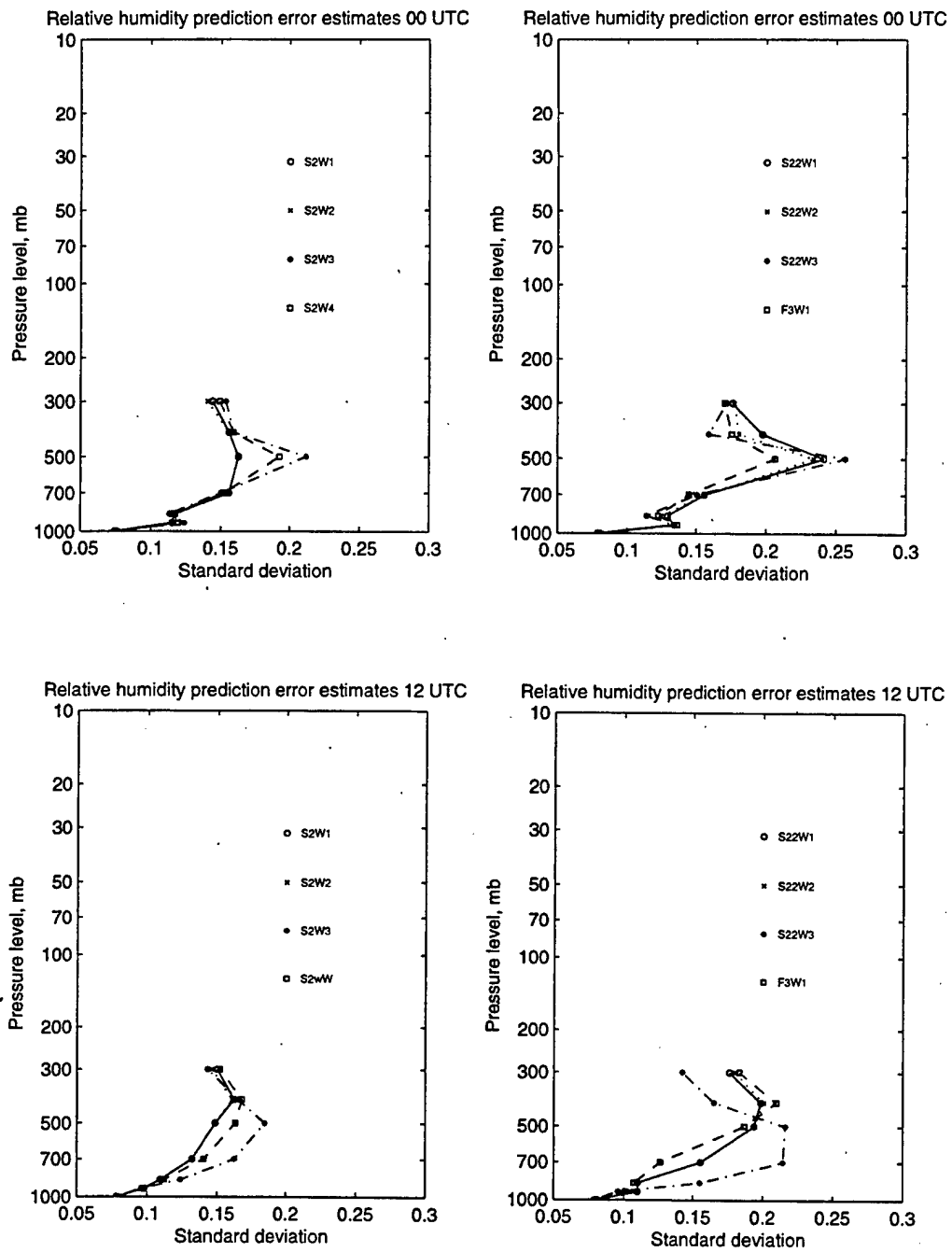


Figure 6: Plots of standard deviations of relative humidity prediction errors inferred from spatial covariance fits 1-8 in Table 1 for times 00 and 12 UTC.

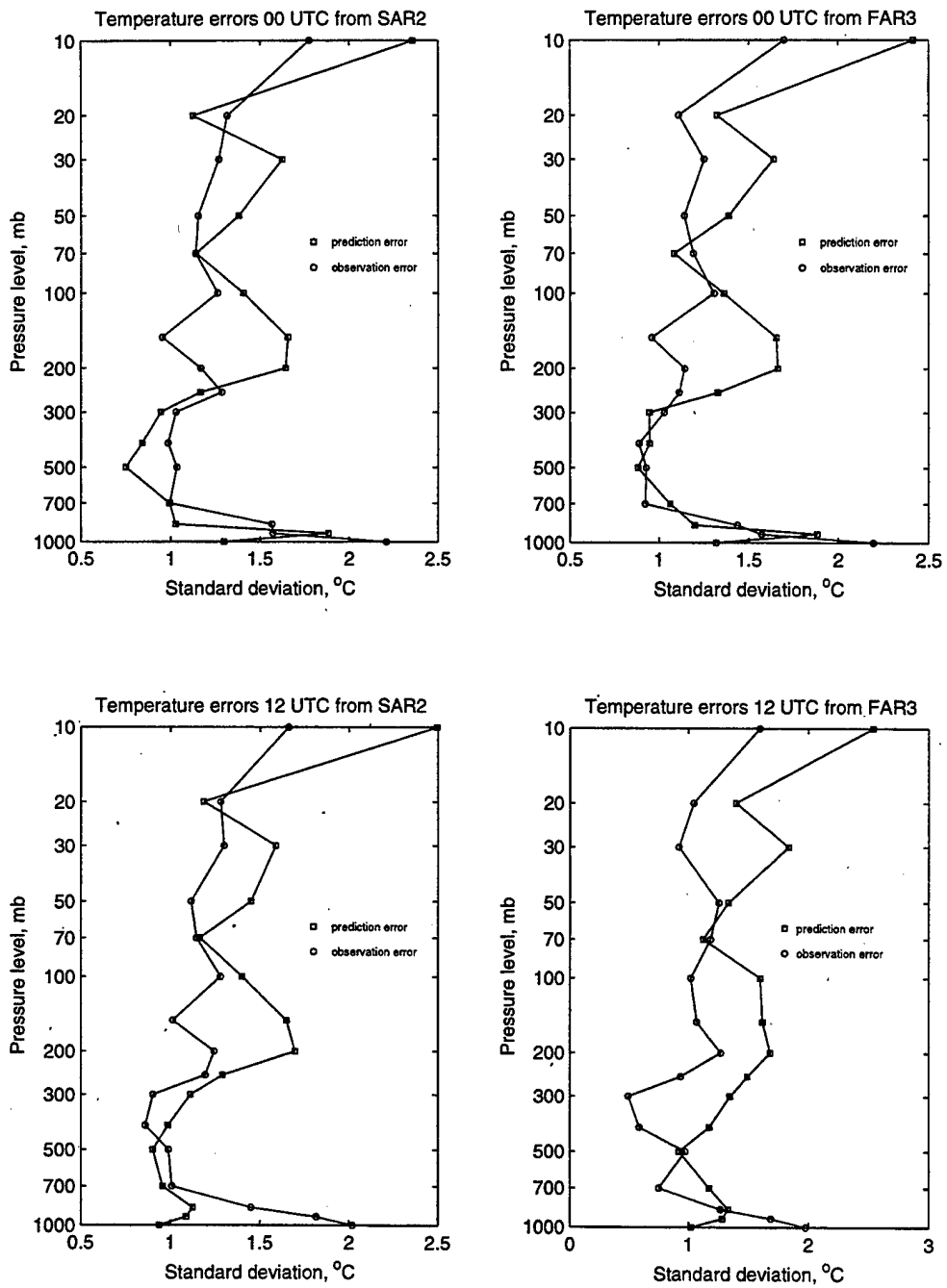


Figure 7: Temperature observation and prediction errors inferred from spatial covariance fits by SAR2 and FAR3 in for times 00 and 12 UTC.

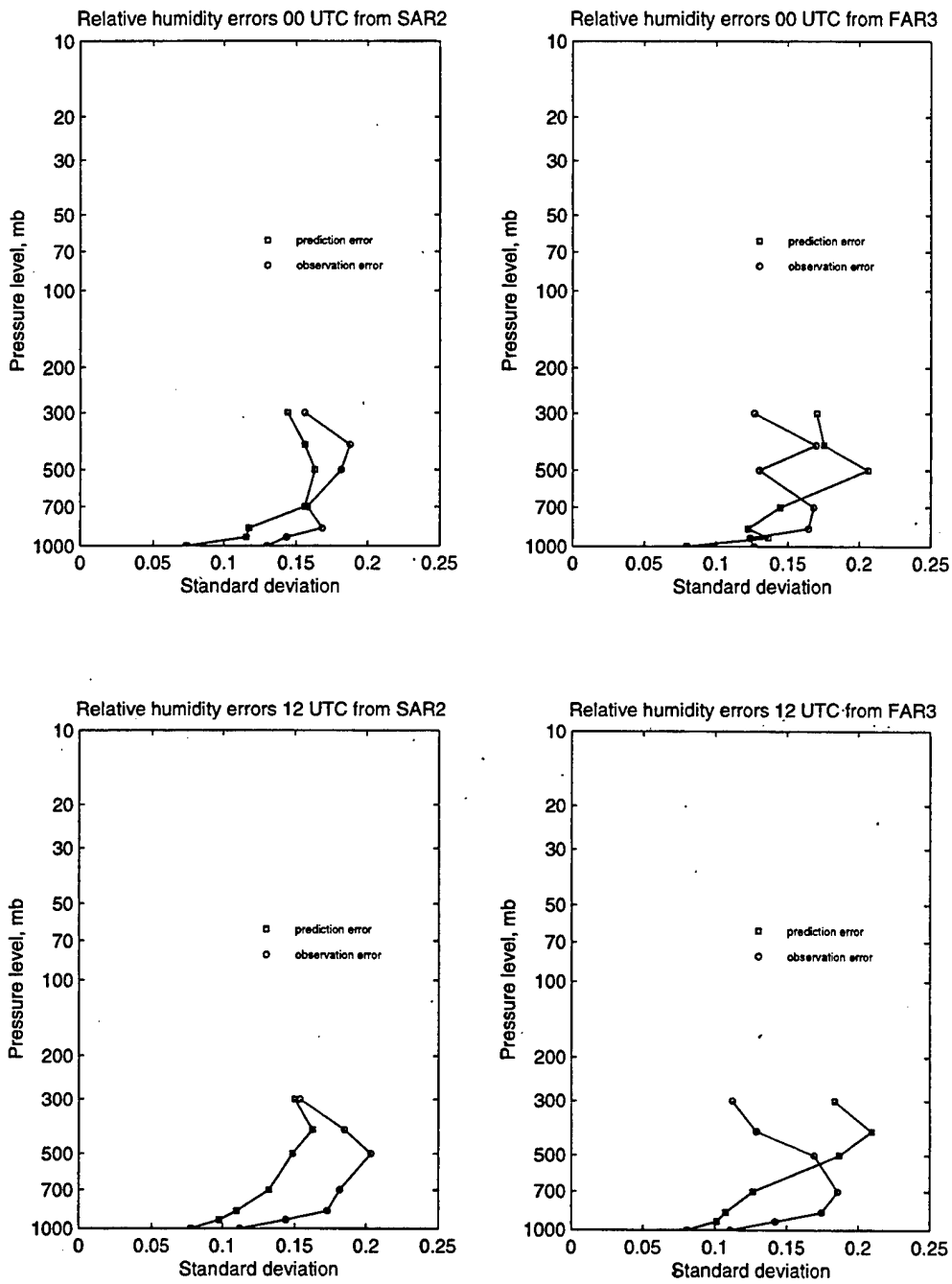


Figure 8: Relative humidity observation and prediction errors inferred from spatial covariance by SAR2 and FAR3 fits for times 00 and 12 UTC.

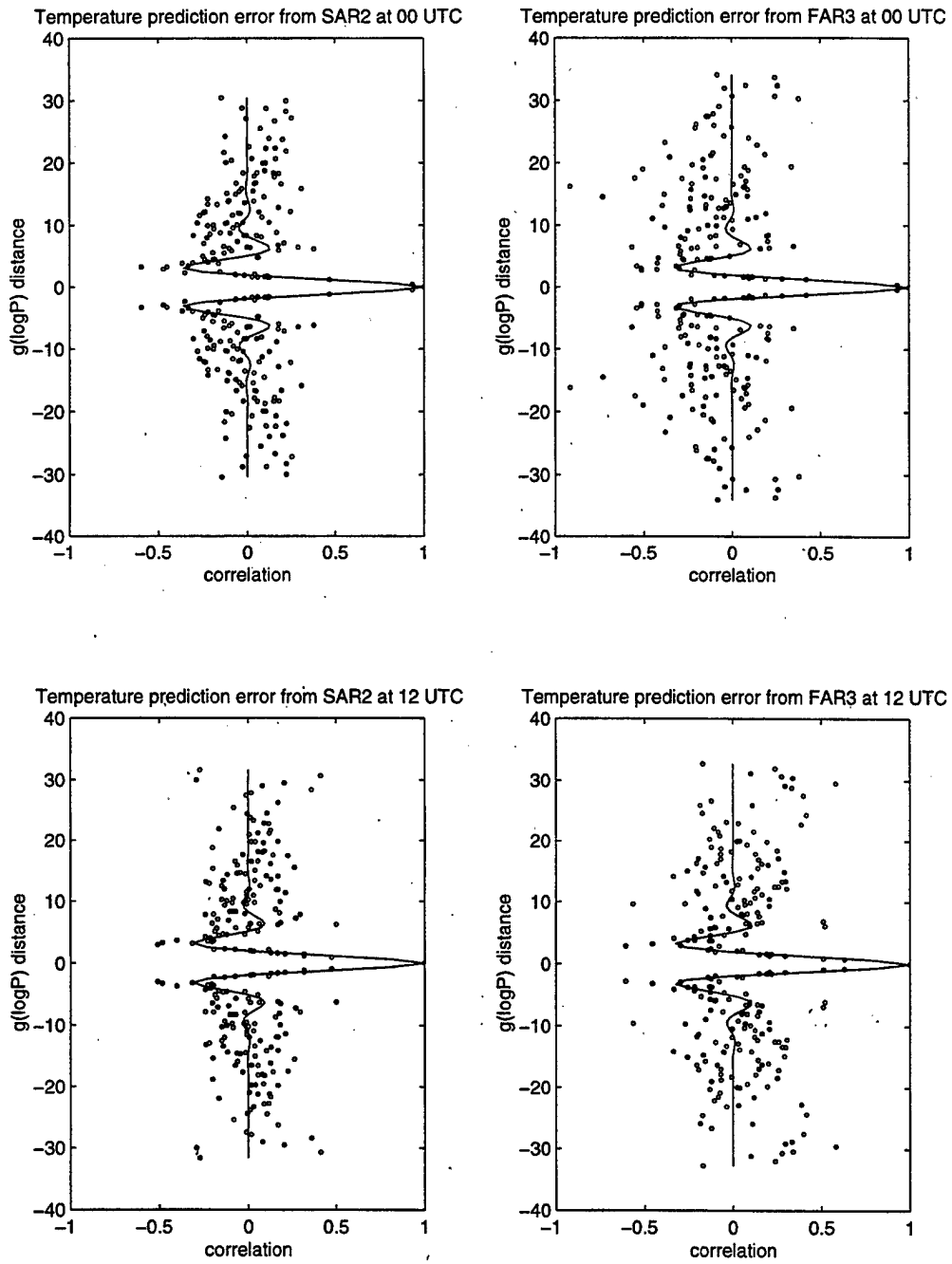


Figure 9: Temperature prediction error correlations in the transformed coordinate system derived from SAR2 and FAR3 fits at 00 and 12 UTC.

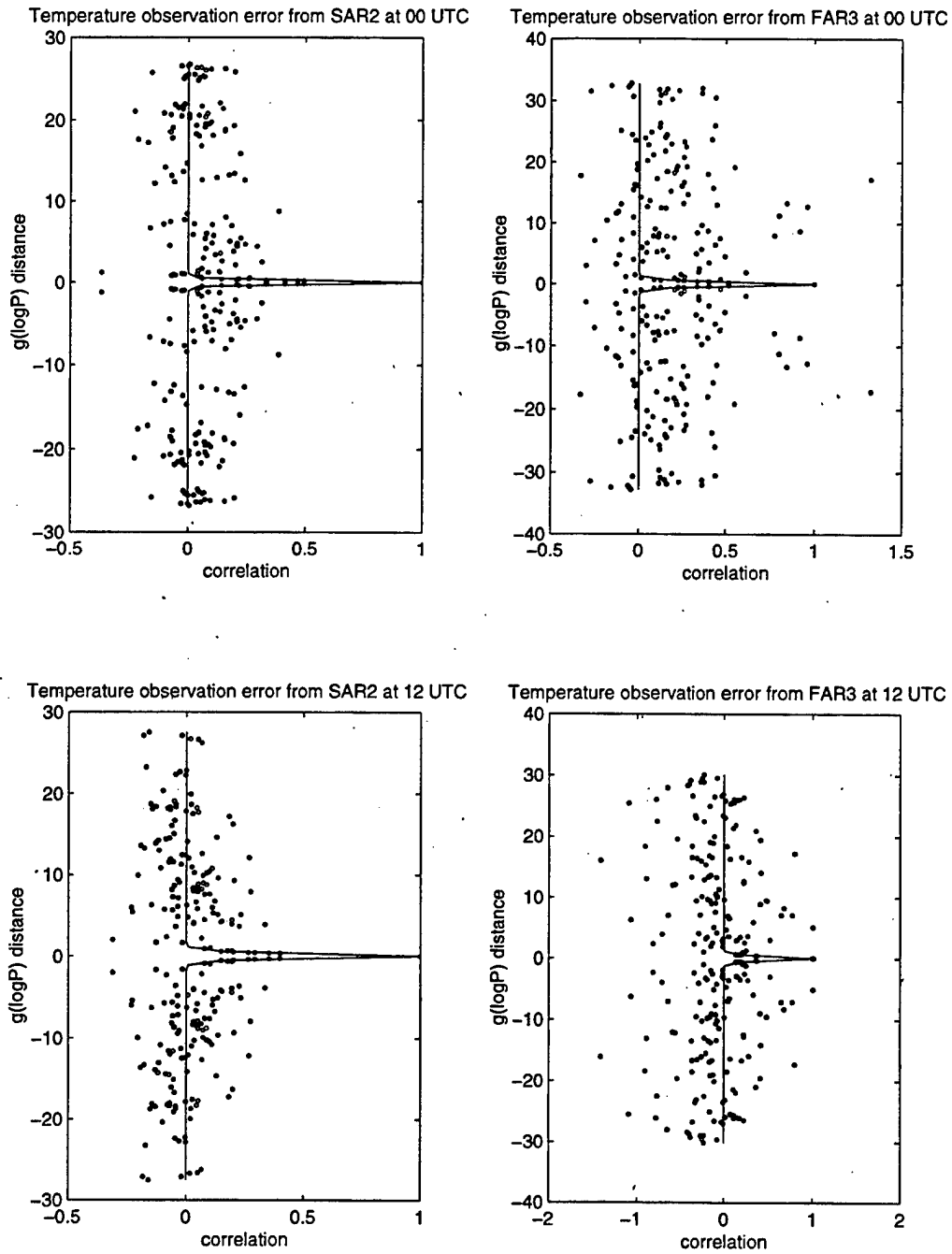


Figure 10: Temperature observation error correlations in the transformed coordinate system derived from SAR2 and FAR3 fits at 00 and 12 UTC.

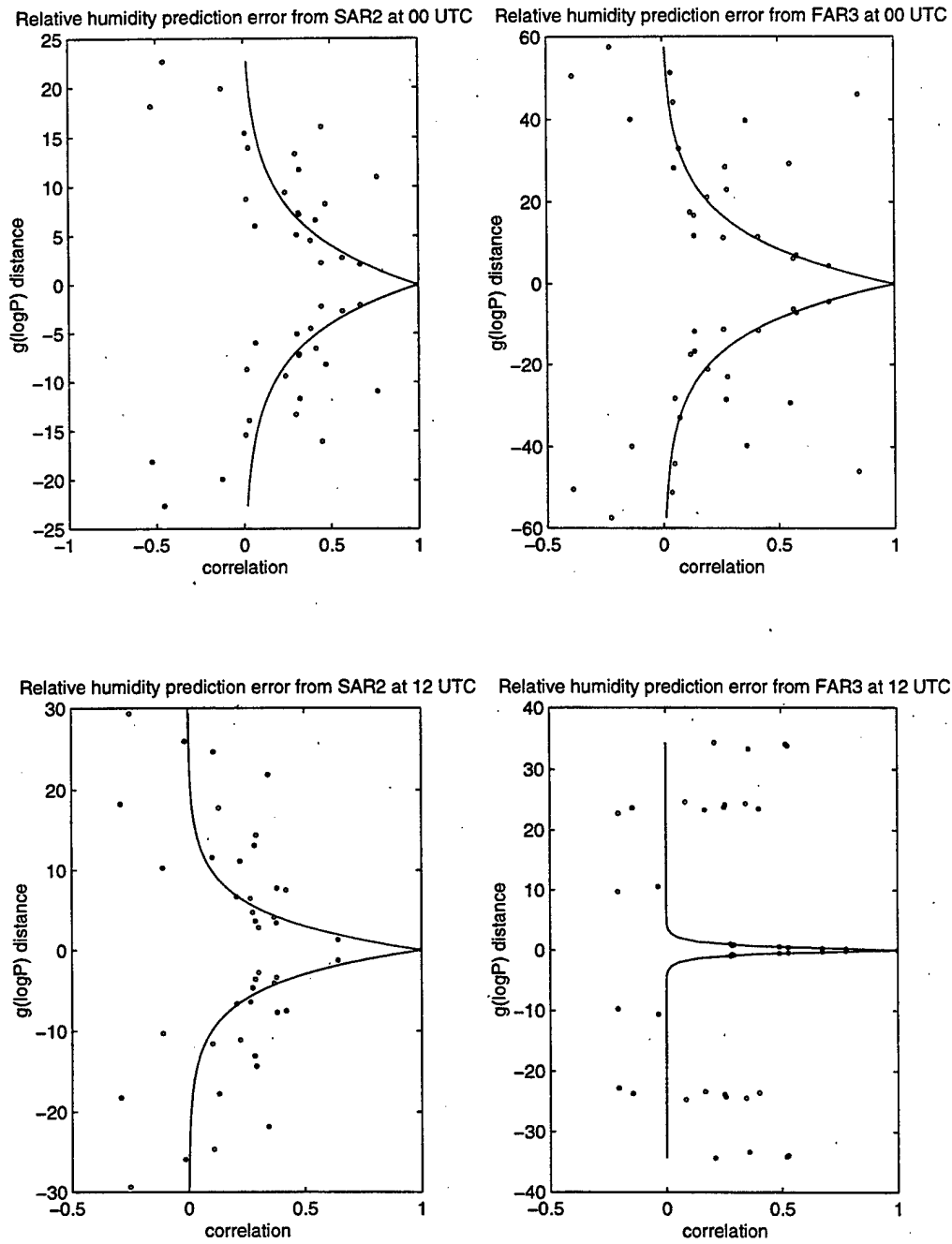
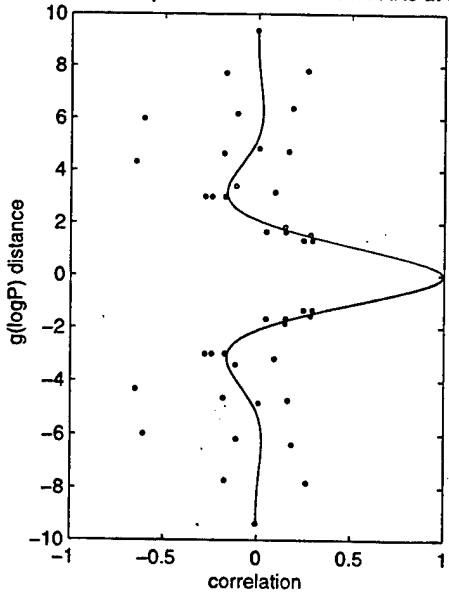
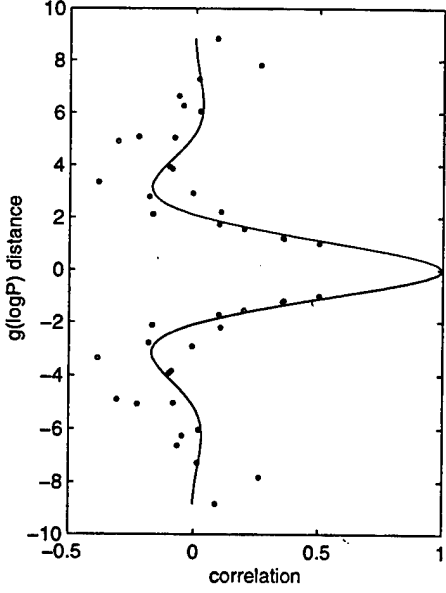


Figure 11: Relative humidity prediction error correlations in the transformed coordinate system derived from SAR2 and FAR3 fits at 00 and 12 UTC.

Relative humidity observation error from SAR2 at 00 UTC Relative humidity observation error from FAR3 at 00 UTC



Relative humidity observation error from SAR2 at 12 UTC Relative humidity observation error from FAR3 at 12 UTC

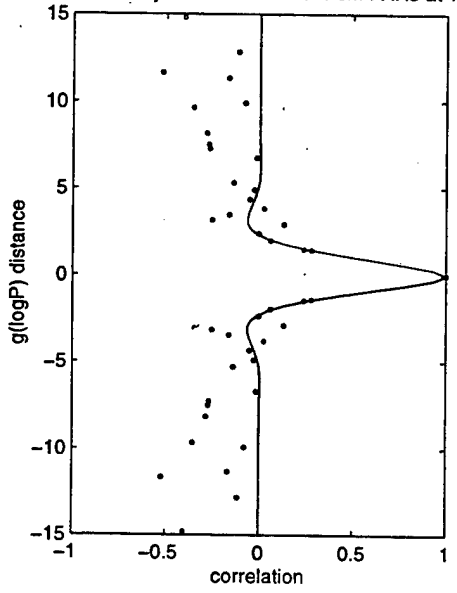
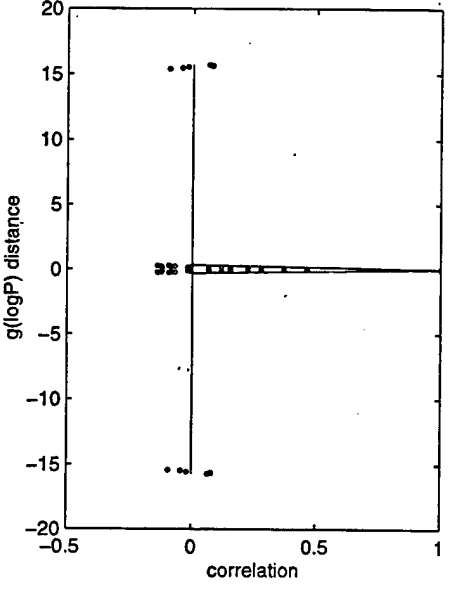


Figure 12: Relative humidity observation error correlations in the transformed coordinate system derived from SAR2 and FAR3 fits at 00 and 12 UTC.

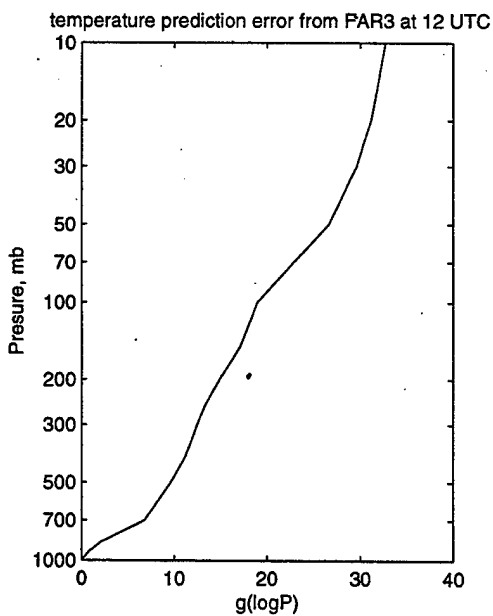
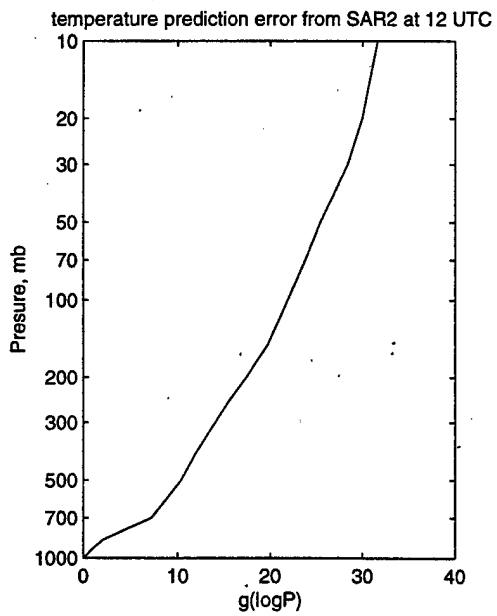
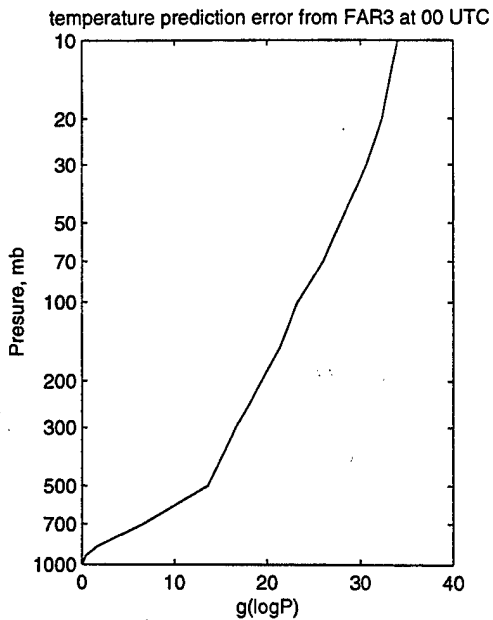
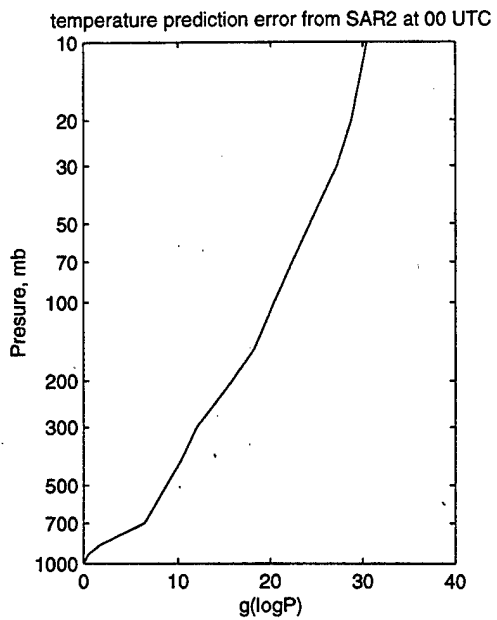


Figure 13: Transformation for Figure 9.

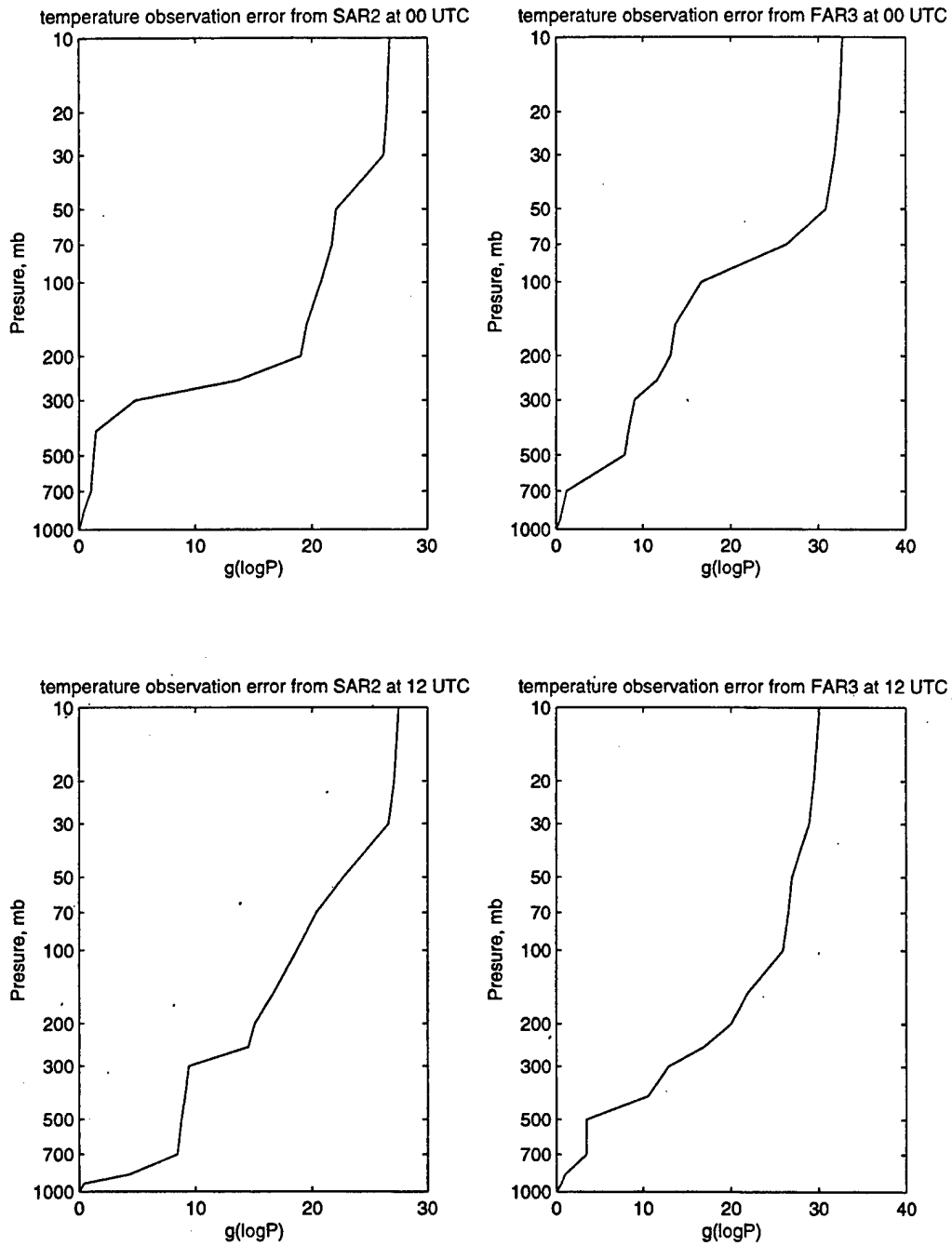


Figure 14: Transformation for Figure 10.

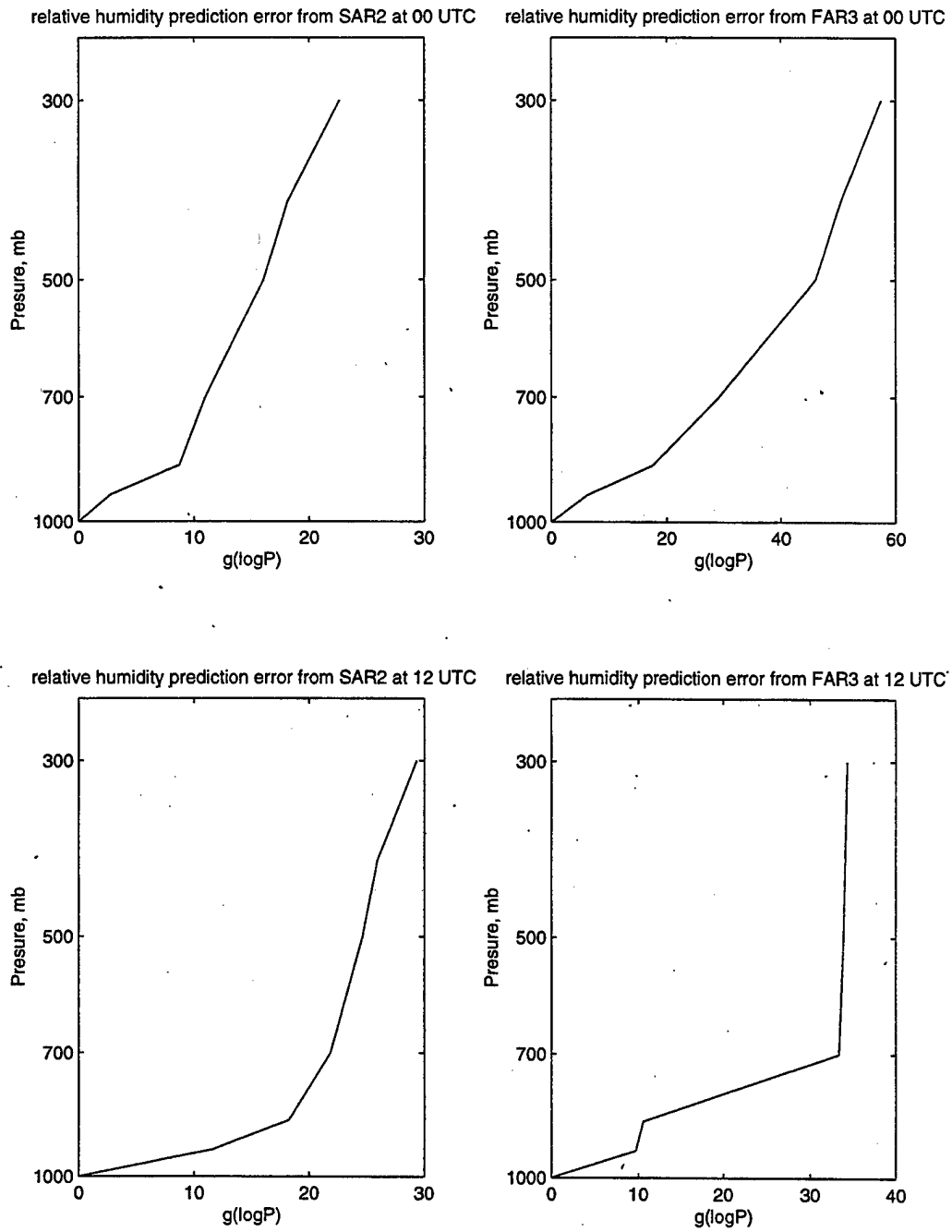


Figure 15: Transformation for Figure 11.

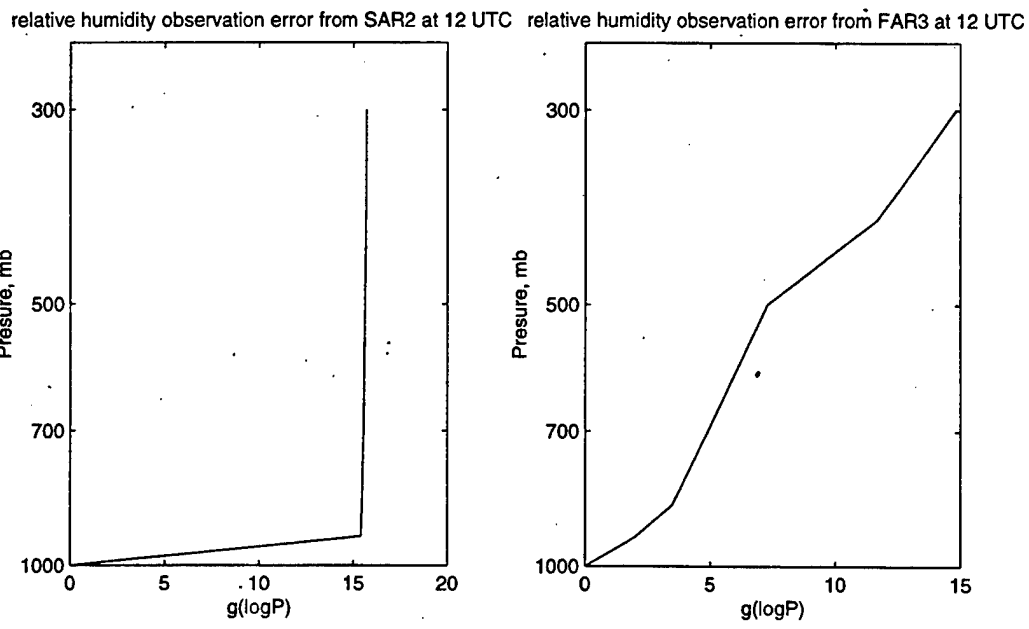
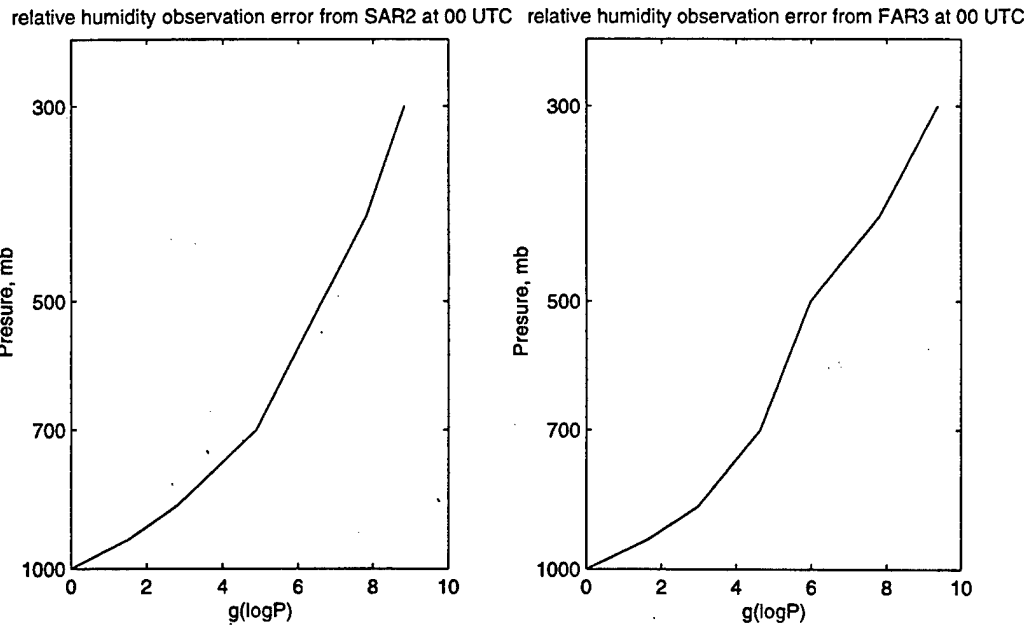


Figure 16: Transformation for Figure 12.

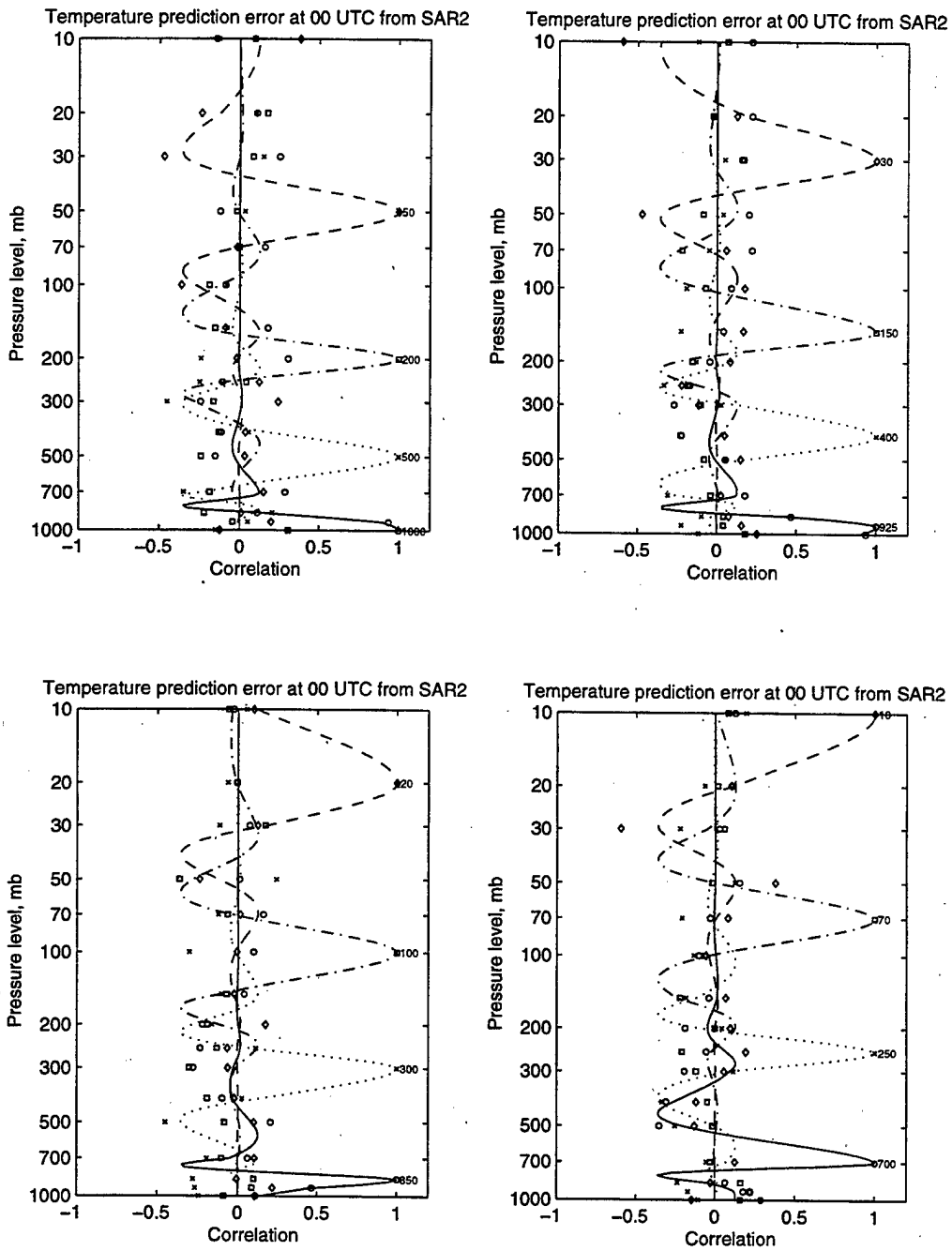


Figure 17: Vertical correlation of temperature prediction errors at time 00 UTC inferred from SAR2. The curves obtained by fitting and transformation of coordinates showing the correlation between errors at the indicated level and other levels are shown.

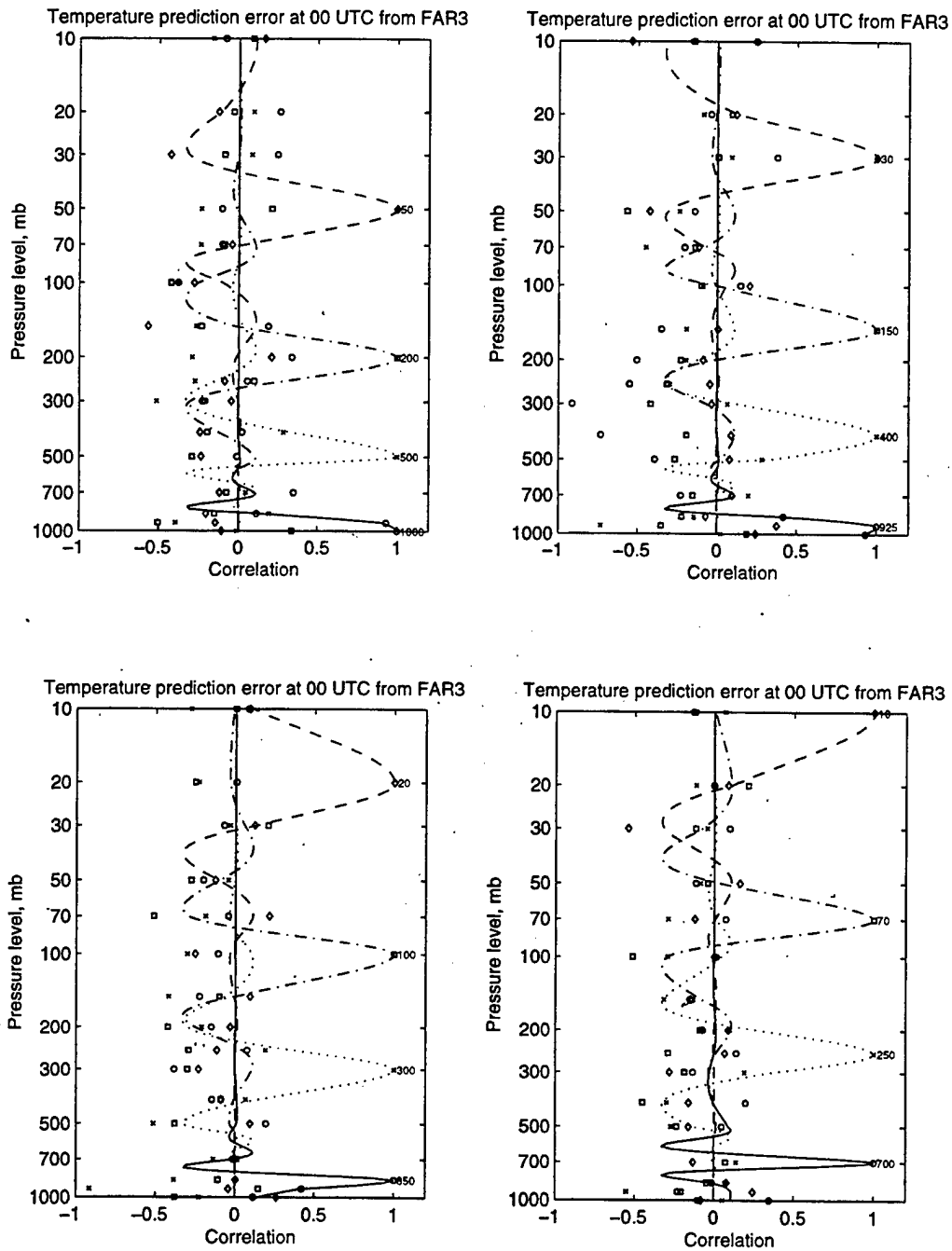


Figure 18: Vertical correlation of temperature prediction errors at time 00 UTC inferred from FAR3. The curves obtained by fitting and transformation of coordinates showing the correlation between errors at the indicated level and other levels are shown.

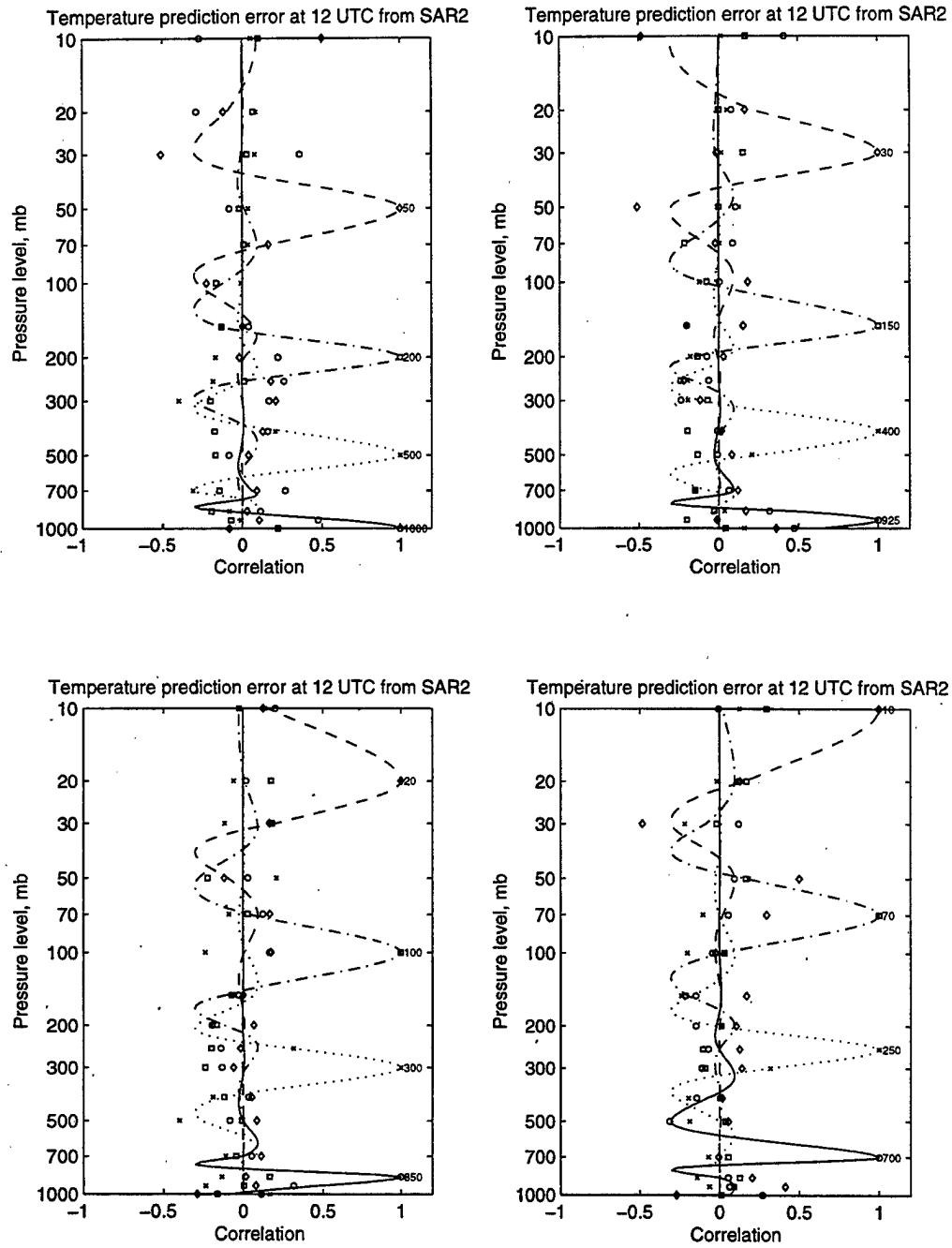


Figure 19: Vertical correlation of temperature prediction errors at time 12 UTC inferred from SAR2. The curves obtained by fitting and transformation of coordinates showing the correlation between errors at the indicated level and other levels are shown.

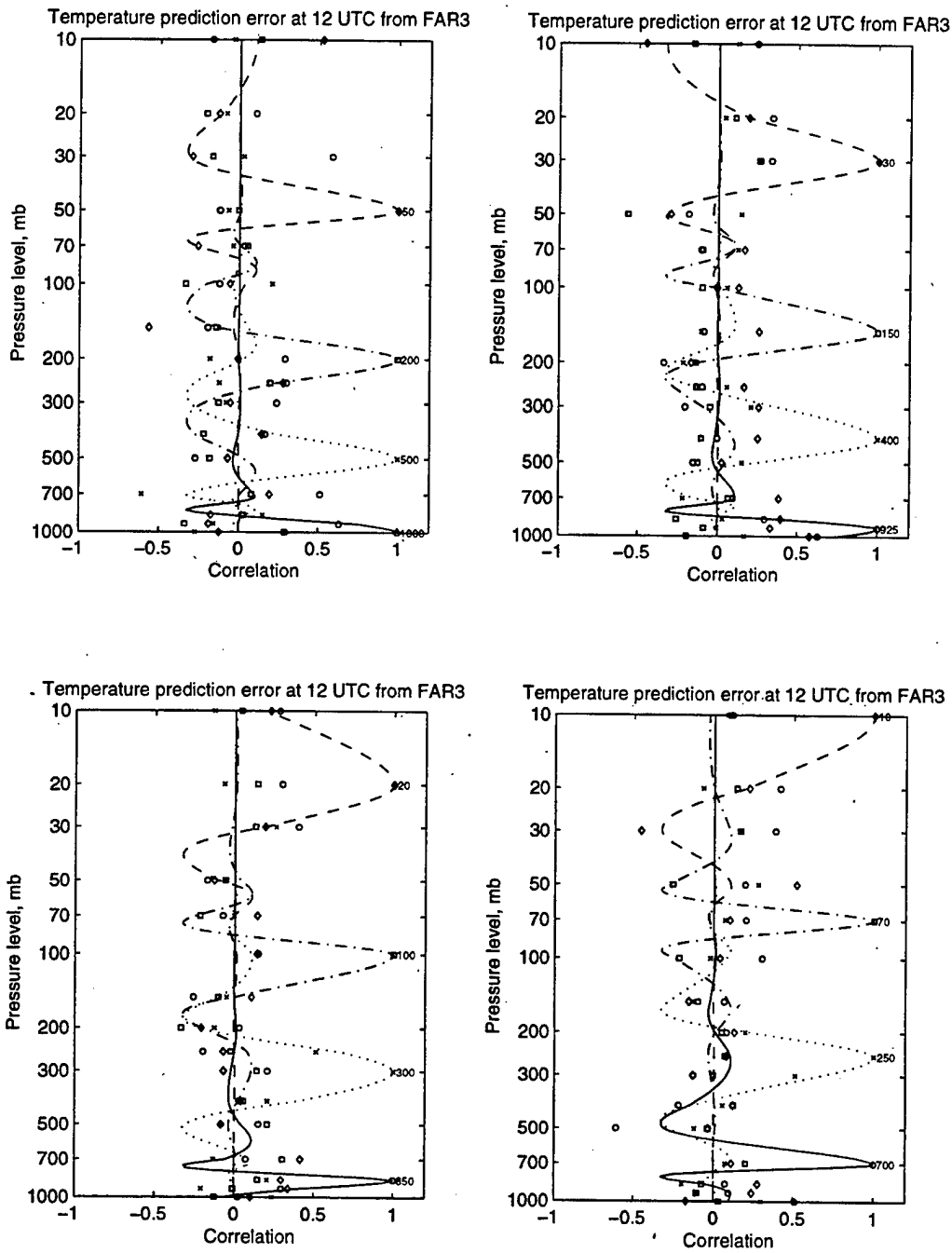


Figure 20: Vertical correlation of temperature prediction errors at time 12 UTC inferred from FAR3. The curves obtained by fitting and transformation of coordinates showing the correlation between errors at the indicated level and other levels are shown.

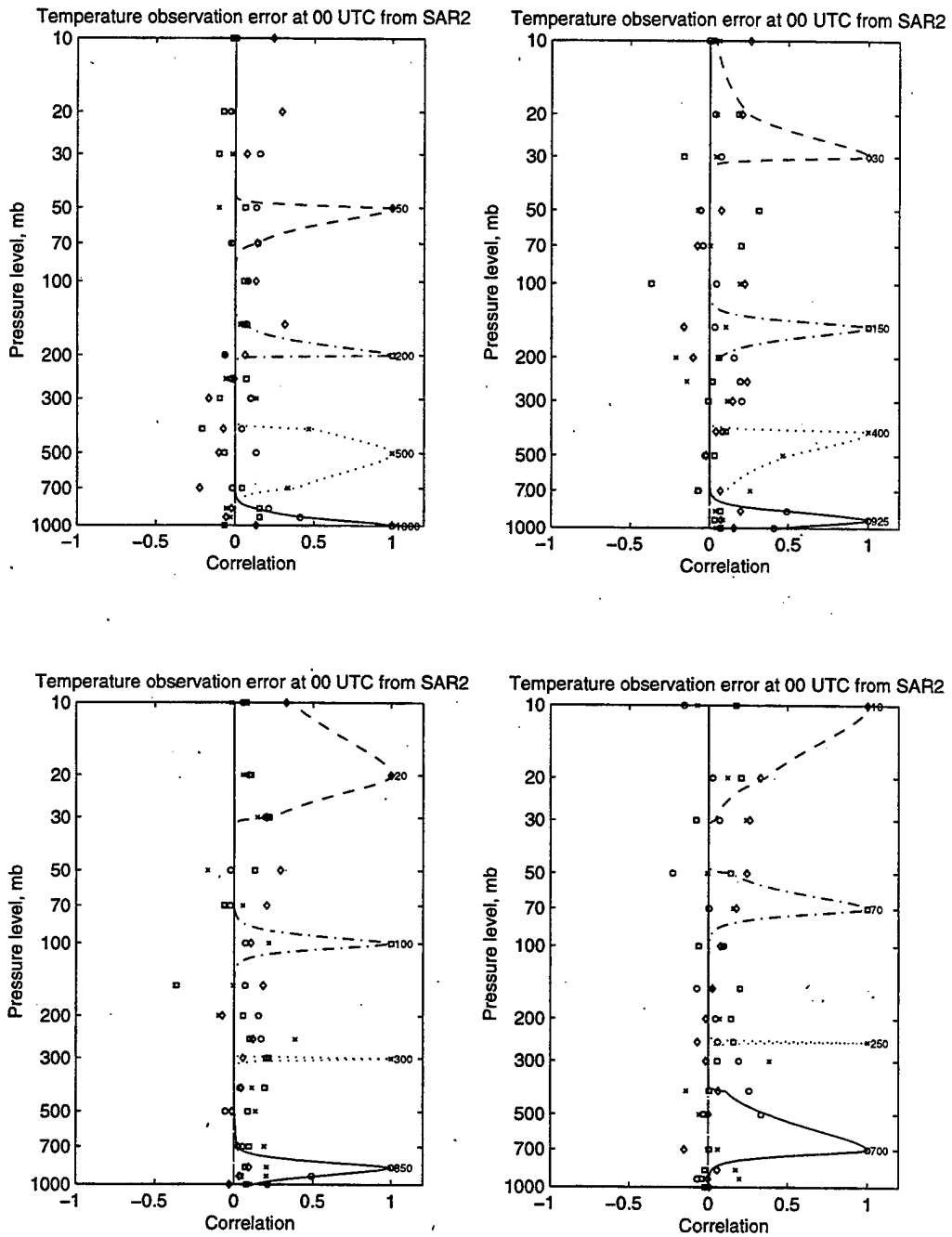


Figure 21: Vertical correlation of temperature observation errors at time 00 UTC inferred from SAR2. The curves obtained by fitting and transformation of coordinates showing the correlation between errors at the indicated level and other levels are shown.

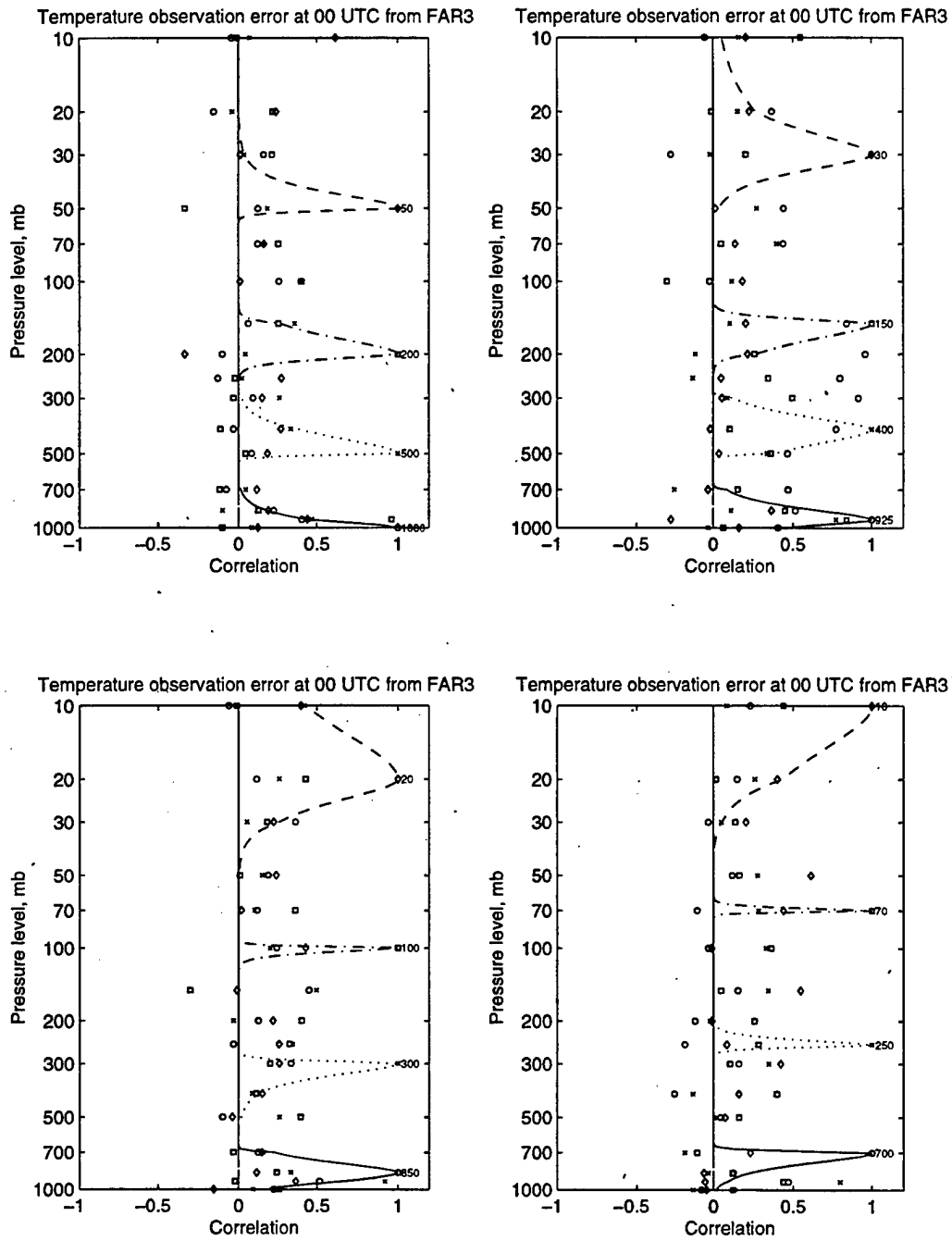


Figure 22: Vertical correlation of temperature observation errors at time 00 UTC inferred from FAR3. The curves obtained by fitting and transformation of coordinates showing the correlation between errors at the indicated level and other levels are shown.

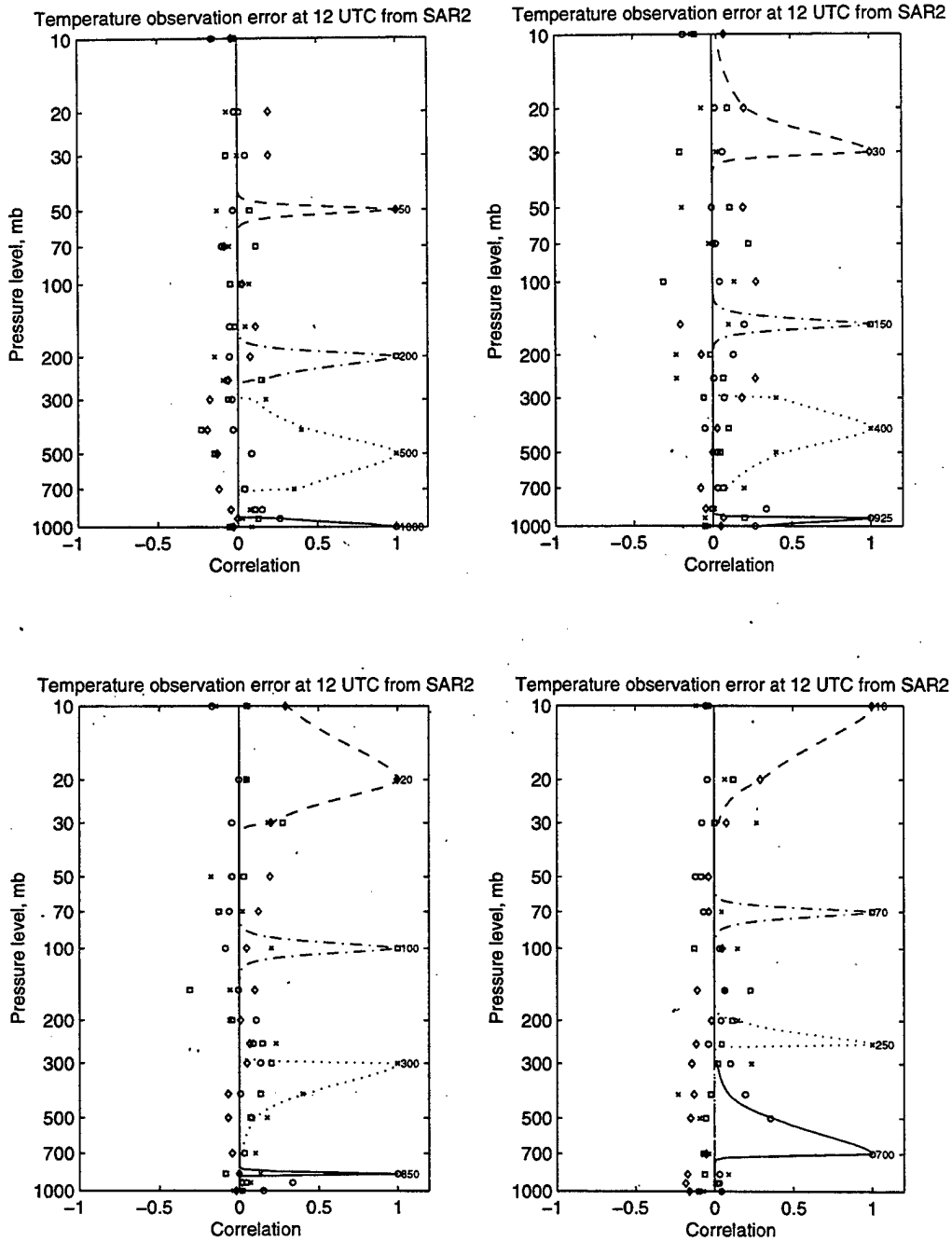


Figure 23: Vertical correlation of temperature observation errors at time 12 UTC inferred from SAR2. The curves obtained by fitting and transformation of coordinates showing the correlation between errors at the indicated level and other levels are shown.

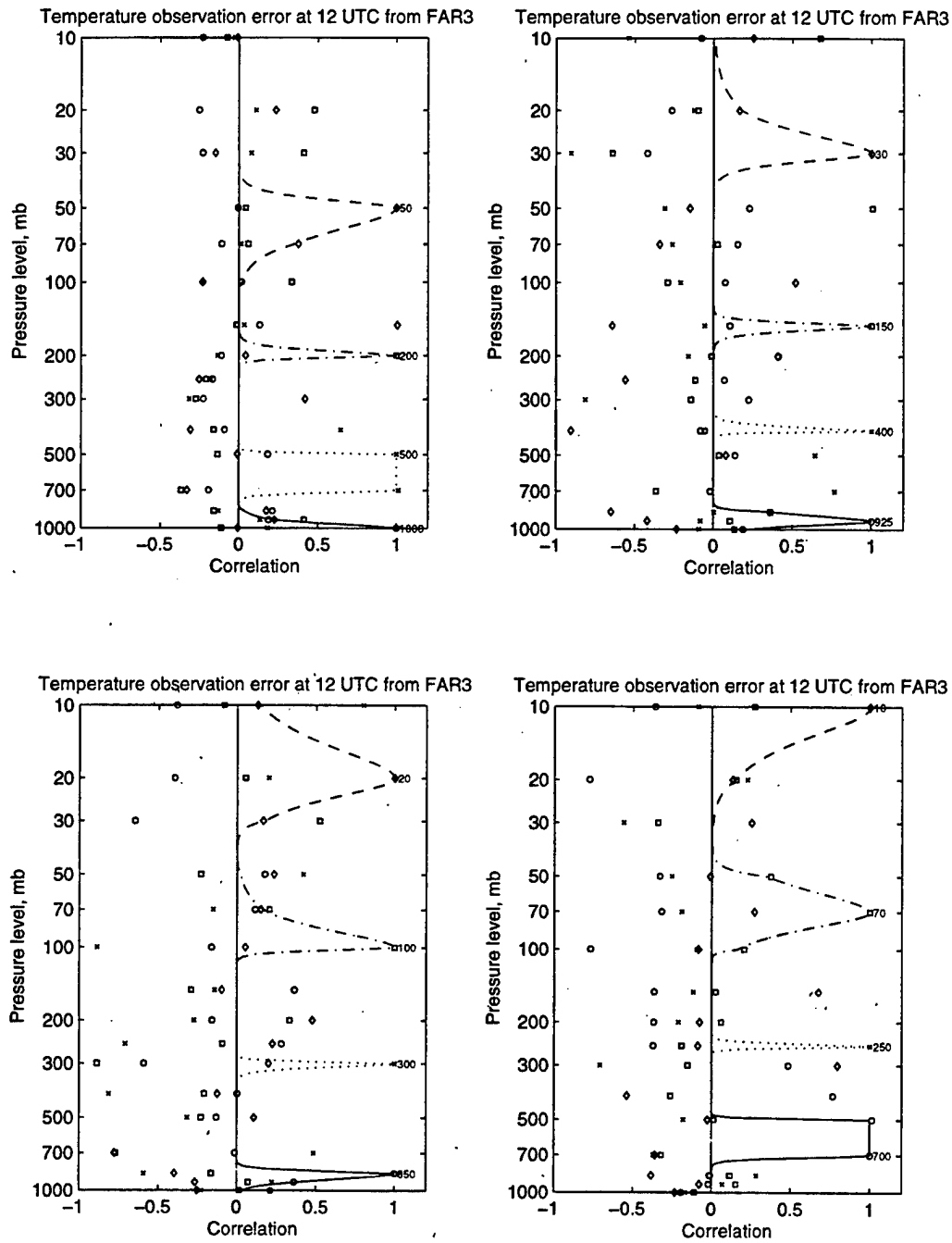


Figure 24: Vertical correlation of temperature observation errors at time 12 UTC inferred from FAR3. The curves obtained by fitting and transformation of coordinates showing the correlation between errors at the indicated level and other levels are shown.

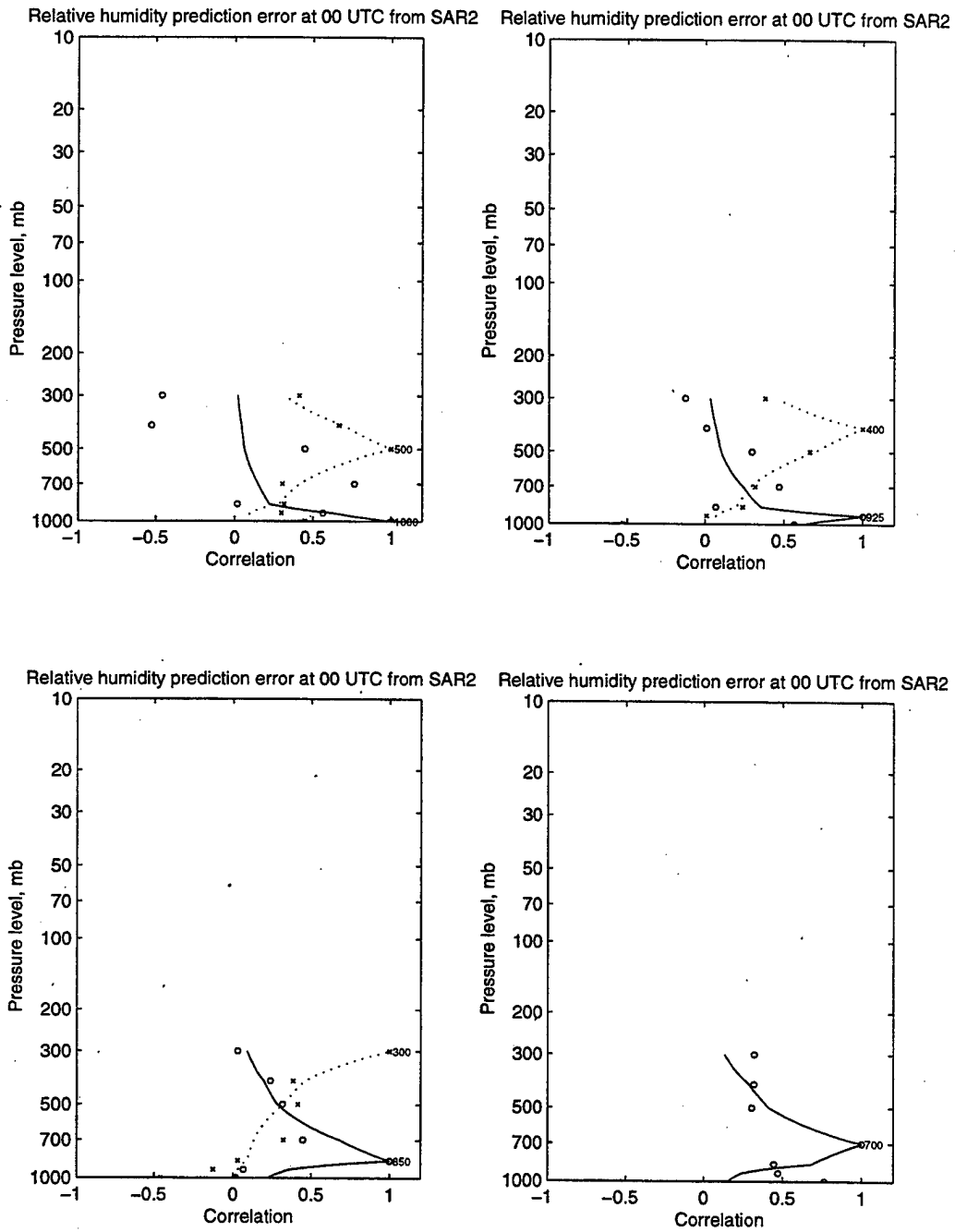


Figure 25: Vertical correlation of relative humidity prediction errors at time 00 UTC inferred from SAR2. The curves obtained by fitting and transformation of coordinates showing the correlation between errors at the indicated level and other levels are shown.

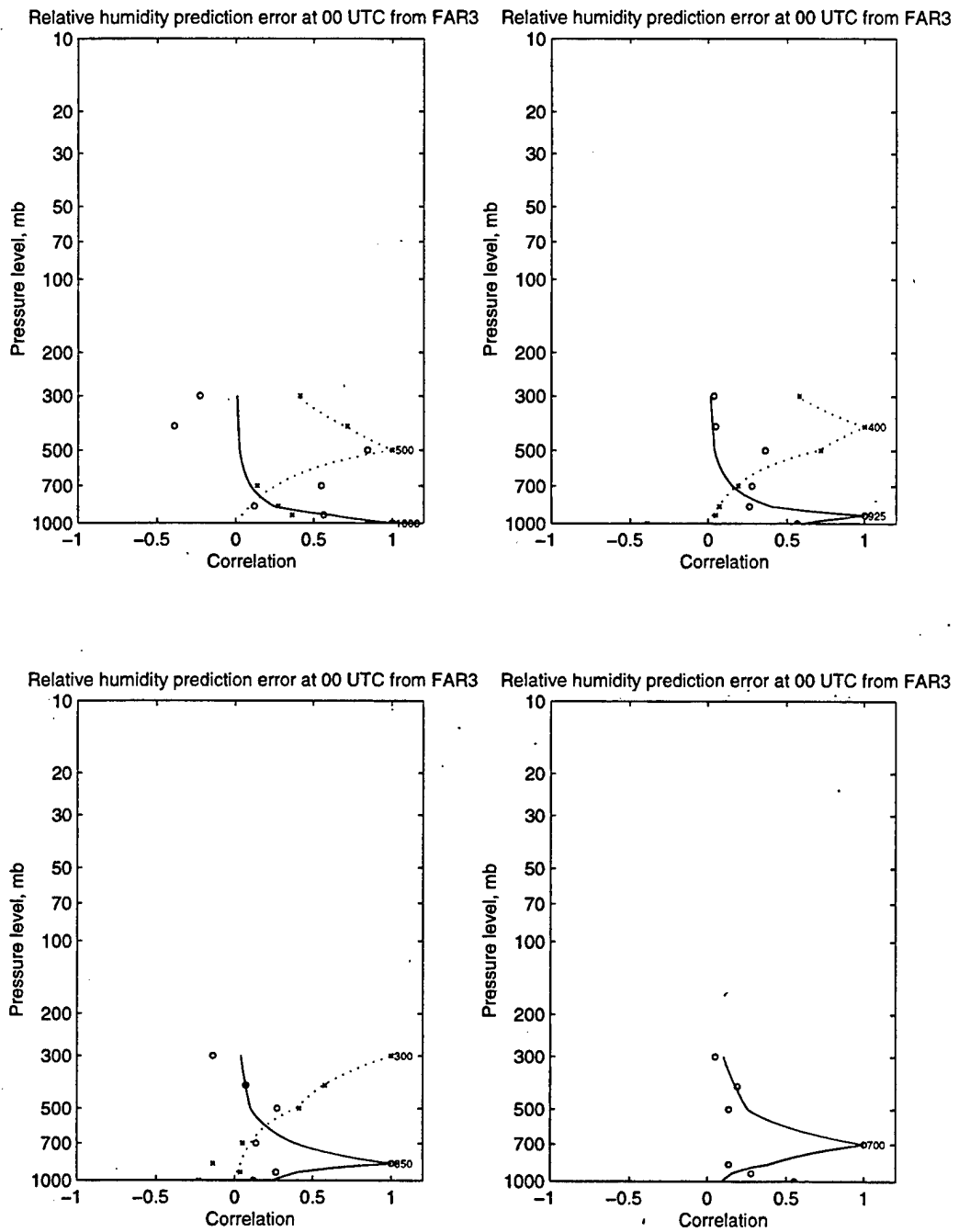


Figure 26: Vertical correlation of relative humidity prediction errors at time 00 UTC inferred from FAR3. The curves obtained by fitting and transformation of coordinates showing the correlation between errors at the indicated level and other levels are shown.

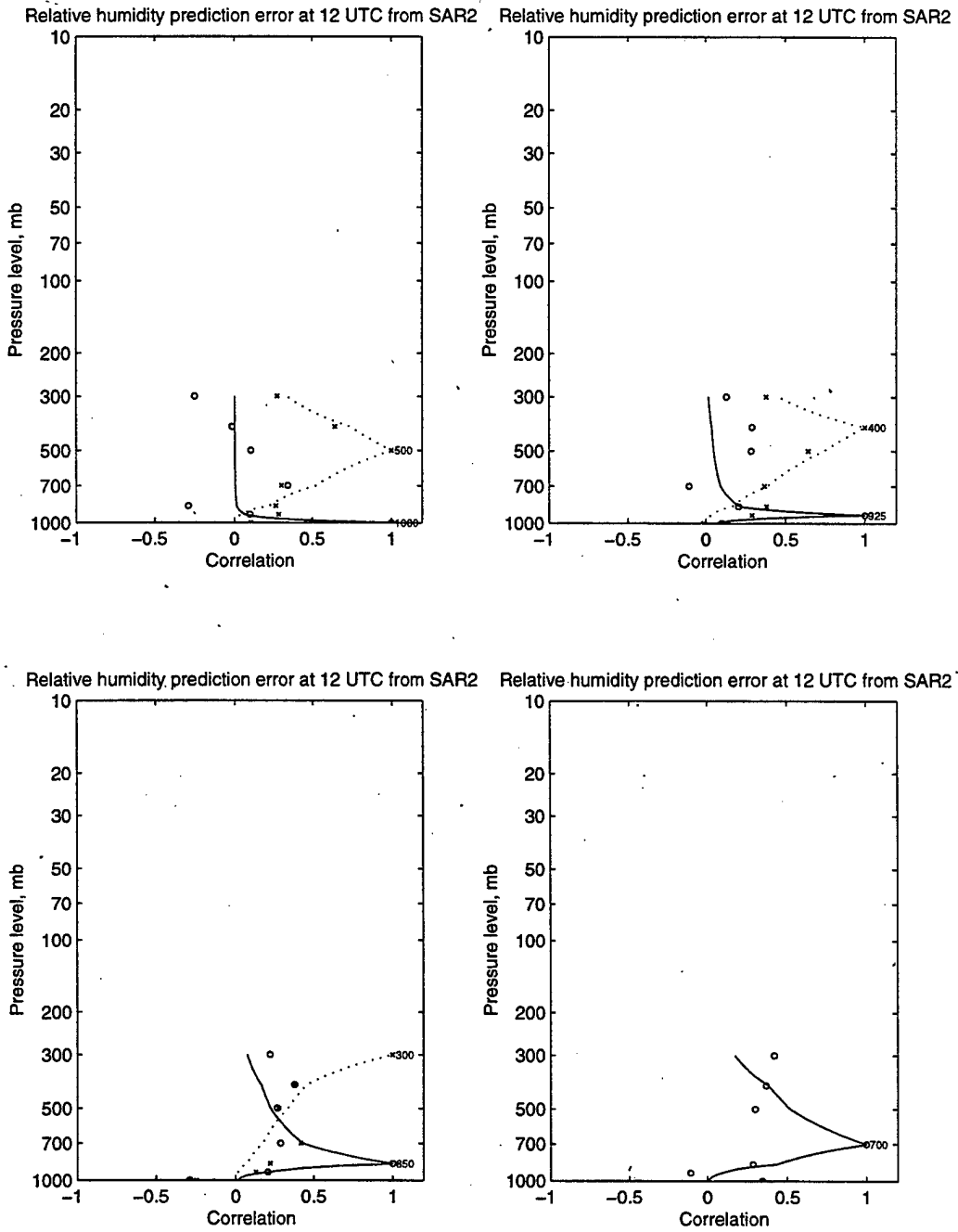


Figure 27: Vertical correlation of relative humidity prediction errors at time 12 UTC inferred from SAR2. The curves obtained by fitting and transformation of coordinates showing the correlation between errors at the indicated level and other levels are shown.

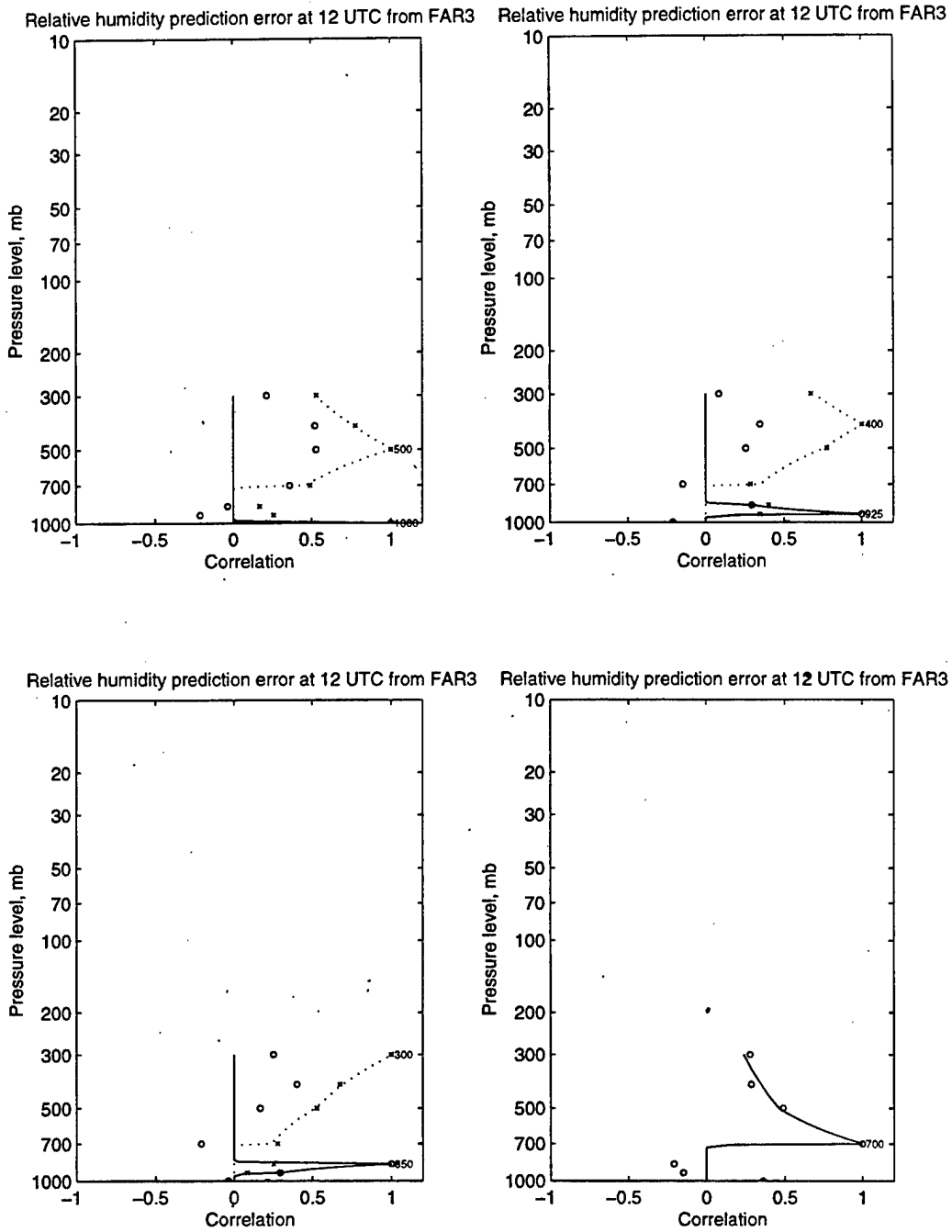


Figure 28: Vertical correlation of relative humidity prediction errors at time 12 UTC inferred from FAR3. The curves obtained by fitting and transformation of coordinates showing the correlation between errors at the indicated level and other levels are shown.

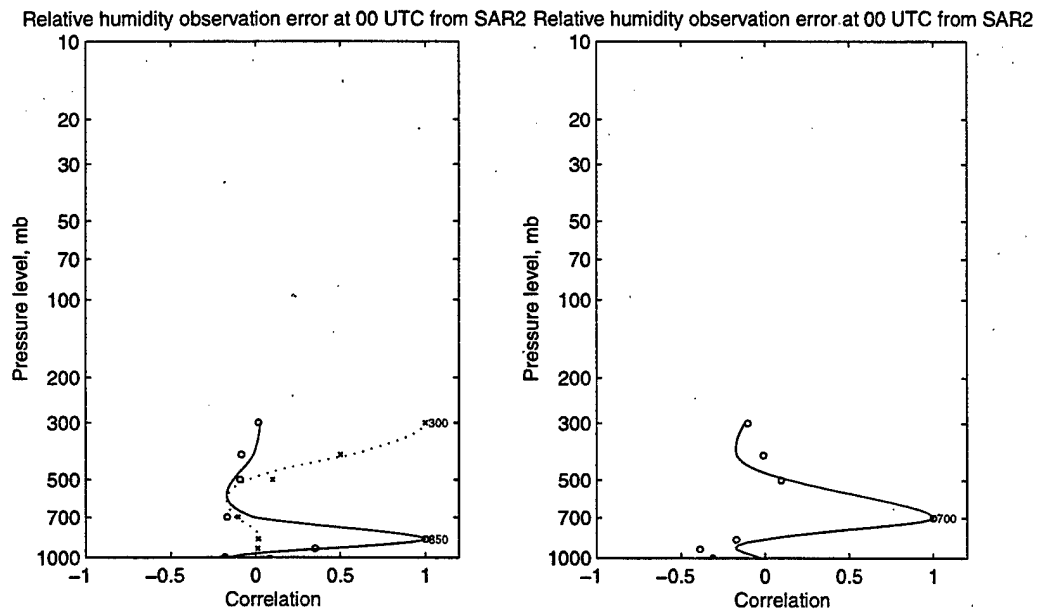
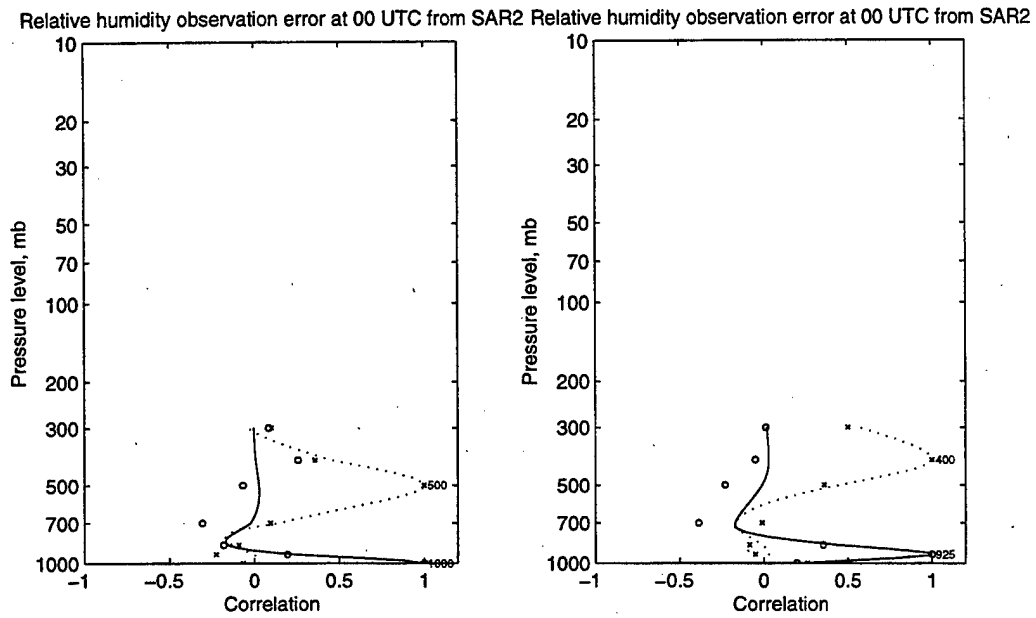


Figure 29: Vertical correlation of relative humidity observation errors at time 00 UTC inferred from SAR2. The curves obtained by fitting and transformation of coordinates showing the correlation between errors at the indicated level and other levels are shown.

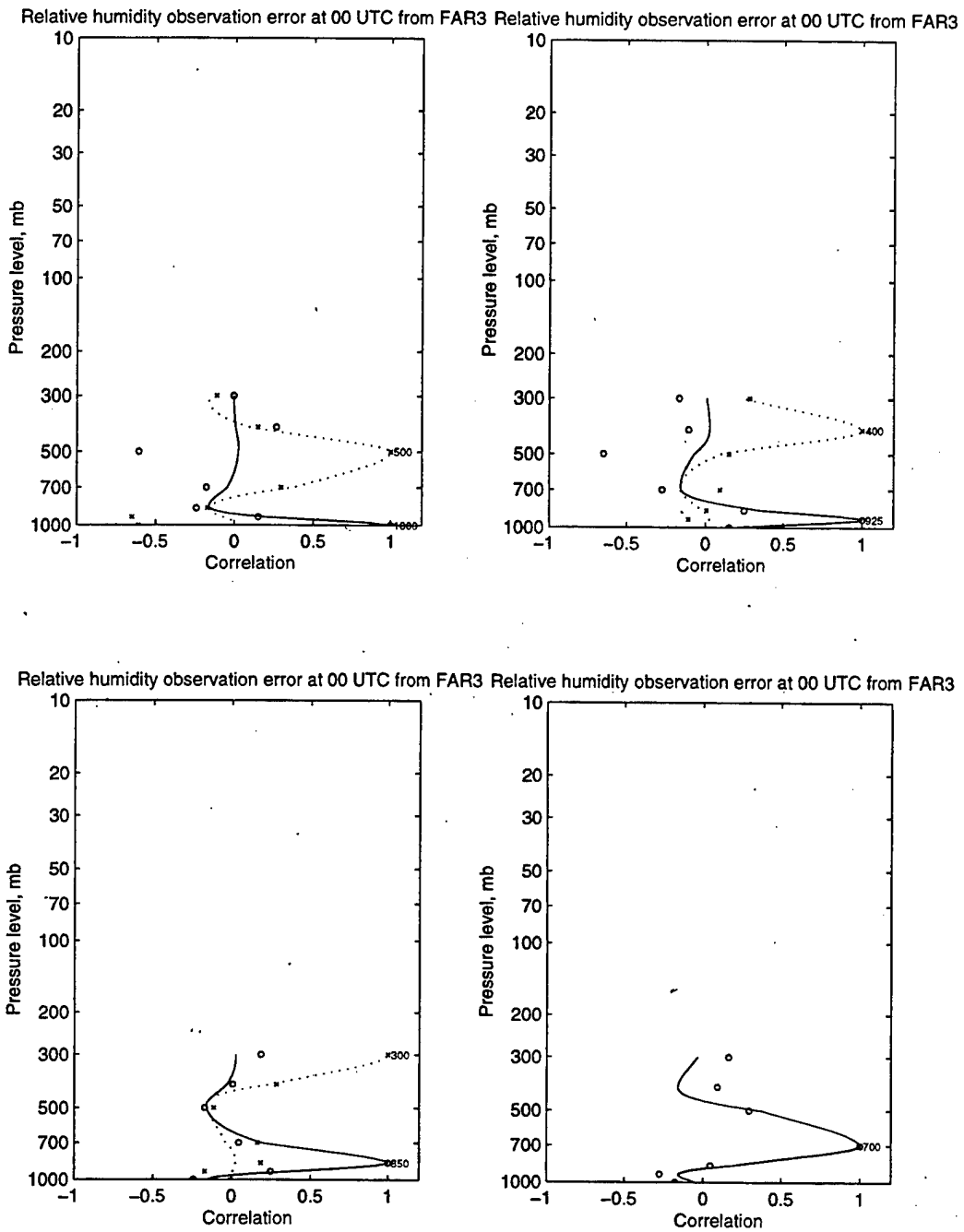


Figure 30: Vertical correlation of relative humidity observation errors at time 00 UTC inferred from FAR3. The curves obtained by fitting and transformation of coordinates showing the correlation between errors at the indicated level and other levels are shown.

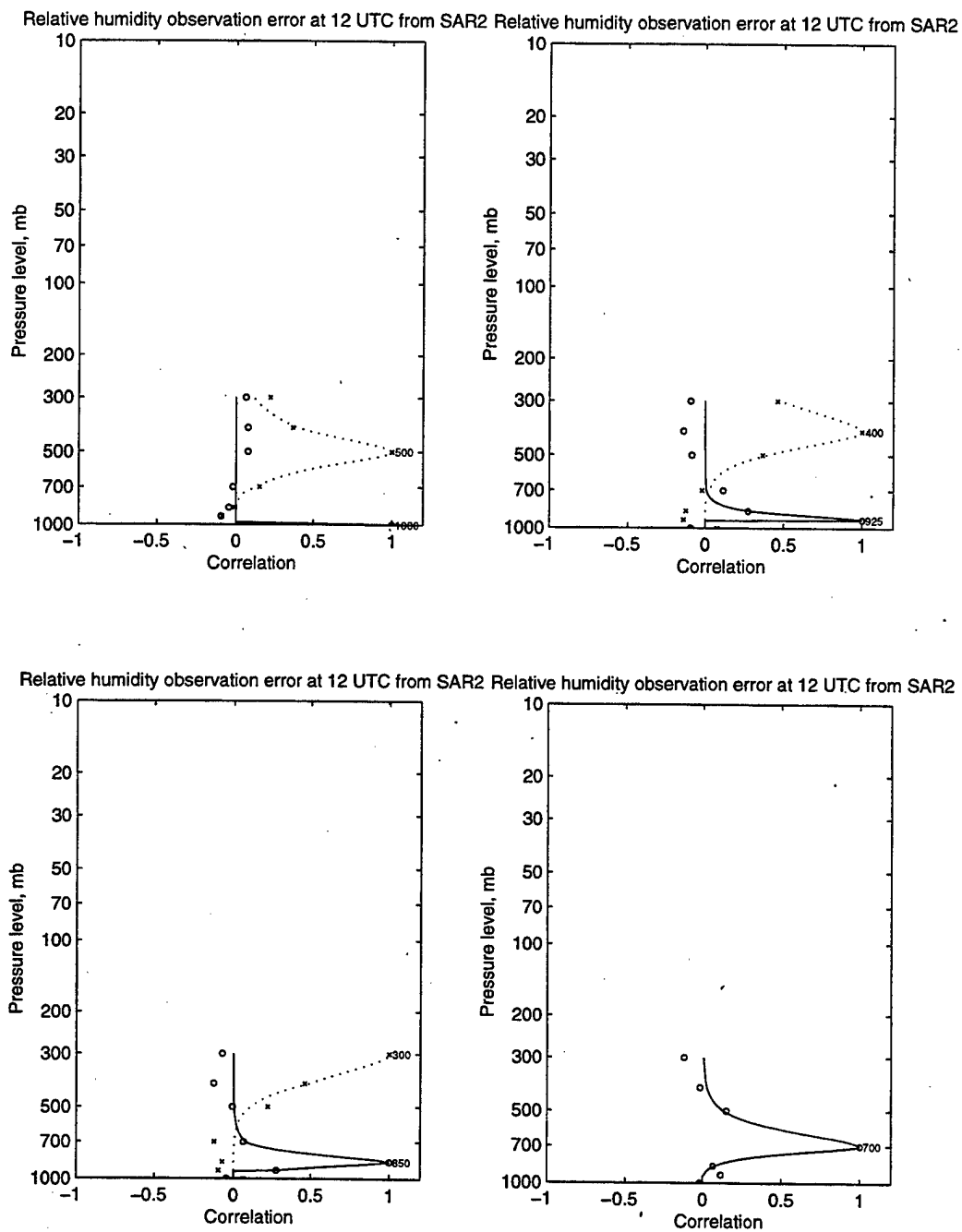


Figure 31: Vertical correlation of relative humidity observation errors at time 12 UTC inferred from SAR2. The curves obtained by fitting and transformation of coordinates showing the correlation between errors at the indicated level and other levels are shown.

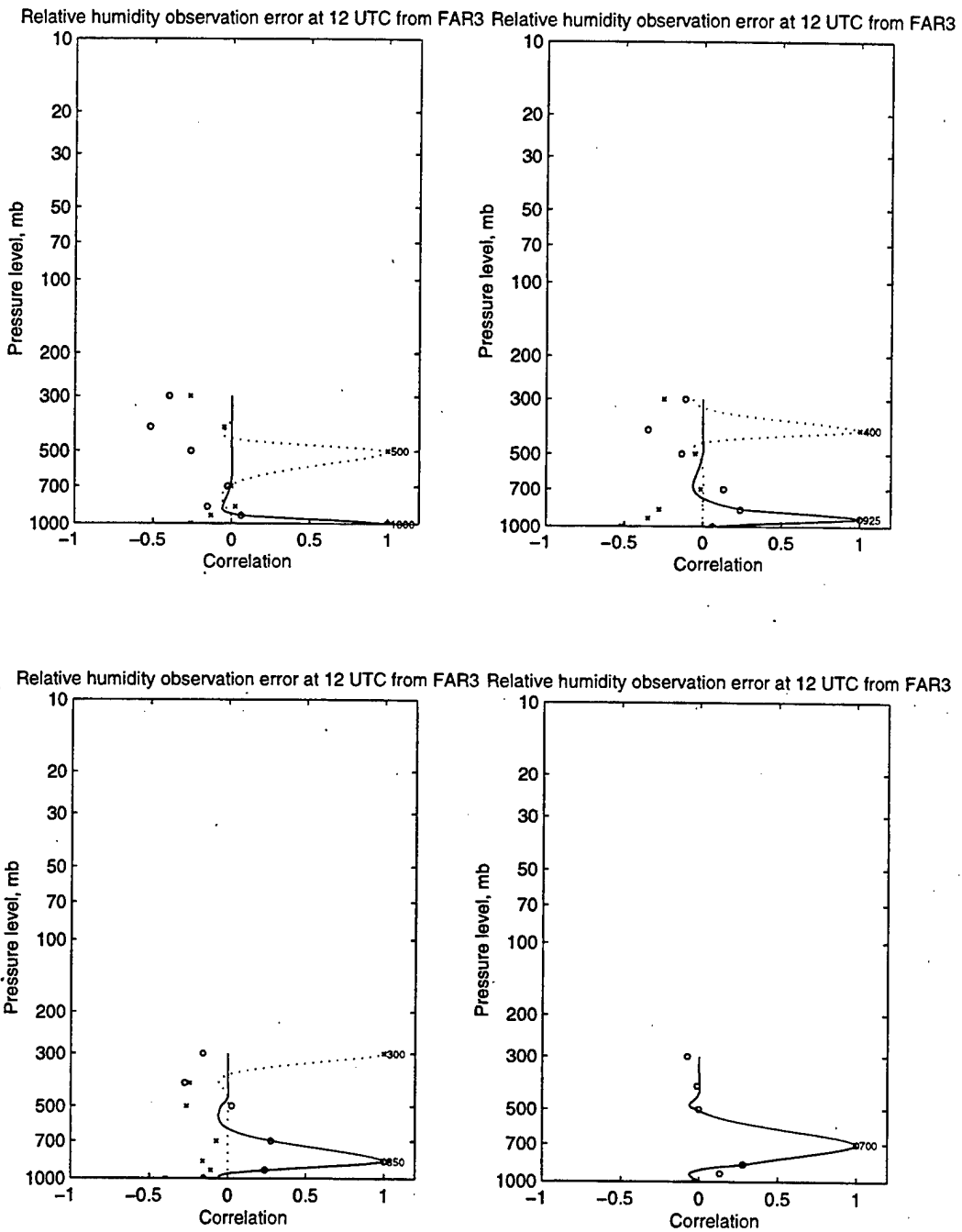


Figure 32: Vertical correlation of relative humidity observation errors at time 12 UTC inferred from FAR3. The curves obtained by fitting and transformation of coordinates showing the correlation between errors at the indicated level and other levels are shown.

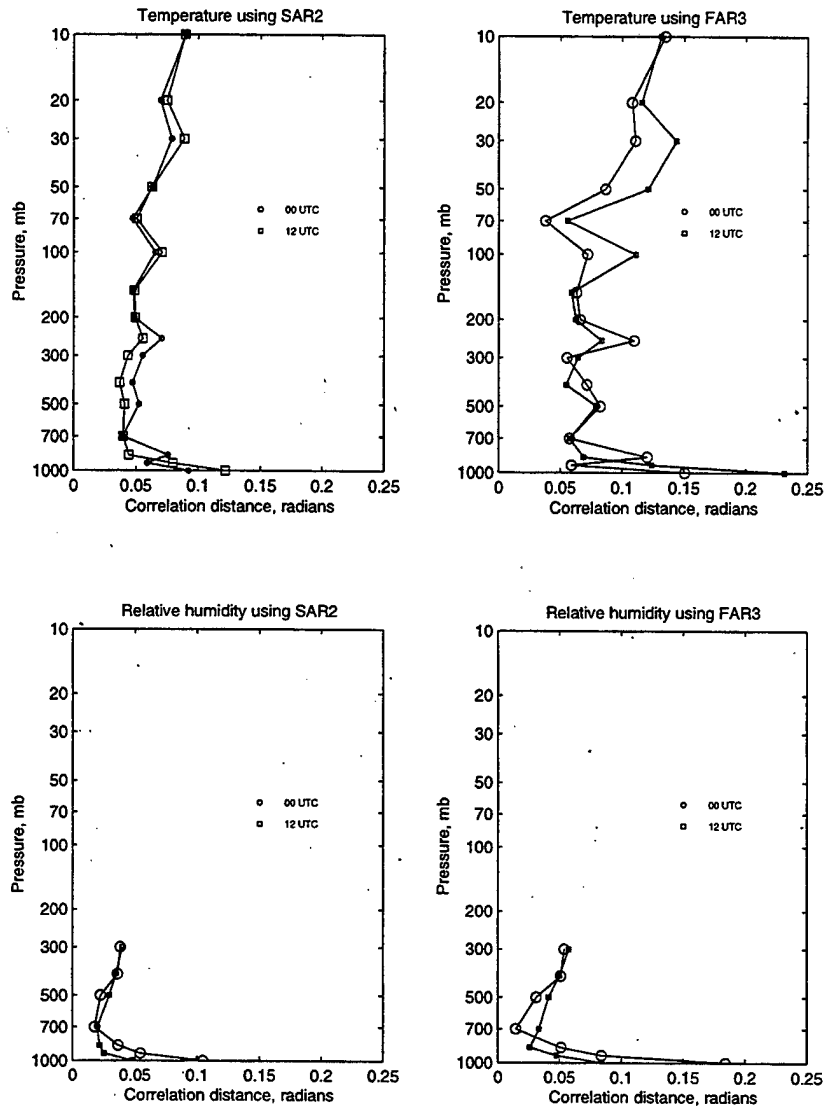


Figure 33: Correlation distance values for spatial covariance fits for temperature and relative humidity prediction errors using SAR2 and FAR3 fits at 00 and 12 UTC.

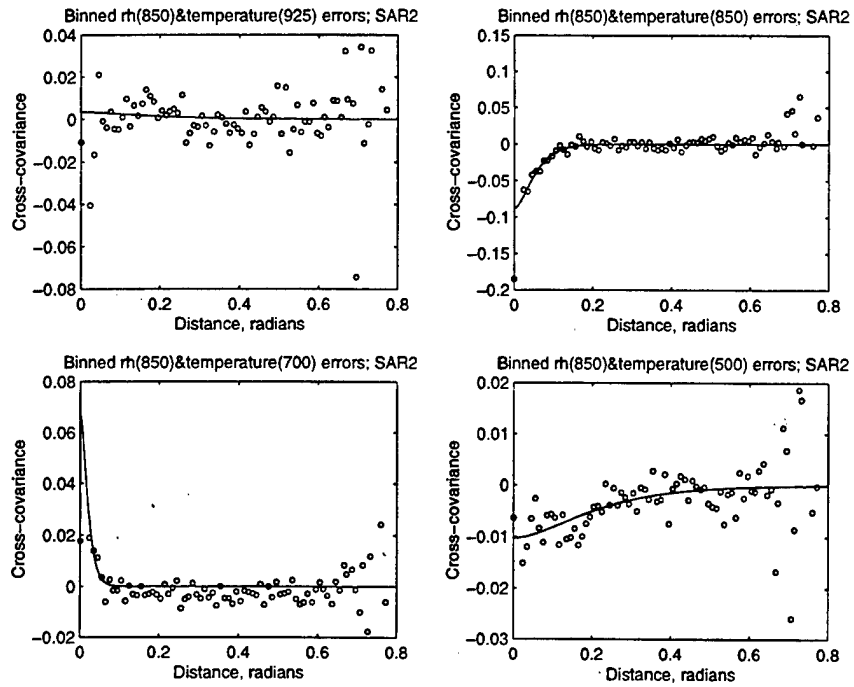


Figure 34: Binned cross-covariances between relative humidity error at 850 mb level and temperature error at 925, 850, 700, and 500 mb at time 00 UTC. Also shown are the SAR2 fits to the data.

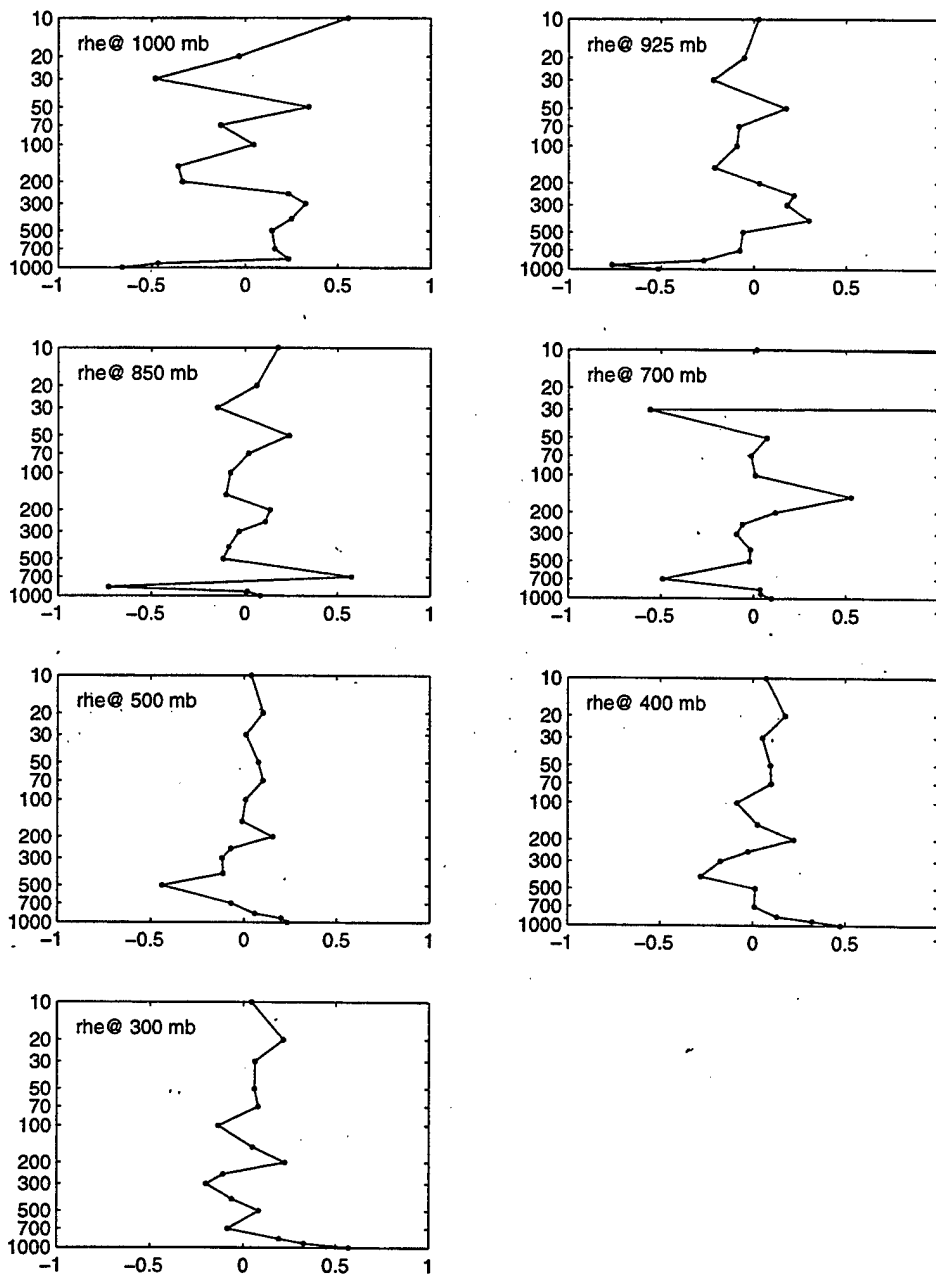


Figure 35: Correlation between relative humidity error at various levels and temperature errors for time 00 UTC. These points were derived from SAR2 fits to spatial covariance of temperature errors, relative humidity errors, and cross-covariance of relative humidity and temperature errors.

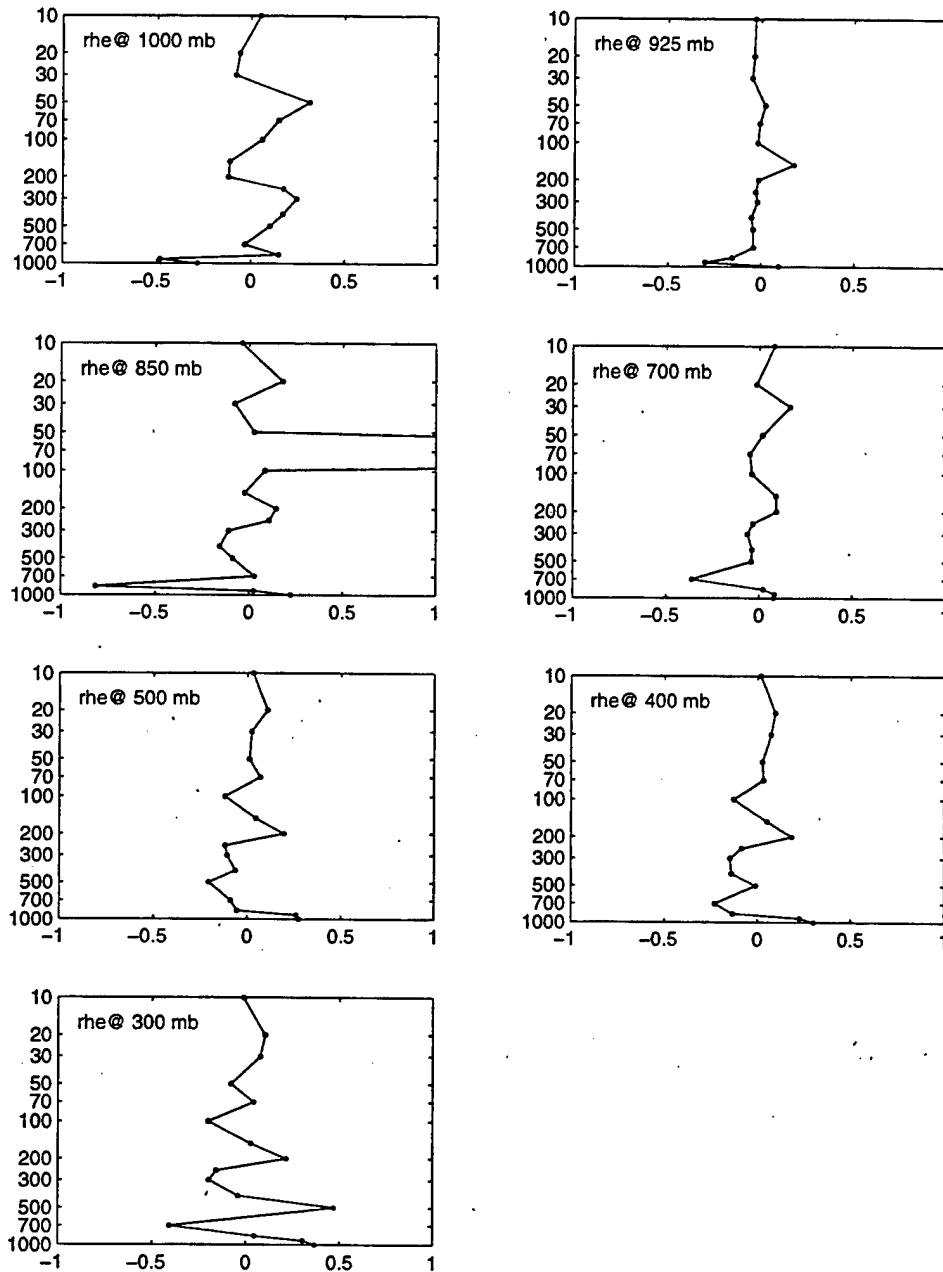


Figure 36: Correlation between relative humidity error at various levels and temperature errors for time 12 UTC. These points were derived from SAR2 fits to spatial covariance of temperature errors, relative humidity errors, and cross-covariance of relative humidity and temperature errors.

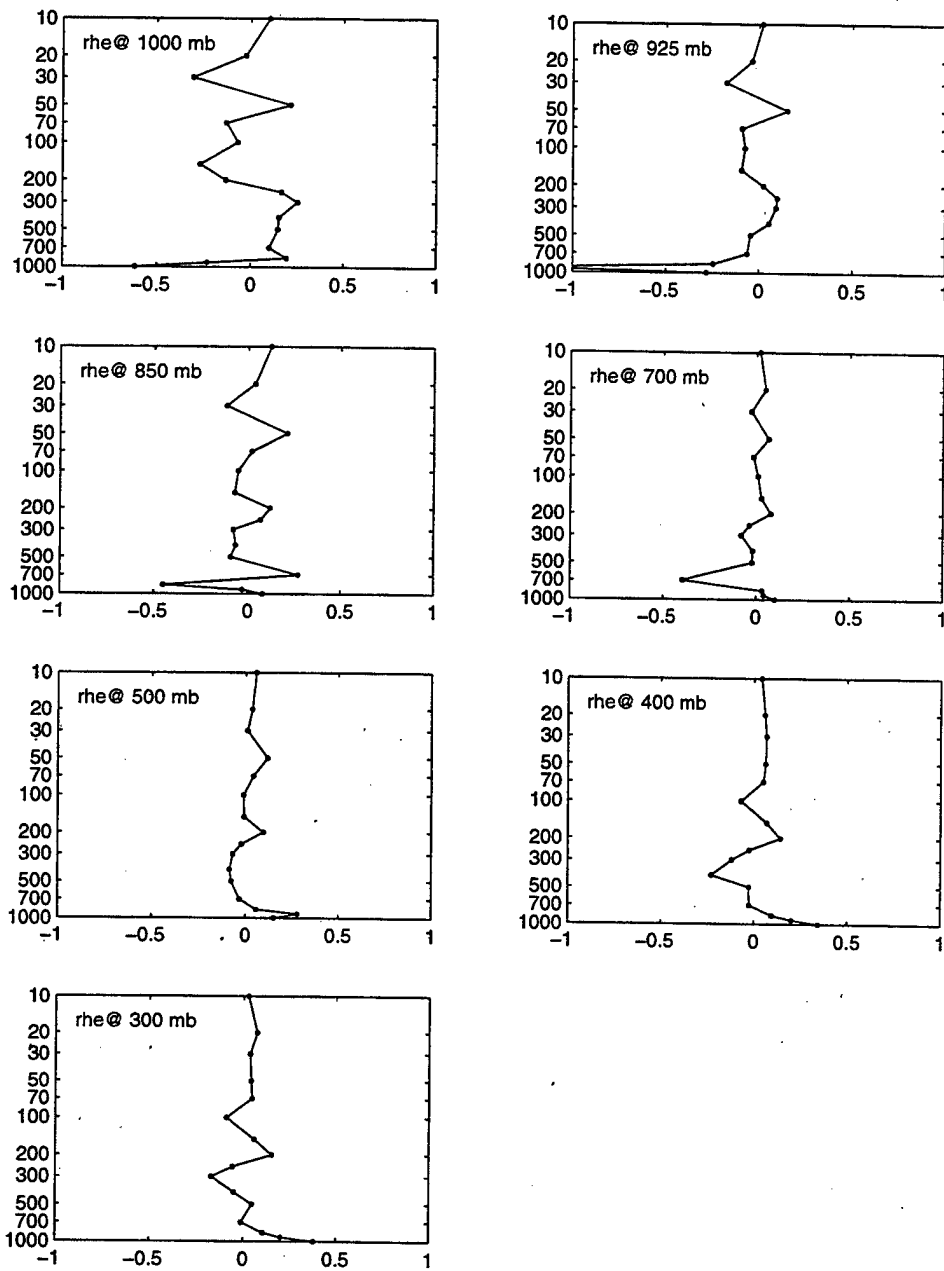


Figure 37: Correlation between relative humidity error at various levels and temperature errors for time 00 UTC. These points were derived from FAR3 fits to spatial covariance of temperature errors, relative humidity errors, and cross-covariance of relative humidity and temperature errors.

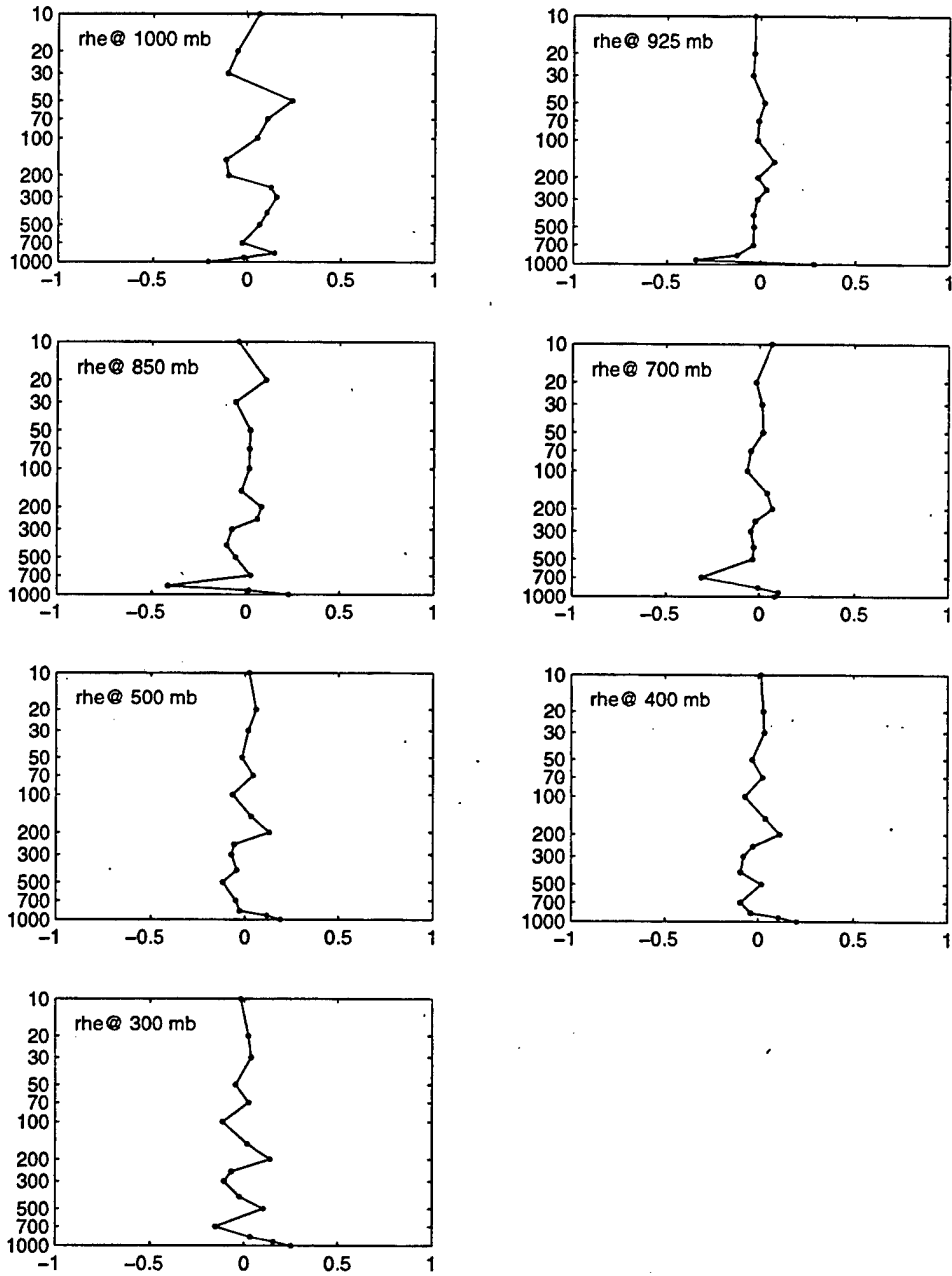


Figure 38: Correlation between relative humidity error at various levels and temperature errors for time 12 UTC. These points were derived from FAR3 fits to spatial covariance of temperature errors, relative humidity errors, and cross-covariance of relative humidity and temperature errors.

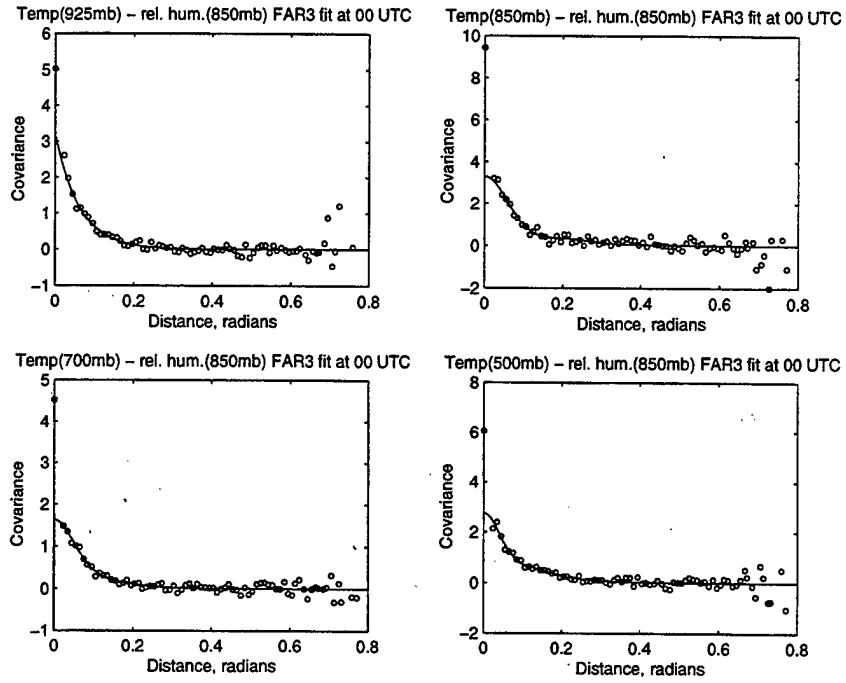


Figure 39: Binned covariances of the difference between normalized relative humidity error at 850 mb level and normalized temperature error at 925, 850, 700, and 500 mb at time 00 UTC. Also shown are the FAR3 fits to the data.

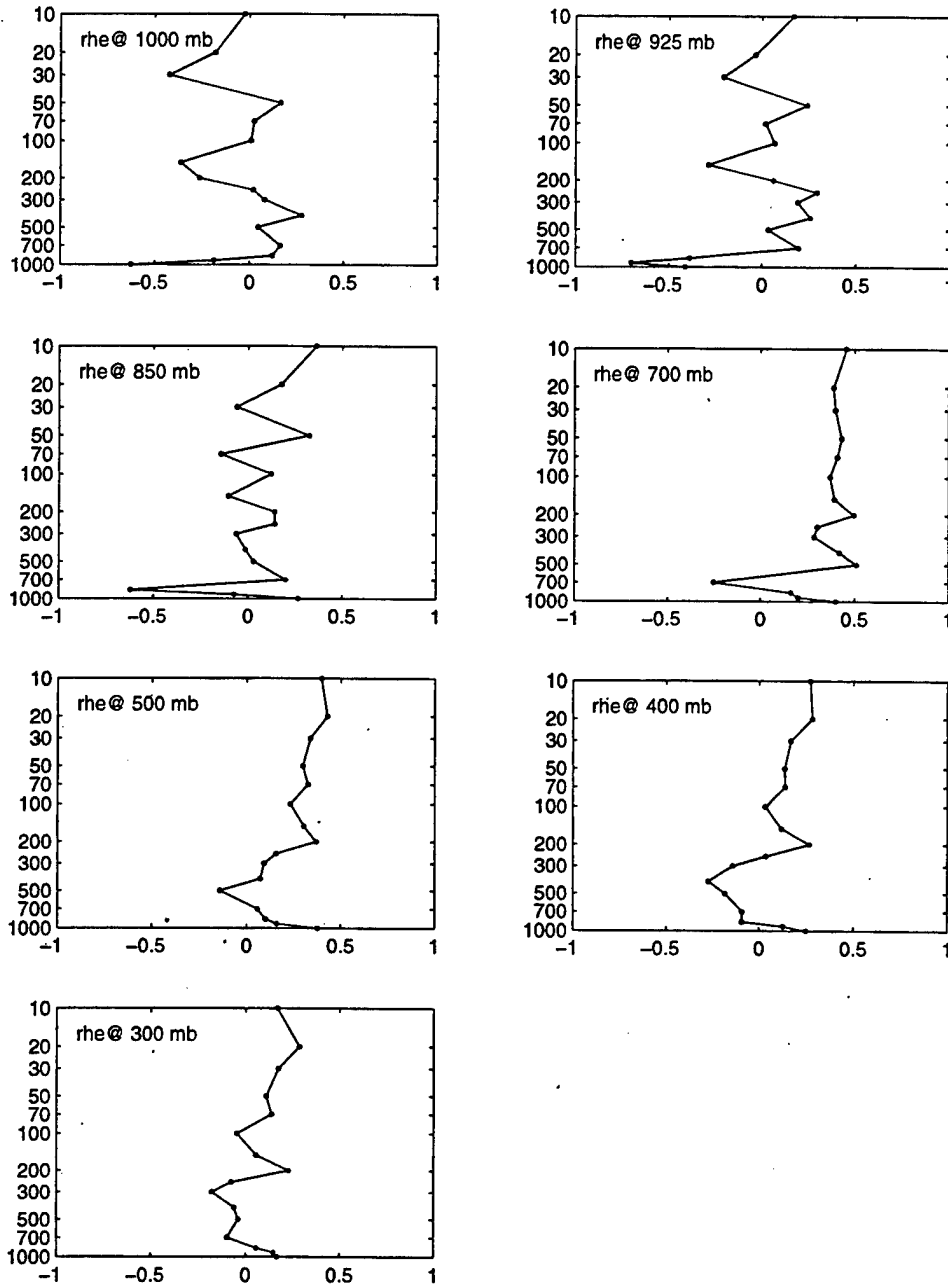


Figure 40: Correlation between temperature error at various heights and relative humidity error at the indicated heights for time 00 UTC. These curves were derived using the difference method and SAR2 fits to the spatial covariance data.

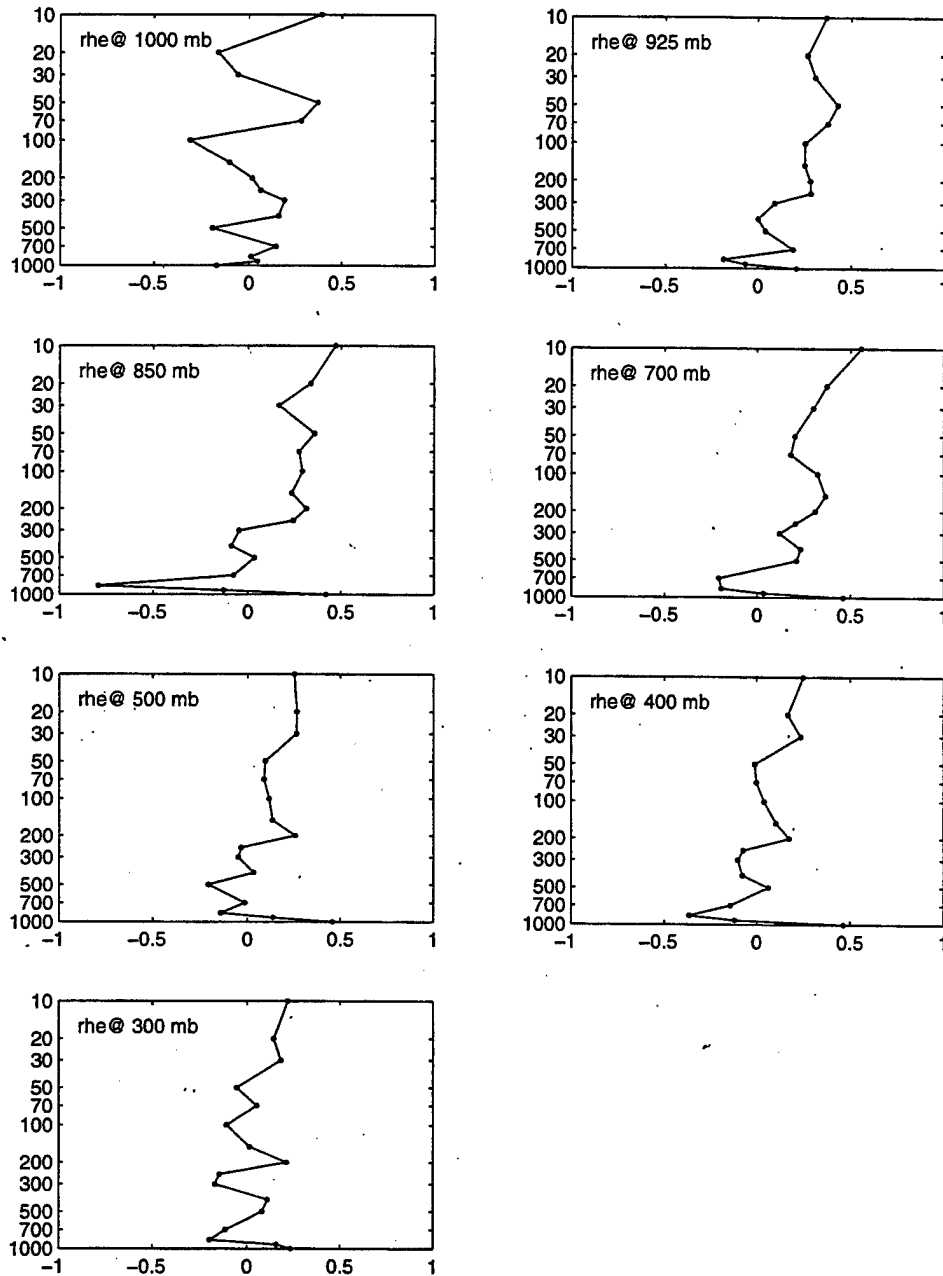


Figure 41: Correlation between temperature error at various heights and relative humidity error at the indicated heights for time 12 UTC. These curves were derived using the difference method and SAR2 fits to the spatial covariance data.

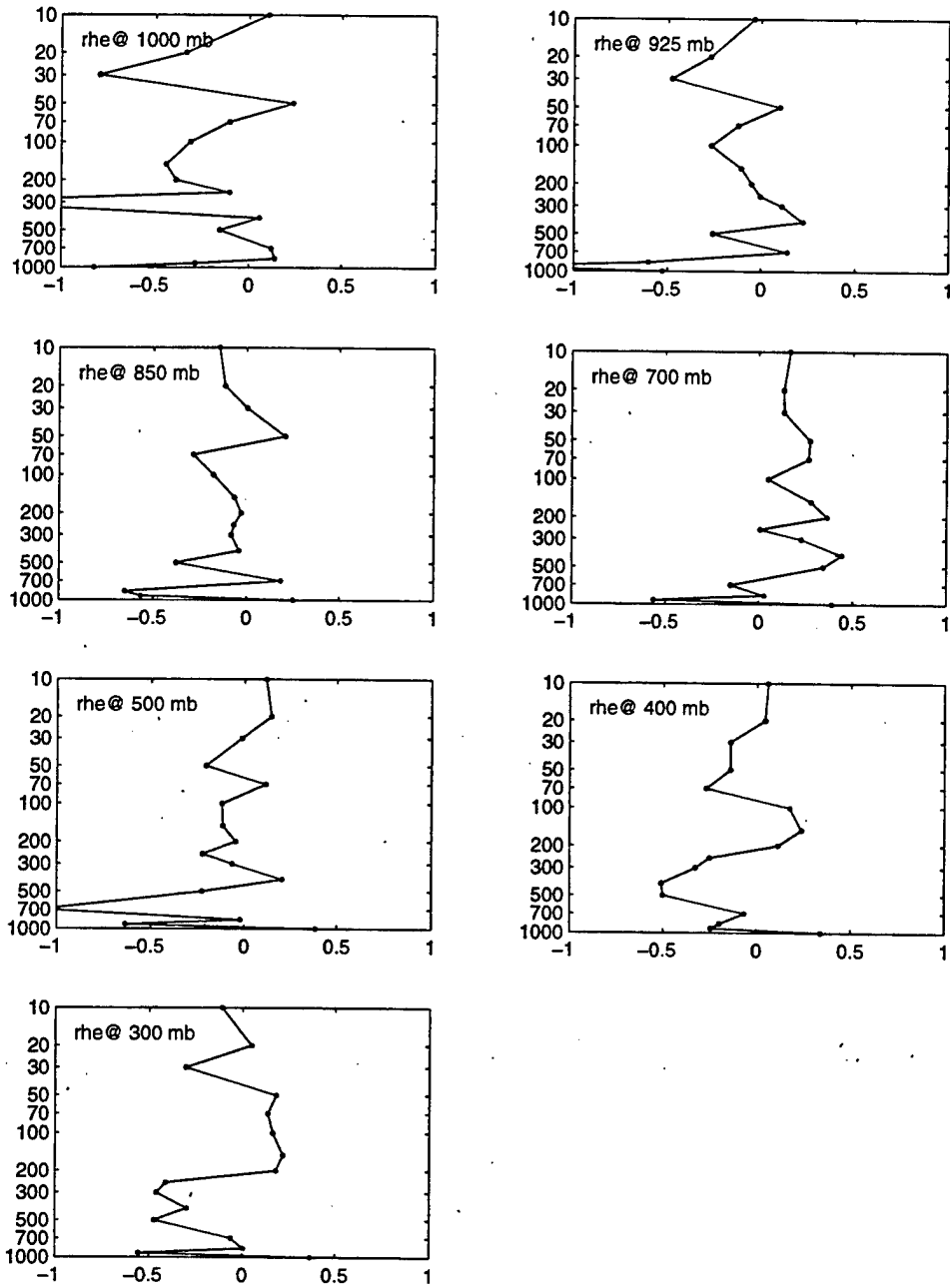


Figure 42: Correlation between temperature error at various heights and relative humidity error at the indicated heights for time 00 UTC. These curves were derived using the difference method and FAR3 fits to the spatial covariance data.

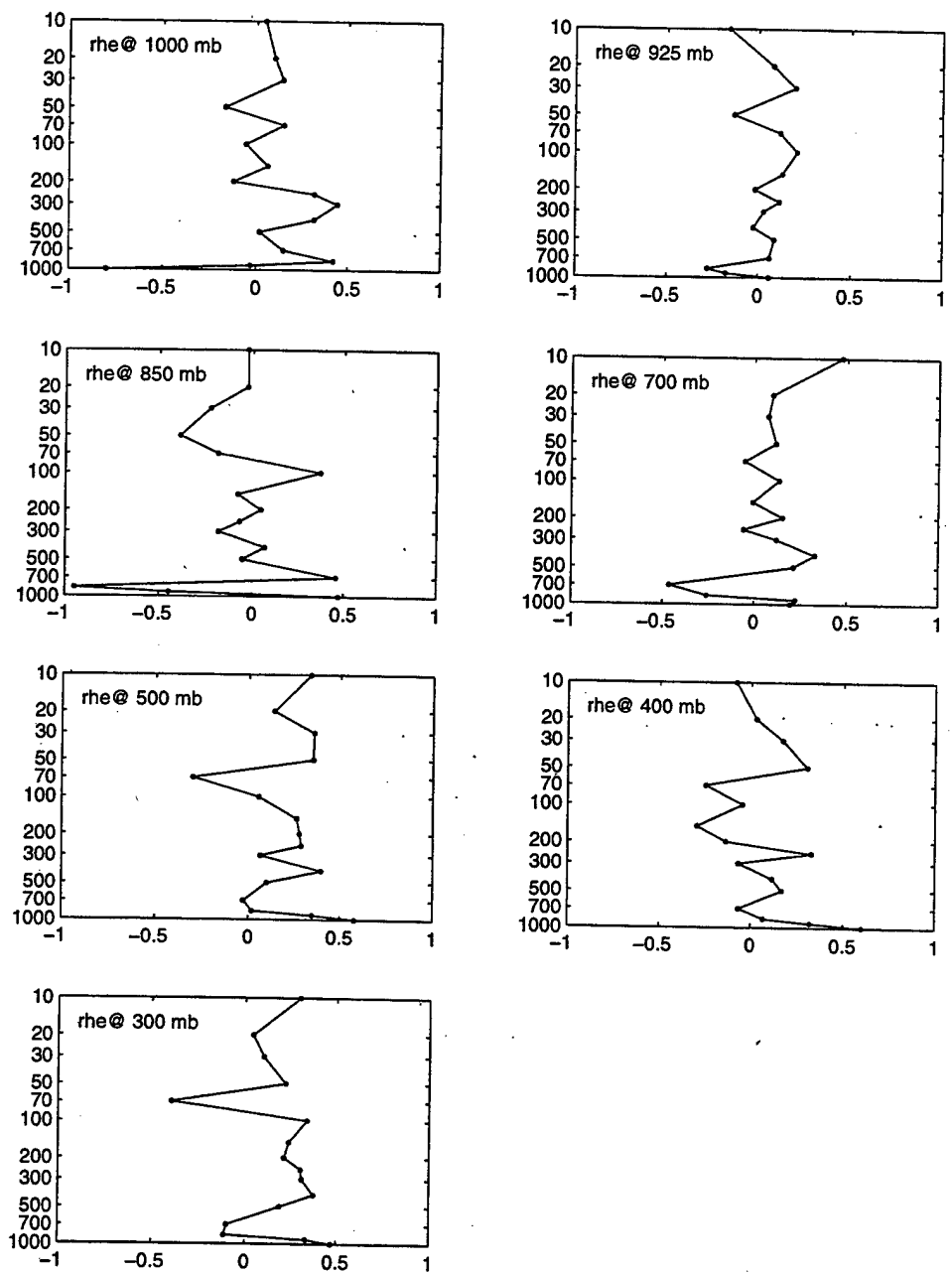


Figure 43: Correlation between temperature error at various heights and relative humidity error at the indicated heights for time 12 UTC. These curves were derived using the difference method and FAR3 fits to the spatial covariance data.

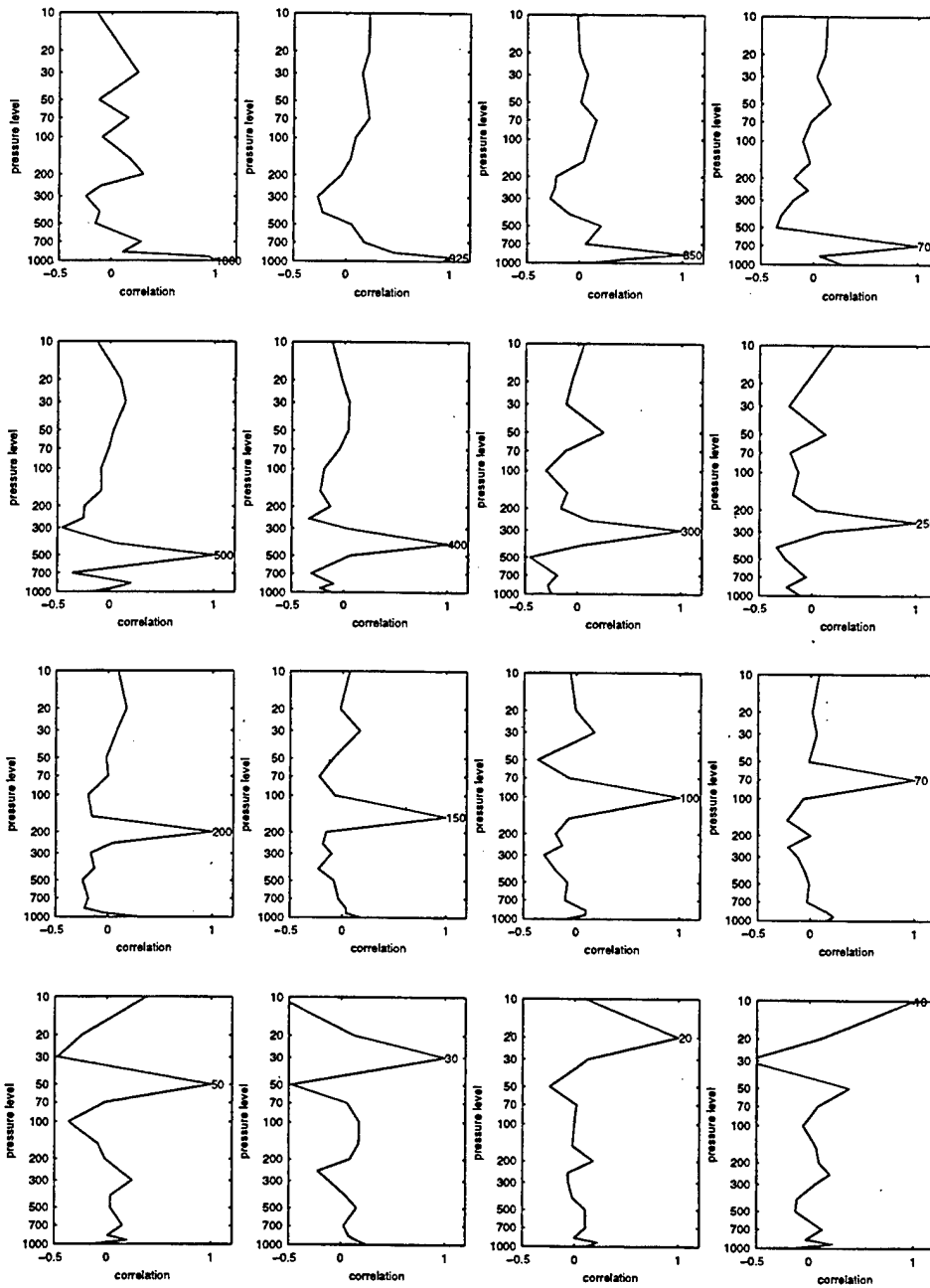


Figure 44: Vertical correlation curves for temperature prediction error at 00 UTC as derived from the SAR2 approximations. Each of the sixteen curves shows the correlation between the error at the indicated level and other levels.

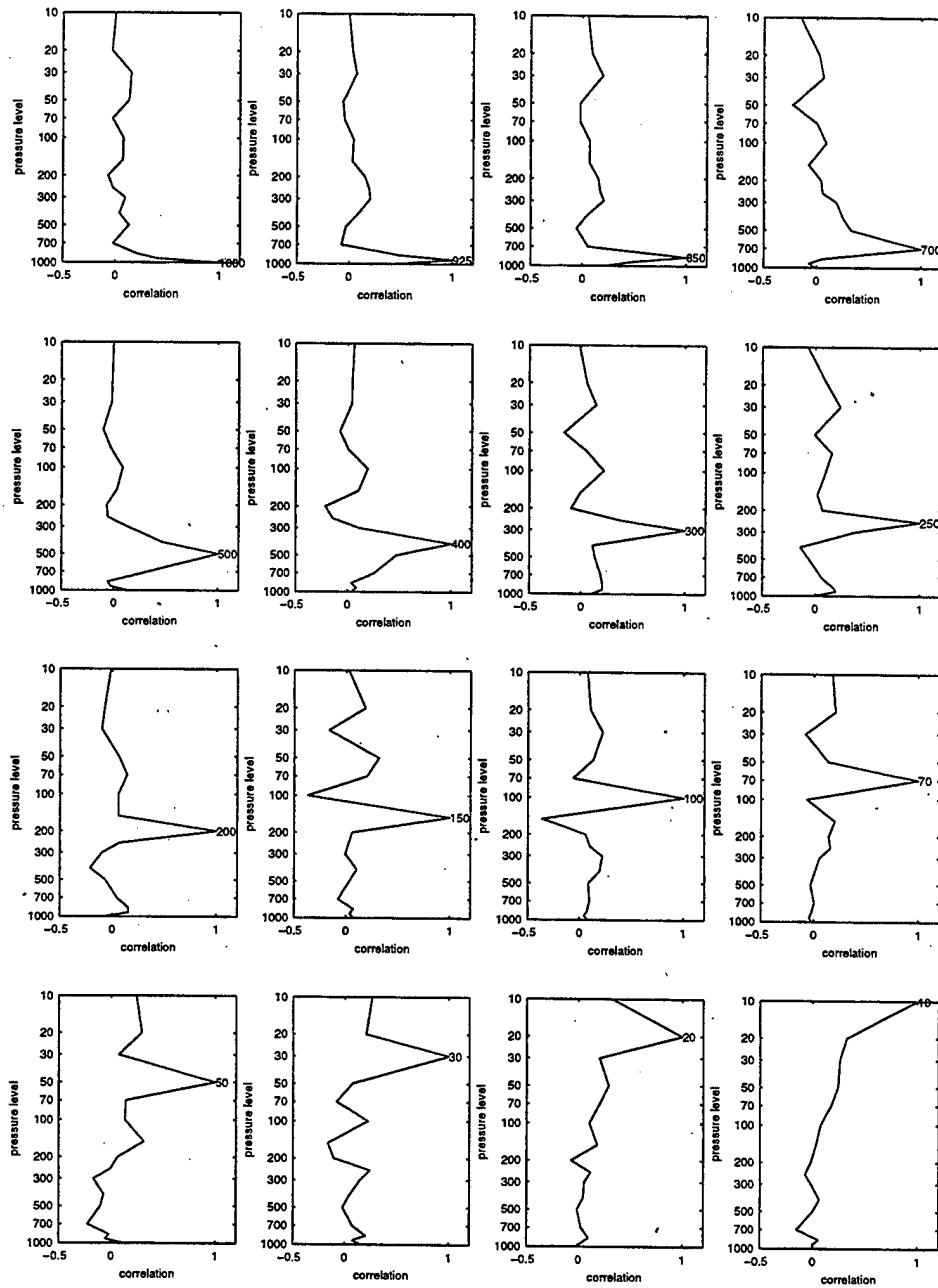


Figure 45: Vertical correlation curves for temperature observation error at 00 UTC as derived from the SAR2 approximations. Each of the sixteen curves shows the correlation between the error at the indicated level and other levels.

Appendix:

level	S2W1	S2W2	S2W3	S2W4	S22W1	S22W2	S22W3	F3W1
10	2.36	2.35	2.36	2.37	2.50	2.48	2.36	2.42
20	1.12	1.15	1.25	1.16	1.29	1.27	1.38	1.33
30	1.63	1.64	1.59	1.62	1.67	1.64	1.59	1.64
50	1.38	1.38	1.47	1.40	1.48	1.52	1.59	1.39
70	1.14	1.13	1.11	1.13	1.14	1.19	1.11	1.09
100	1.41	1.40	1.41	1.41	1.50	1.54	1.42	1.36
150	1.66	1.66	1.68	1.66	1.70	1.69	1.75	1.65
200	1.64	1.65	1.72	1.67	1.78	1.78	1.86	1.66
250	1.17	1.25	1.22	1.20	1.35	1.39	1.28	1.33
300	0.94	1.00	0.98	0.97	1.07	1.11	1.02	0.94
400	0.84	0.87	0.87	0.86	0.92	1.00	0.89	0.95
500	0.75	0.83	0.86	0.82	0.87	0.99	0.90	0.88
700	0.99	1.01	1.05	1.02	1.16	1.09	1.16	1.06
850	1.03	1.19	1.18	1.09	1.19	1.32	1.27	1.20
925	1.88	1.92	2.14	1.98	2.18	2.18	2.40	1.88
1000	1.30	1.32	1.26	1.28	1.34	1.32	1.35	1.32

**Table 1: Temperature prediction error at 00 UTC using various fitting schemes.
This data is shown graphically in Figure 5 (top two plots).**

level	S2W1	S2W2	S2W3	S2W4	S22W1	S22W2	S22W3	F3W1
10	2.50	2.53	2.58	2.51	2.63	2.60	2.71	2.54
20	1.18	1.20	1.28	1.22	1.30	1.32	1.40	1.40
30	1.59	1.64	1.67	1.61	1.69	1.70	1.75	1.83
50	1.45	1.41	1.45	1.45	1.45	1.50	1.45	1.33
70	1.16	1.16	1.27	1.18	1.21	1.23	1.41	1.12
100	1.40	1.42	1.35	1.42	1.56	1.56	1.35	1.60
150	1.65	1.65	1.48	1.62	1.65	1.65	1.48	1.62
200	1.70	1.69	1.70	1.71	1.79	1.83	1.70	1.68
250	1.29	1.31	1.34	1.32	1.47	1.49	1.40	1.49
300	1.11	1.13	1.26	1.16	1.35	1.35	1.39	1.35
400	0.99	1.01	1.06	1.03	1.09	1.20	1.14	1.17
500	0.90	0.94	0.97	0.93	1.01	1.06	1.01	0.92
700	0.96	0.96	1.24	1.03	1.16	1.16	1.45	1.17
850	1.12	1.21	1.37	1.28	1.31	1.50	1.43	1.33
925	1.09	1.29	1.63	1.25	1.29	1.49	1.73	1.28
1000	0.94	0.89	1.45	0.99	0.94	0.90	1.43	1.02

**Table 2: Temperature prediction error at 12 UTC using various fitting schemes.
This data is shown graphically in Figure 5 (bottom two plots).**

level	S2W1	S2W2	S2W3	S2W4	S22W1	S22W2	S22W3	F3W1
300	0.144	0.141	0.154	0.149	0.176	0.177	0.172	0.170
400	0.156	0.156	0.159	0.159	0.197	0.181	0.159	0.175
500	0.163	0.162	0.212	0.193	0.241	0.234	0.257	0.206
700	0.156	0.156	0.150	0.153	0.156	0.156	0.150	0.145
850	0.117	0.118	0.114	0.117	0.129	0.125	0.114	0.122
925	0.115	0.122	0.124	0.120	0.134	0.135	0.134	0.136
1000	0.074	0.079	0.077	0.075	0.079	0.082	0.081	0.080

Table 3: Relative humidity prediction error at 00 UTC using various fitting schemes. This data is shown graphically in Figure 6 (top two plots).

level	S2W1	S2W2	S2W3	S2W4	S22W1	S22W2	S22W3	F3W1
300	0.150	0.146	0.143	0.152	0.176	0.180	0.142	0.183
400	0.162	0.161	0.165	0.168	0.199	0.201	0.165	0.210
500	0.149	0.148	0.184	0.163	0.194	0.194	0.216	0.187
700	0.132	0.132	0.162	0.140	0.155	0.156	0.214	0.126
850	0.110	0.109	0.124	0.112	0.110	0.109	0.155	0.107
925	0.098	0.098	0.096	0.097	0.110	0.110	0.096	0.101
1000	0.078	0.079	0.079	0.079	0.080	0.079	0.079	0.081

Table 4: Relative humidity prediction error at 12 UTC using various fitting schemes. This data is shown graphically in Figure 6 (bottom two plots).

level	00 UTC				12 UTC			
	SAR2		FAR3		SAR2		FAR3	
	Pred	Obs	Pred	Obs	Pred	Obs	Pred	Obs
10	2.36	1.78	2.42	1.70	2.50	1.66	2.54	1.59
20	1.12	1.32	1.33	1.11	1.18	1.28	1.40	1.04
30	1.63	1.27	1.64	1.25	1.59	1.30	1.83	0.92
50	1.38	1.15	1.39	1.14	1.45	1.12	1.33	1.25
70	1.14	1.14	1.09	1.19	1.16	1.14	1.12	1.18
100	1.41	1.26	1.36	1.31	1.40	1.28	1.60	1.02
150	1.66	0.95	1.65	0.96	1.65	1.01	1.62	1.07
200	1.64	1.17	1.66	1.14	1.70	1.24	1.68	1.27
250	1.17	1.28	1.33	1.11	1.29	1.19	1.49	0.93
300	0.94	1.03	0.94	1.03	1.11	0.90	1.35	0.49
400	0.84	0.99	0.95	0.89	0.99	0.86	1.17	0.58
500	0.75	1.03	0.88	0.93	0.90	0.99	0.92	0.97
700	0.99	0.99	1.06	0.92	0.96	1.01	1.17	0.75
850	1.03	1.57	1.20	1.44	1.12	1.45	1.33	1.27
925	1.88	1.57	1.88	1.57	1.09	1.82	1.28	1.68
1000	1.30	2.21	1.32	2.19	0.94	2.02	1.02	1.98

Table 5: Temperature prediction and observation errors using two fitting schemes. This data is shown graphically in Figure 7.

level	00 UTC				12 UTC			
	SAR2		FAR3		SAR2		FAR3	
	Pred	Obs	Pred	Obs	Pred	Obs	Pred	Obs
300	0.144	0.156	0.170	0.127	0.150	0.154	0.183	0.112
400	0.156	0.188	0.175	0.170	0.162	0.185	0.210	0.129
500	0.163	0.181	0.206	0.130	0.149	0.203	0.187	0.169
700	0.156	0.158	0.145	0.168	0.132	0.181	0.126	0.186
850	0.117	0.168	0.122	0.164	0.110	0.173	0.107	0.174
925	0.115	0.143	0.136	0.124	0.098	0.144	0.101	0.142
1000	0.074	0.130	0.080	0.127	0.078	0.112	0.081	0.110

Table 6: Relative humidity prediction and observation errors using two fitting schemes. This data is shown graphically in Figure 8.

coefficient	00 UTC		12 UTC	
	SAR2	FAR3	SAR2	FAR3
a	1.000	1.000	1.000	1.000
b	0.327	9.211	0.353	4.820
c	11.533	51.193	23.914	27.385

Table 7: FAR3 parameters for vertical correlation approximations to temperature prediction error derived from horizontal approximations by indicated method at given times. The curves are shown graphically in Figure 9.

coefficient	00 UTC		12 UTC	
	SAR2	FAR3	SAR2	FAR3
a	1.000	1.000	1.000	1.000
b	0.378	5.968	0.356	5.398
c	9.584	45.270	21.208	18.985

Table 8: FAR3 parameters for vertical correlation approximations to temperature observation error derived from horizontal approximations by indicated method at given times. The curves are shown graphically in Figure 10.

coefficient	00 UTC		12 UTC	
	SAR2	FAR3	SAR2	FAR3
a	1.000	1.000	1.000	1.000
b	13049.771	0.559	13047.033	0.582
c	0.172	25936.027	0.081	19806.409

Table 9: FAR3 parameters for vertical correlation approximations to relative humidity prediction error derived from horizontal approximations by indicated method at given times. The curves are shown graphically in Figure 11.

coefficient	00 UTC		12 UTC	
	SAR2	FAR3	SAR2	FAR3
a	1.000	1.000	1.000	1.000
b	86709.162	47.665	187.995	0.886
c	0.232	419684.256	1.438	5609.970

Table 10: FAR3 parameters for vertical correlation approximations to relative humidity observation error derived from horizontal approximations by indicated method at given times. The curves are shown graphically in Figure 12.

log(level)	00 UTC		12 UTC	
	SAR2	FAR3	SAR2	FAR3
1.00	30.438	26.753	34.062	32.797
1.30	28.748	26.513	32.337	32.404
1.48	27.164	26.217	30.657	31.871
1.70	24.242	22.056	27.812	30.858
1.85	22.348	21.680	25.976	26.356
2.00	20.392	20.738	23.241	16.647
2.18	18.318	19.524	21.335	13.654
2.30	15.878	19.036	19.377	13.128
2.40	13.798	13.622	17.929	11.630
2.48	12.041	4.854	16.601	9.074
2.60	10.382	1.431	14.927	8.348
2.70	8.775	1.247	13.553	7.923
2.85	6.456	1.017	6.649	1.205
2.93	1.656	0.387	1.672	0.631
2.97	0.460	0.207	0.408	0.385
3.00	0.000	0.000	0.000	0.000

Table 11: $g(\log P)$ transformations for the temperature prediction error vertical correlation curve shown in Figure 9. The transformations are shown graphically in Figure 13.

log(level)	00 UTC		12 UTC	
	SAR2	FAR3	SAR2	FAR3
1.00	31.624	27.525	32.732	30.113
1.30	29.963	27.122	31.160	29.485
1.48	28.387	26.637	29.571	28.901
1.70	25.416	22.685	26.634	26.941
1.85	23.780	20.362	22.880	26.523
2.00	21.893	18.698	18.969	25.918
2.18	19.731	16.698	17.061	21.878
2.30	17.466	15.069	14.867	19.998
2.40	15.497	14.518	13.345	16.806
2.48	14.074	9.405	12.461	12.893
2.60	11.870	9.079	11.166	10.546
2.70	10.402	8.777	9.645	3.448
2.85	7.223	8.428	6.824	3.448
2.93	2.112	4.299	2.047	0.932
2.97	0.932	0.416	0.753	0.535
3.00	0.000	0.000	0.000	0.000

Table 12: $g(\log P)$ transformations for the temperature observation error vertical correlation curve shown in figure 10. The transformations are shown graphically in Figure 14.

log(level)	00 UTC		12 UTC	
	SAR2	FAR3	SAR2	FAR3
2.48	22.652	8.832	57.468	9.365
2.60	18.139	7.820	50.401	7.814
2.70	16.052	6.628	45.984	5.972
2.85	10.962	4.903	29.261	4.642
2.93	8.730	2.786	17.503	2.985
2.97	2.732	1.555	6.261	1.650
3.00	0.000	0.000	0.000	0.000

Table 13: $g(\log P)$ transformations for the relative humidity prediction error vertical correlation curve shown in Figure 11. The transformations are shown graphically in Figure 15.

log(level)	00 UTC		12 UTC	
	SAR2	FAR3	SAR2	FAR3
2.48	29.356	15.699	34.338	14.809
2.60	25.967	15.663	34.074	11.640
2.70	24.670	15.620	33.878	7.289
2.85	21.863	15.546	33.334	4.899
2.93	18.237	15.457	10.563	3.471
2.97	11.583	15.404	9.703	1.985
3.00	0.000	0.000	0.000	0.000

Table 14: $g(\log P)$ transformations for the relative humidity observation error vertical correlation curve shown in Figure 12. The transformations are shown graphically in Figure 16.

level	Temperature				Humidity			
	SAR2		FAR3		SAR2		FAR3	
	00 UTC	12 UTC	00 UTC	12 UTC	00 UTC	12 UTC	00 UTC	12 UTC
10	0.0900	0.0897	0.1347	0.1314				
20	0.0698	0.0751	0.1079	0.1158				
30	0.0788	0.0890	0.1106	0.1437				
50	0.0633	0.0629	0.0867	0.1209				
70	0.0474	0.0504	0.0380	0.0558				
100	0.0657	0.0710	0.0722	0.1111				
150	0.0478	0.0488	0.0632	0.0593				
200	0.0487	0.0494	0.0661	0.0627				
250	0.0707	0.0555	0.1097	0.0836				
300	0.0556	0.0435	0.0556	0.0644	0.0382	0.0395	0.0538	0.0574
400	0.0471	0.0369	0.0717	0.0549	0.0358	0.0346	0.0510	0.0497
500	0.0524	0.0407	0.0824	0.0794	0.0223	0.0292	0.0310	0.0410
700	0.0395	0.0396	0.0575	0.0577	0.0176	0.0197	0.0144	0.0333
850	0.0760	0.0443	0.1202	0.0689	0.0363	0.0216	0.0511	0.0259
925	0.0591	0.0798	0.0591	0.1241	0.0543	0.0250	0.0839	0.0474
1000	0.0925	0.1219	0.1506	0.2314	0.1047	0.0475	0.1843	0.0840

Table 15: Correlation distance values for prediction and observation temperature errors from two approximations at the indicated times, and correlation distance values for prediction and observation relative humidity errors from two approximations at the indicated times. The data is shown graphically in Figure 33.

temperature level	humidity levels						
	1000	925	850	700	500	400	300
10	0.556	0.026	0.179	0.018	0.039	0.073	0.045
20	-0.033	-0.051	0.063	26.493	0.103	0.175	0.217
30	-0.480	-0.219	-0.147	-0.557	0.011	0.053	0.063
50	0.343	0.175	0.238	0.072	0.077	0.094	0.061
70	-0.131	-0.079	0.021	-0.013	0.103	0.098	0.080
100	0.046	-0.092	-0.078	0.009	0.010	-0.086	-0.135
150	-0.357	-0.211	-0.102	0.530	-0.009	0.026	0.050
200	-0.335	0.031	0.136	0.117	0.155	0.221	0.225
250	0.233	0.216	0.111	-0.062	-0.069	-0.026	-0.109
300	0.325	0.181	-0.031	-0.092	-0.118	-0.175	-0.198
400	0.249	0.298	-0.086	-0.018	-0.113	-0.281	-0.061
500	0.144	-0.059	-0.116	-0.022	-0.438	0.013	0.084
700	0.160	-0.077	0.575	-0.490	-0.066	0.009	-0.084
850	0.232	-0.271	-0.730	0.037	0.059	0.130	0.194
925	-0.467	-0.763	0.015	0.040	0.200	0.320	0.327
1000	-0.660	-0.516	0.085	0.097	0.234	0.475	0.569

Table 16: Correlation between temperature error and relative humidity error at various levels at time 00 UTC. The points were derived from SAR2 fits to spatial covariance of temperature errors, relative humidity errors, and the cross-covariance of temperature and relative humidity errors. The data is shown graphically in Figure 33.

temperature level	humidity levels						
	1000	925	850	700	500	400	300
10	0.053	-0.029	-0.037	0.080	0.033	0.017	-0.013
20	-0.059	-0.037	0.179	-0.014	0.109	0.095	0.104
30	-0.080	-0.046	-0.076	0.165	0.024	0.072	0.079
50	0.310	0.021	0.030	0.018	0.013	0.026	-0.080
70	0.148	-0.006	5.790	-0.050	0.071	0.032	0.043
100	0.061	-0.017	0.087	-0.040	-0.118	-0.128	-0.202
150	-0.112	0.176	-0.022	0.089	0.048	0.050	0.027
200	-0.119	-0.014	0.146	0.092	0.196	0.184	0.215
250	0.175	-0.028	0.109	-0.034	-0.117	-0.085	-0.159
300	0.244	-0.019	-0.106	-0.062	-0.106	-0.147	-0.197
400	0.172	-0.050	-0.155	-0.037	-0.062	-0.139	-0.041
500	0.104	-0.041	-0.085	-0.041	-0.206	-0.009	0.468
700	-0.030	-0.040	0.031	-0.359	-0.088	-0.227	-0.408
850	0.151	-0.153	-0.815	0.022	-0.054	-0.131	0.046
925	-0.484	-0.297	0.028	0.084	0.260	0.225	0.302
1000	-0.283	0.096	0.223	0.079	0.275	0.300	0.365

Table 17: Correlation between temperature error and relative humidity error at various levels at time 12 UTC. The points were derived from SAR2 fits to spatial covariance of temperature errors, relative humidity errors, and the cross-covariance of temperature and relative humidity errors. The data is shown graphically in Figure 34.

temperature level	humidity levels						
	1000	925	850	700	500	400	300
10	0.100	0.020	0.122	0.021	0.056	0.041	0.027
20	-0.026	-0.037	0.038	0.048	0.036	0.060	0.074
30	-0.309	-0.171	-0.114	-0.025	0.010	0.068	0.037
50	0.216	0.154	0.210	0.066	0.118	0.063	0.042
70	-0.130	-0.088	0.021	-0.015	0.043	0.051	0.047
100	-0.068	-0.074	-0.052	0.010	-0.010	-0.067	-0.090
150	-0.272	-0.092	-0.069	0.029	-0.008	0.070	0.059
200	-0.134	0.026	0.119	0.080	0.095	0.142	0.152
250	0.166	0.100	0.068	-0.036	-0.020	-0.023	-0.057
300	0.253	0.093	-0.077	-0.079	-0.067	-0.116	-0.171
400	0.153	0.056	-0.064	-0.017	-0.085	-0.225	-0.049
500	0.148	-0.042	-0.092	-0.021	-0.077	-0.025	0.048
700	0.100	-0.061	0.271	-0.394	-0.031	-0.024	-0.009
850	0.194	-0.240	-0.450	0.034	0.058	0.097	0.106
925	-0.233	-1.277	-0.030	0.043	0.280	0.204	0.201
1000	-0.614	-0.277	0.080	0.102	0.153	0.344	0.379

Table 18: Correlation between temperature error and relative humidity error at various levels at time 00 UTC. The points were derived from FAR3 fits to spatial covariance of temperature errors, relative humidity errors, and the cross-covariance of temperature and relative humidity errors. The data is shown graphically in Figure 35.

temperature level	humidity levels						
	1000	925	850	700	500	400	300
10	0.065	-0.028	-0.040	0.064	0.022	0.013	-0.017
20	-0.052	-0.030	0.106	-0.016	0.059	0.026	0.023
30	-0.101	-0.038	-0.055	0.014	0.017	0.031	0.038
50	0.241	0.021	0.022	0.020	-0.014	-0.031	-0.044
70	0.107	-0.008	0.019	-0.043	0.044	0.022	0.025
100	0.053	-0.015	0.017	-0.063	-0.065	-0.069	-0.112
150	-0.111	0.073	-0.024	0.041	0.034	0.036	0.017
200	-0.097	-0.013	0.082	0.068	0.130	0.114	0.139
250	0.127	0.031	0.061	-0.020	-0.056	-0.026	-0.066
300	0.157	-0.015	-0.073	-0.043	-0.070	-0.077	-0.105
400	0.105	-0.035	-0.100	-0.027	-0.042	-0.092	-0.024
500	0.066	-0.032	-0.054	-0.034	-0.115	0.017	0.103
700	-0.024	-0.036	0.025	-0.307	-0.047	-0.093	-0.151
850	0.147	-0.123	-0.412	-0.005	-0.026	-0.038	0.033
925	-0.016	-0.343	0.016	0.101	0.118	0.106	0.155
1000	-0.206	0.281	0.230	0.083	0.191	0.202	0.251

Table 19: Correlation between temperature error and relative humidity error at various levels at time 12 UTC. The points were derived from FAR3 fits to spatial covariance of temperature errors, relative humidity errors, and the cross-covariance of temperature and relative humidity errors. The data is shown graphically in Figure 36.

temperature level	humidity levels						
	1000	925	850	700	500	400	300
10	-0.025	0.166	0.362	0.455	0.396	0.271	0.169
20	-0.180	-0.034	0.177	0.388	0.428	0.283	0.286
30	-0.420	-0.203	-0.059	0.397	0.337	0.168	0.175
50	0.166	0.240	0.324	0.430	0.298	0.135	0.109
70	0.025	0.019	-0.141	0.407	0.326	0.137	0.138
100	0.008	0.067	0.123	0.370	0.234	0.034	-0.045
150	-0.361	-0.284	-0.103	0.393	0.303	0.119	0.056
200	-0.262	0.061	0.142	0.497	0.369	0.267	0.228
250	0.021	0.294	0.143	0.301	0.158	0.035	-0.074
300	0.081	0.190	-0.062	0.285	0.094	-0.139	-0.176
400	0.278	0.257	-0.013	0.419	0.074	-0.269	-0.060
500	0.046	0.034	0.030	0.510	-0.138	-0.180	-0.039
700	0.165	0.194	0.201	-0.249	0.059	-0.088	-0.096
850	0.122	-0.387	-0.620	0.161	0.102	-0.090	0.057
925	-0.185	-0.702	-0.072	0.200	0.161	0.127	0.148
1000	-0.626	-0.411	0.267	0.401	0.377	0.248	0.168

Table 20: Correlation between temperature error and relative humidity error at various levels at time 00 UTC. The points were derived using the difference method and SAR2 fits to the spatial covariance data. The data is shown graphically in Figure 40.

temperature level	humidity levels						
	1000	925	850	700	500	400	300
10	0.390	0.368	0.470	0.559	0.251	0.249	0.218
20	-0.159	0.268	0.335	0.374	0.263	0.169	0.143
30	-0.057	0.307	0.165	0.301	0.260	0.236	0.180
50	0.368	0.428	0.357	0.203	0.096	-0.010	-0.052
70	0.280	0.376	0.273	0.182	0.088	-0.001	0.052
100	-0.308	0.255	0.291	0.323	0.117	0.041	-0.107
150	-0.103	0.253	0.233	0.366	0.134	0.105	0.014
200	0.018	0.282	0.313	0.310	0.255	0.176	0.211
250	0.063	0.284	0.242	0.207	-0.032	-0.073	-0.143
300	0.190	0.090	-0.044	0.121	-0.046	-0.101	-0.168
400	0.158	0.002	-0.086	0.235	0.033	-0.076	0.109
500	-0.190	0.041	0.036	0.212	-0.205	0.064	0.080
700	0.146	0.190	-0.076	-0.207	-0.013	-0.142	-0.112
850	0.012	-0.185	-0.793	-0.194	-0.138	-0.366	-0.195
925	0.045	-0.066	-0.126	0.035	0.138	-0.117	0.156
1000	-0.168	0.208	0.418	0.462	0.457	0.464	0.233

Table 21: Correlation between temperature error and relative humidity error at various levels at time 12 UTC. The points were derived using the difference method and SAR2 fits to the spatial covariance data. The data is shown graphically in Figure 41.

temperature level	humidity levels						
	1000	925	850	700	500	400	300
10	0.105	-0.038	-0.146	0.166	0.116	0.059	-0.109
20	-0.336	-0.269	-0.116	0.132	0.144	0.043	0.049
30	-0.796	-0.478	0.004	0.134	-0.013	-0.140	-0.301
50	0.238	0.102	0.208	0.271	-0.205	-0.141	0.183
70	-0.103	-0.121	-0.285	0.264	0.115	-0.269	0.138
100	-0.312	-0.265	-0.178	0.051	-0.118	0.176	0.164
150	-0.442	-0.106	-0.064	0.277	-0.115	0.237	0.218
200	-0.390	-0.050	-0.028	0.363	-0.045	0.114	0.180
250	-0.102	-0.003	-0.067	0.008	-0.222	-0.252	-0.410
300	-1.600	0.113	-0.081	0.225	-0.063	-0.326	-0.461
400	0.059	0.224	-0.040	0.441	0.204	-0.510	-0.297
500	-0.154	-0.257	-0.376	0.342	-0.225	-0.501	-0.470
700	0.121	0.141	0.184	-0.149	-1.080	-0.066	-0.060
850	0.141	-0.602	-0.650	0.030	-0.020	-0.198	0.005
925	-0.285	-1.417	-0.565	-0.562	-0.637	-0.245	-0.556
1000	-0.825	-0.527	0.251	0.389	0.384	0.340	0.366

Table 22: Correlation between temperature error and relative humidity error at various levels at time 00 UTC. The points were derived using the difference method and FAR3 fits to the spatial covariance data. The data is shown graphically in Figure 42.

temperature level	humidity levels						
	1000	925	850	700	500	400	300
10	0.046	-0.159	-0.027	0.471	0.337	-0.080	0.298
20	0.098	0.084	-0.027	0.100	0.138	0.030	0.044
30	0.143	0.202	-0.226	0.076	0.357	0.176	0.100
50	-0.168	-0.131	-0.388	0.117	0.352	0.307	0.220
70	0.150	0.122	-0.185	-0.052	-0.298	-0.246	-0.394
100	-0.055	0.211	0.372	0.136	0.056	-0.044	0.339
150	0.062	0.134	-0.080	-0.007	0.261	-0.295	0.238
200	-0.122	-0.017	0.046	0.156	0.277	-0.135	0.213
250	0.318	0.117	-0.068	-0.058	0.286	0.330	0.304
300	0.444	0.031	-0.181	0.122	0.065	-0.065	0.310
400	0.316	-0.025	0.069	0.329	0.396	0.119	0.374
500	0.020	0.089	-0.051	0.215	0.100	0.171	0.188
700	0.150	0.064	0.456	-0.464	-0.027	-0.065	-0.098
850	0.423	-0.276	-0.948	-0.258	0.021	0.071	-0.111
925	-0.028	-0.176	-0.445	0.226	0.348	0.322	0.332
1000	-0.801	0.063	0.471	0.197	0.579	0.600	0.470

Table 23: Correlation between temperature error and relative humidity error at various levels at time 12 UTC. The points were derived using the difference method and FAR3 fits to the spatial covariance data. The data is shown graphically in Figure 43.

References

- P. Courtier, E. Andersson, W. Heckley, G. Kelly, J. Pailleux, F. Rabier, J.-N. Thépaut, P. Undén, D. Vasiljevic, C. Cardinali, J. Eyre, M. Hamrud, J. Haseler, A. Hollingsworth, A. McNally, A. Stoffelen, 1993: Variation Assimilation at ECMWF, *Technical Memorandum No. 194*, ECMWF, 84 pp.
- Cressie, Noel A. C., 1993: *Statistics for Spatial Data*, John Wiley & Sons, Inc, 900 pp.
- Richard Franke, 1998: Three dimensional covariance functions for NOGAPS data, submitted to *Mon. Wea. Rev.* , 37 pp.
- Franke, Richard , 1986: Covariance functions for statistical interpolation, TR# NPS-53-86-007, Naval Postgraduate School, Monterey, CA 93943, 80 pp.
- Mitchell, Herschel L., Cécilien Charette, Clément Chouinard, and Bruce Brasnett, 1990: Revised interpolation statistics for the Canadian data assimilation procedure: their derivation and application, *Mon. Weather Rev.* **118**, 1591-1614.
- Office of the Federal Coordinator for Meteorological Services and Supporting Research, *Federal Meteorological Handbook No. 3, Rawinsonde and Pibal Observations*, FCM-H3-1997, U. S. Department of Commerce, 1997.
- Parrish, D., and J. Derber, 1992: The National Meteorological Center's spectral statistical interpolation analysis system, *Mon. Wea. Rev.* **109**, 1747-1763.
- P. Steinle and R. Seaman, 1995: A new 3-D variational analysis scheme, BMRC Research Report No 54, Bur Met, Australia, pp. 139-144.